Control of the Mechanical Properties of the Synthetic Anterior Longitudinal Ligament and its Effect on the Mechanical Analogue Lumbar Spine Model

By
Leighton J. LaPierre

Submitted to the graduate degree program in Mechanical Engineering and the Graduate Faculty of the University of Kansas School of Engineering in partial fulfillment of the requirements for the degree of Master of Science.

Dr. Elizabeth Friis, *Committee Chair*

Dr. Kenneth Fischer, *Committee Member*

Dr. Sara Wilson, *Committee Member*

Date Defended

The Thesis Committee for Leighton J. LaPierre certifies
that this is the approved version of the following thesis:

Control of the Mechanical Properties of the Synthetic Anterior Longitudinal Ligament and its Effect on the Mechanical Analogue Lumbar Spine Model

Dr. Elizabeth Friis, *Committee Chair*

Dr. Kenneth Fischer, *Committee Member*

Dr. Sara Wilson, *Committee Member*

Date Approved

Abstract

The development and validation of an anatomically correct mechanical analogue spine model would serve as a valuable tool in helping researchers and implant designers understand and alleviate low back pain. Advanced composite ligaments were designed to mimic the tensile mechanical properties of human spinal ligaments. By changing the composite properties, the stiffness and deformation at toe were controlled in a repeatable manner. Five analogue spine models, with three different Anterior Longitudinal Ligament (ALL) stiffness configurations, were tested in bending and compression using displacement control in a MTS load frame. The bending stiffness and kinematic ranges of motion of the spines were compared for each ALL stiffness configuration. The ALL stiffness had a significant effect on the stiffness and peak moment in extension of the overall spine model. The study demonstrated that a change in the synthetic ligament properties successfully controls the biomechanics of the analogue spine model and the model effectively mimics the human cadaveric biomechanical response.

Acknowledgements

I would like to extend a sincere amount of gratitude to several people who have helped to make my graduate experience at KU extremely rewarding and enlightening.

- Dr. Elizabeth Friis for her guidance and positive encouragement. I am thankful for her strong belief in my abilities and for her constantly pushing me to be a better researcher and to do my personal best. Her innovative and product based sense of research and education has taught me so much about how to be successful in the field of biomedical engineering.

- Dr. Kenneth Fischer and Dr Sara Wilson for agreeing to be a part of my thesis committee and for their time and guidance.

- All faculty members in the Department of Mechanical Engineering for their time, effort, and guidance towards providing me with a quality engineering education that I can be proud of

- My fellow researchers and friends…Mark Pacey, Amber Reeve, Amit Mane, Chad Clary for their constant willingness to drop what they were doing and lend a hand or mind; Nic Jaumard for his leadership, wisdom, and knowledge (I couldn't have done it without you); Gene Avidano for his partnership in every aspect of this project and for constantly pushing me to think outside the box and to not just accept the status quo (and of course for your continued friendship).

- John James and Amy Johnson at Pacific Research Laboratories for their hard work in the development and manufacturing of the specimens for this study.

- Carol Gonce, Lucas Jacobsen, and Shelby Stice for their willingness to try and answer any crazy question I could throw at them.

- My family for their constant love and support. Thank you Mom and Dad for always being proud of me and always inspiring me to do my best.

- Last and certainly not least…My wonderful wife, Morgan, for her never-ending love and support through this entire process. It was your positive encouragement and drive that kept me going many times. Thank you for your constant understanding on all the late nights and time spent doing "thesis stuff."

This work was supported in part by NIH SBIR Grant AR054289-01 and by Pacific Research Laboratories, Inc.

Table of Contents

List of Figures

List of Tables

List of Abbreviations

A/P – Anterior-Posterior
ACS – Anatomic Coordinate System
AF – Annulus Fibrosis
ALE – Adjacent Level Effects
ALL – Anterior Longitudinal Ligament
aROM – angular Range of Motion
ASTM – American Society for Testing and Materials
AVG ALL – Analogue spine model with an average stiffness ALL ligament
AX – Axial Torsion
C - Compression
CEZ – Compression Neutral Zone
CL – Capsular Ligament
CNC – Computer Numerical Control
CNZ – Compression Neutral Zone
CT – Computed Tomography
DEFTOE – Deformation at Toe in Compression
EEZ – Extension Elastic Zone
EZ – Elastic Zone (secondary stiffness)
FDA – Food and Drug Administration
FE – Flexion/Extension
FE6ROM – Flexion/Extension Range of Motion at ± 6 Nm
FEA – Finite Element Analysis
FEM – Finite Element Method
FENZ – Flexion/Extension Neutral Zone
FEZ – Flexion Elastic Zone
FSU – Functional Spinal Unit
IDE – Investigational Device Exemption
IRED – Infrared Light Emitting Diodes
ISL – Interspinous Ligament
IVD – Intervertebral Disc
KU – The University of Kansas
LBP – Low Back Pain
LED – Light Emitting Diode
LEZ – Left Elastic Zone
LF – Ligamentum Flavum
M/L – Medial-Lateral
MANOVA – Multivariate Analysis of Variance
MRI – Magnetic Resonance Imaging
MTS – Material Test System
NONE ALL – Analogue spine model with no ALL ligament
NP – Nucleus Pulposus
NZ – Neutral Zone (initial stiffness)

PE – Polyethylene
PGs - Proteoglycans
PLL – Posterior Longitudinal Ligament
PMMA – Polymethylmethacralate
PRL – Pacific Research Laboratories
PU – Polyurethane
PZ – Plastic Zone
RB – Rigid Body
REZ – Right Elastic Zone
RL – Right/Left Lateral Bending
RL6ROM – Right/Left Range of Motion at ± 6 Nm
RLNZ – Right/Left Neutral Zone
ROM – Range of Motion
SBIR – Small Business Innovation Research
SSL – Supraspinous Ligament
STIFF ALL – Analogue spine model with a stiffer than average ALL ligament
TL – Transverse Ligaments
tROM – translational Range of Motion
UHMWPE – Ultra High Molecular Weight Polyethylene
Vf – Volume Fraction

Chapter 1 – Introduction

The intended purpose of the research presented in this study was to further the development of the mechanical analogue spine model and to investigate how various parameters such as ligament stiffness can be altered in order to control the spine's biomechanical response. Development and validation of an anatomically correct mechanical analogue spine for quasistatic loading would open the doors for researchers and manufacturers to examine a multitude of clinical questions and implant design issues. The following is a discussion of the need for a mechanical analogue lumbar spine model, the shortcomings of the methods currently used, and how the model will help in evaluating medical devices.

1.1 Significance of Low Back Pain:

Low back pain (LBP) is a major public health problem in the United States and around the world and is beginning to exhibit epidemic proportions [1-3]. Various studies have shown that 70-85% of all people have back pain at some point in their life [1, 2, 4]. In the United States, back pain is the second most common reason cited for visiting a physician and the most common reason for limited activity in people younger than age 45. It is also the fifth most common reason for being admitted to a hospital and the third most common cause for having surgical procedure [2, 5, 6]. Also, in people under the age of 45 it is the most common work-related disability and the most expensive cause of work-related disability, in terms of workers' compensation and medical expenses [2]. Several studies have attempted to calculate the workplace absence and costs associated with LBP. Equally distributed among

men and women, an estimated loss of 149 million workdays equaling an estimated annual productivity loss of $28 billion annually [3, 7, 8].

Annually, more than 50 million physician office visits in the United States are attributed to back pain. LBP has been reported as the second-most common reason for seeking medical consultation with a doctor, second only to upper respiratory infections. In 2005, $86 billion was spent on back pain, up from $52 billion in 1997 [9].

The etiology of LBP is not well understood, and there is no clear consensus on the best treatment for the condition [3]. Experimental studies suggest that low back pain may originate from many different spinal structures including ligaments, facet joints, vertebral periosteum, the annulus fibrosis, and other structures. The most common source of low back pain may be musculo-ligamentous injuries and the age degenerative process in the intervertebral disc (IVD) and facet joints [1, 10]. Injury or age degeneration in the spinal ligaments may also lead to spinal instability and may alter the overall biomechanics of the spine. Spine fusion procedures were initially performed to stabilize vertebral fractures, spinal tuberculosis, and deformities such as scoliosis, but in recent years a majority has been performed for degenerative spinal conditions. These include disc degeneration, herniated disc, spinal stenosis, and degenerative spondylolisthesis as well as patients with symptomatic back pain associated with degenerative changes in the lumbar spine [11].

Spinal fusion has traditionally been considered the gold standard of back pain management, representing 85% of procedures, and 78% of spinal implant sales in

2006 according to the National Library of Medicine (Bethesda, MD). The most common spinal area treated is the lower (lumbar) spine [12]. However, it is predicted that as less-invasive procedures and motion preserving technology (such as total disc arthroplasty, nucleus replacement, interspinous process spacers, posterior dynamic stabilization devices, and others) are developed, spinal fusions may become less of a common place.

1.2 Current Market Growth:

Over the last decade and a half, spinal surgeries, namely fusions, have increased dramatically. In 2001, there were approximately 356,638 hospitalizations for lumbar surgery with over 122,000 of these being fusion procedures, representing a 220% increase in fusion procedures from 1990. There was a sharp increase in 1996 when the Food and Drug Administration (FDA) approved intervertebral fusion cages for use in the U.S. From 1996 to 2001 there was a 113% increase in spinal fusions versus a 10-13% increase in hip and knee arthroplasty. The most rapid increase was seen in adults age 60 and over [13].

Similar to the general orthopedics sector, spine sector growth can be attributed to aging populations, product innovation, and the market demand of the baby-boom generation who typically lead very active lifestyles. In addition, the rising incidence of obesity, which can place larger loads on the back creating a higher incidence of spinal degeneration, has been frequently cited as a contributing factor [12].

It is estimated that by 2010 the US spine industry will earn more than $10 billion in revenue, with non-fusion products comprising more than 90% of the

revenues [14]. This increase in spinal surgery procedures has led to a multi-billion dollar industry. Considering that worldwide spinal market revenues were less than a $100 million in 1990, grew to $3.5 billion by 2004, and reached more than $6 billion last year, growth of the segment has indeed been impressive [12]. As the baby-boomer population ages, there is a growing need to develop innovative new types of spinal implants for the benefit of society. Much research and development in this area is currently underway, as resolution of medical-legal issues have allowed implant manufacturers to forge new paths in the area. It is, however, estimated by some in industry that technology development in the spine field is approximately 15 years behind that of other orthopaedic areas such as hip and total knee related implants.

There is a large demand for evaluating new spinal device technology and determining how it affects the kinetics and kinematics of the lumbar spine. Many biomechanical evaluations have been performed to determine the changes in segmental motion, adjacent level effects (ALE), intradiscal pressures, facet contact patterns, and other parameters of the lumbar spine after fusion, nucleus replacement, or disc arthroplasty. Both animal and cadaveric studies have demonstrated increased motion and/or mechanical stress adjacent to lumbar fusion constructs [15-25]. There are still many unknowns in the area of spinal implants and their affects on the spine. The use of a biomechanically accurate synthetic mechanical analogue lumbar spine model would help to investigate the wide spectrum of unknowns in the spinal device field.

Testing of new spinal implant technologies and surgical approaches is necessary and often required by the FDA in order to be approved for sale in the United States. The purpose of this testing is to evaluate the new technology's safety and effectiveness. Often times implant testing helps in the product development process to determine failure modes, fatigue properties, and maximum load and deformation limits.

1.3 Motivation for Synthetic Analogue Lumbar Spine Model:

The analogue lumbar spine model is not intended to completely replace the current standard of testing non-pathological fresh frozen human cadaveric lumbar spines. It is purely intended to act as a supplement and tool in better guiding research understanding and product development, which ultimately will lead to better spinal implants and surgical procedures. The basic concept of designing the mechanical analogue lumbar spine model is to develop a vertebrae and soft tissues with anatomically correct geometry and rigidities and to assemble them together in appropriate anatomical positions so that the structural rigidity of the human spine (without muscles) is replicated. This will allow for a biomechanically accurate test model that can be manufactured to be both repeatable and controllable. This idea is identical to the engineering steps taken in the development of many computational models (i.e., finite element analysis). Finite element analysis, however, has many limitations, including replicating the complex geometries and mechanical interactions of the spinal elements.

Currently, the most common methods to evaluate the effects of spinal implant devices on the lumbar spine is in the form of in-vitro human cadaveric spine testing, animal spine testing, computer modeling via finite element analysis (FEA), and in-vivo investigational device exemption (IDE) clinical trials. The major factors supporting a synthetic mechanical analogue of the lumbar spine relate to the deficits in current testing methods of spinal implants.

The most realistic in vitro representation of the lumbar spine, or any spinal region, is provided through cadaveric samples. These segments – removed from sheep, cattle, and some humans – are used extensively to test and evaluate newly developed spinal fusion devices. There are many difficulties and inadequacies associated with cadaveric (human and animal) testing of spinal stabilization and arthroplasty devices. There are handling and biohazard concerns, high cost and limited availability of specimens, specimen quality, and large inter-specimen variability [26], as well as degradation and testing time constraints [27]. There is also difficulty associated with testing specific parameters in a cadaveric specimen such as facet joint load, disc pressures, and ligament stresses and strains. All of these difficulties can be overcome through the use of the synthetic mechanical analogue spine model.

Specifically, the in vitro time allotted for the display of accurate in vivo biomechanical properties is severely limited by the degradation of the biologic tissue once exposed to air. This prevents extensive testing with one model, forcing researchers and engineers to work with several different samples, which display

significant changes in tissue properties as time passes. There is also tremendous inherent inter-specimen variation in the mechanical response of the human cadaveric spine segments (i.e., up to 500% variation in normal intervertebral disc pressures in normal specimens [26]). This variation makes statistical comparison of surgical variations difficult with a reasonable sample size. The synthetic mechanical analogue spine model will have much lower variation in mechanical properties and disc pressures.

Other concepts in mechanical analogue spinal modeling exist, but these models do not display appropriate biomechanical characteristics and are thus limited in marketing capability. These custom analogues are typically assembled by researchers for non-commercial use to satisfy their own testing conditions, and originate from ASTM testing standards. They are usually constructed from two or more rigid polyurethane foam blocks linked in series to mimic the spine structure only. Even when physical assembly in these makeshift replicas is accurate, the stabilization provided by soft tissues such as ligaments is absent, preventing rigorous testing in flexion, extension, and lateral bending. These models are neither intended nor designed for load levels experienced in in-vivo loading.

In addition to providing an efficient means for biomechanical testing of spinal implant devices on the lumbar spine and aiding in product development, the synthetic mechanical analogue lumbar spine model will help in the understanding of the different roles various spinal elements have on the overall biomechanics of the spinal column. The effect of surgical procedures and various implants on potential patient

outcomes will also be able to be evaluated. It is intended for use by researchers and designers in both the academic and medical industry.

The basic technologies (specifically the soft tissue) developed for the mechanical analogue spine model can be applied to make variations of the analogue spine model appropriate for simulating situations such as pathological conditions, degenerative affects due to age, and models of varying laxity. These technologies could also be extended to develop models of typical spinal deformities, such as scoliosis.

Chapter 2 – Background and Significance

According to White and Panjabi, the human spinal column is a mechanical structure that has three fundamental biomechanical functions [28]: 1) It transfers the loads and the resultant bending moments of the head, trunk, and any weights being lifted to the pelvis. 2) It allows sufficient physiologic motions between these three body parts. 3) It protects the delicate spinal cord from potentially damaging forces and motions produced by both physiologic movements and trauma. The vertebral bodies articulate with each other through a series of complex semi-movable joints, passive structures, and active structures. The intervertebral disc (cartilaginous joint) and facet joints (synovial) act as the primary articulating joints, the ligaments act as the passive stabilizing structures, and the muscles act as the active structures that move and stabilize the spine by applying forces and moments to the spinal via a complex dynamic neuromuscular control system.

2.1 Spinal Anatomy and Functional Structures:

In order to better understand the biomechanics of the lumbar spine it is important to review some of the anatomy and function of the components that make up the spinal complex.

The spinal column consists of a total of 33 vertebral bodies: 7 cervical vertebrae (neck region), 12 thoracic vertebrae (chest region), 5 lumbar vertebrae (lower back region), and 5 fused sacral vertebrae (pelvic region), and 2-4 fused coccyx vertebrae (tailbone) (Figure 1). The vertebral bodies are the primary weight bearing structures in the spinal column. Between each set of two vertebrae are

intervertebral discs and a set of articulating facet joints (also referred to as zygapophyseal joints). The vertebra are also connected by several ligaments, most of them running up and down the length of the spine.

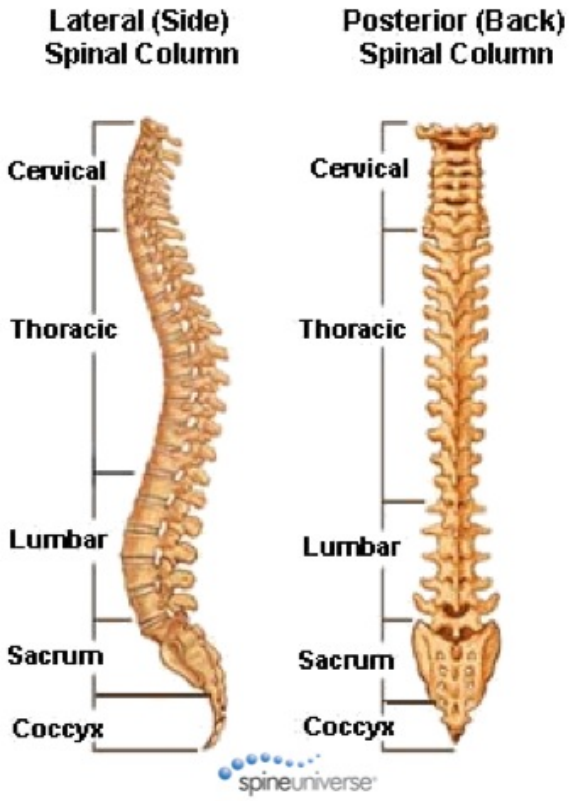

Figure 1. The different vertebral body regions of the spinal column. (Image courtesy of spineuniverse.com via http://www.spineuniverse.com/displayarticle.php/article1286.html)

2.1.1 Vertebrae:

The lumbar region will be highlighted since the vertebrae and other structures in this region bear the majority of the load of the upper body and related biomechanical stress. Incidentally, this is where back pain tends to originate from and has resulted in a large amount of attention by researchers and clinicians alike. The vertebrae consist of several components (Figure 2). Some of the features that set

the lumbar vertebrae apart from their counterparts are larger anterior vertebral bodies with larger intervertebral discs, longer and wider pedicles, more horizontal and square shaped spinous processes. The exterior vertebral body consists of very hard bone shell (cortical bone), with more spongy bone (cancellous or trabecular bone) and blood vessels inside [29].

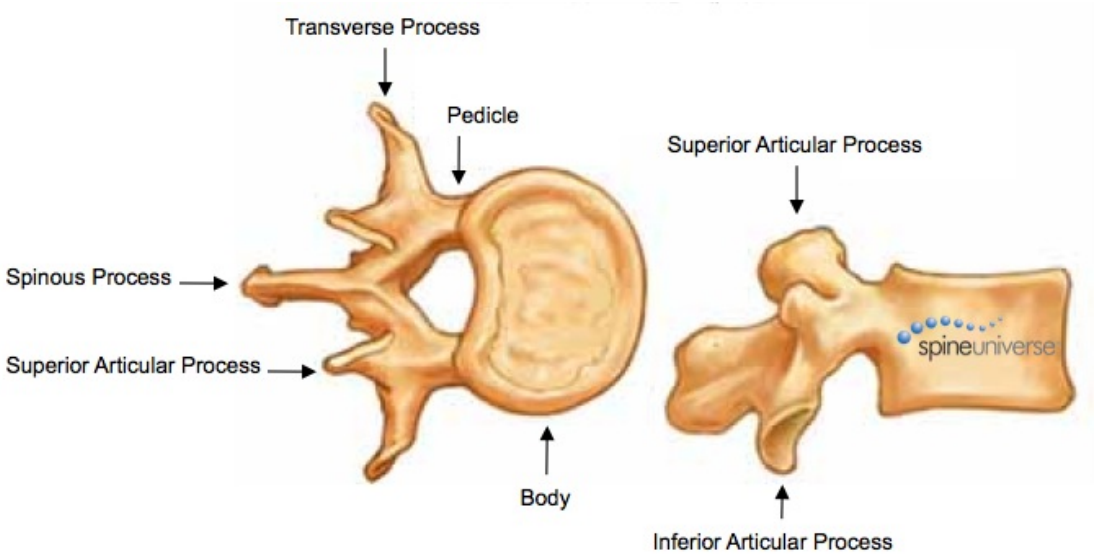

Figure 2. Distinctive features of the lumbar vertebrae (Image courtesy of spineuniverse.com via http://www.spineuniverse.com/displayarticle.php/article1286.html)

- Spinal canal – Opening in the posterior part of the vertebrae that the spinal cord runs through.
- Pedicles – Thick bony structures that consist of cortical bone and connects the posterior aspects of the spine to the anterior column.
- Transverse Process – Bilateral projections from the vertebrae that serve as the sight for muscle and ligament attachments.

- Spinous Process – Large posterior directed projection that makes up part of the vertebral arch. Serves as a sight for ligament and muscle and ligament attachments.

- Facet Joints – Each vertebra contains a superior and inferior articular process. The inferior articular process is convex and faces laterally and the superior articular process is concave and faces medially. These processes come together to form a synovial facet joint that helps in giving the spine stability and limiting spinal motion. Primarily limits axial rotation and extension in the lumbar spine.

2.1.2 Intervertebral Disc:

The intervertebral discs are the one of the main structures of the spinal column and separate the vertebral bodies. They occupy one-third of the spinal column's height. They consist of a gel-like nucleus pulposus, a collagen fiber rich annulus fibrosis, and cartilaginous endplates (Figure 3). The intervertebral disc is primarily an avascular structure with the only blood supply going to the cartilaginous endplates [30]. There is no doubt that the discs play a large mechanical role in transmitting load through the spinal column. In compression and bending, the intervertebral disc acts hydrostatically with the nucleus pulposus pressurizing and the annulus fibrosis containing the NP like a bulging tire. The discs give the spine much of its flexibility thus allowing bending, flexion, extension, and axial rotation. In bending, the fibers on one side of the AF act in tension and the fibers on the opposites side act in

compression [31, 32]. The lumbar IVDs are approximately 7-10 mm thick and approximately 4 cm in diameter [33, 34].

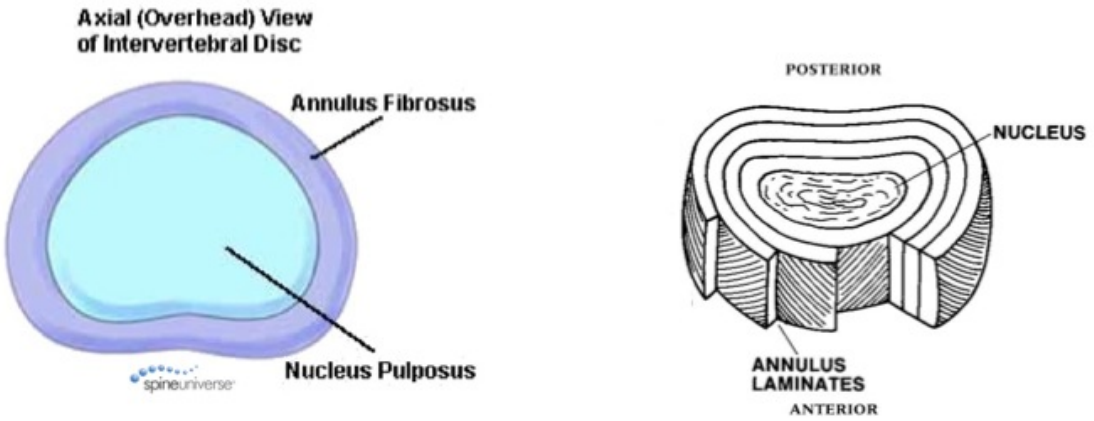

Figure 3. Components of the intervertebral disc. Image on left courtesy of spineuniverse.com via http://www.spineuniverse.com/displayarticle.php/article1267.html. Image on right is from White, A. and M. Panjabi, Clinical Biomechanics of the Spine 2nd Edition. ed. 2 ed. 1990, Philadelphia: J.B. Lippincott Company.

- Nucleus Pulposus – Composed of randomly organized collagen fibers [35] and radially arranged short elastin fibers embedded in a highly hydrated aggrecan-containing gel [36]. The nucleus pulposus contains a high concentration of proteoglycans (PGs), which attract and retain water. It is this concentration of water that hydrostatically resists compression as the spine compresses and bends. The amount of water in the nucleus varies throughout the day depending on the activity.

- Annulus Fibrosis – Composed of 15 to 25 concentric rings or lamellae with the collagen fibers running parallel to each other within the lamellae. The fibers are oriented at ± 30° to the transverse plane [28] and alternate directions

in adjacent lamellae. Elastic fibers lie between the lamellae to possibly help the disc return to its original orientation after bending or compression [37].

- Endplate – Hyaline cartilage usually less than 1mm thick. This interfaces with the intervertebral disc and the vertebral body with no clear boundary between the endplate and the vertebral body. The collagen fibers in the endplate run horizontal and parallel to the vertebral bodies, with the fibers continuing into the disc [34]. Nutrients diffuse through the endplate to in order to feed the nucleus pulposus.

2.1.3 Spinal Ligaments:

Spinal ligaments are uniaxial structures comprised of fibrous bands or sheets of connective tissue that are most effective in carrying tensile loads along the direction that the fibers run. White and Panajabi describe them as rubber bands that "readily resist tensile forces but buckle when subjected to compression."

There are seven spinal ligaments in the lumbar spine. The ligaments are as follows and can be seen in Figure 4: anterior longitudinal ligament (ALL), posterior longitudinal ligament (PLL), ligamentum flavum (LF), transverse ligaments (TL), capsular ligaments (CL), interspinous / supraspinous ligament complex (ISL / SSL).

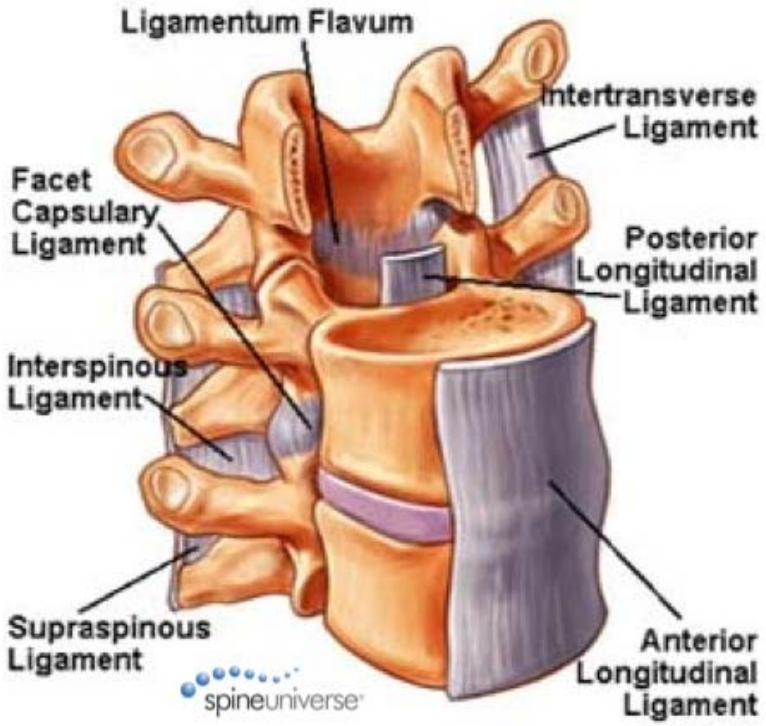

Figure 4. Spinal ligaments of the lumbar spine. (Image courtesy of spineunivers.com via http://www.spineuniverse.com/displayarticle.php/article1268.html)

- ALL: This ligament attaches firmly to the anterior portion of the vertebral bodies but is not as firmly attached to the annulus fibrosis of the intervertebral disc. Comprised of highly organized type I collagen fibers and very few elastin fibers that run parallel to the length of the spine. It provides major stability to the spinal column. It primarily resists hyperextension and bulging of the disc. Due to its high concentration of collagen fibers and few elastin fibers it is able to withstand sudden applications of stress [38].

- PLL: This ligament attaches to the posterior portion of the vertebral bodies in the spinal canal and has an interwoven connection with the intervertebral disc. It primarily prevents hyperflexion and bulging of the disc [28].

- LF: This ligament connects the borders of adjacent laminae. It forms a cover over the dura mater and connects under the facet joints to help prevent the spinal nerve roots from mechanical impingement. This ligament is often referred to as the yellow ligaments because of its yellowish appearance. This ligament is composed of a high amount of elastic fibers and is one of the most pure elastic tissues in the human body [39, 40]. It is stretched during flexion and since it is further from the axis of rotation than the PLL it stretches more for the same amount of flexion [32].

- ISL: The ISL is a fanlike ligament that connects the spinous processes of adjacent vertebrae. Collagen fibers run in a direction parallel to the spinous processes so fibers are not stretched in their longitudinal direction in either flexion or extension [38]. The function of these ligaments are unknown, but it may be to transfer stress from the surrounding muscles [32].

- SSL: A long ligament on the posterior part of the spinous processes that extends from the top of the spine and terminates around L3 and L5. It has very little tensile strength and thus provides little resistance to flexion. The purpose is not primarily mechanical but to provide cushioning for the posterior part of the spine. This ligament also plays a sensory role in terms of a ligamento-muscular protective reflex in the spinal column [41, 42]. Tendons of the erector spinae muscles blend into this ligament. Experiments on pig SSLs showed that it simply falls apart and fails completely at low loads of 28 – 81N [43].

- TL: These ligaments pass between the transverse processes in the thoracic region and are characterized as rounded cords that are connected with the deep muscles in the back. The high failure stress with low failure strain in the thoracic region explains the restricted intervertebral movements in this region. They have little or no mechanical significance in the lumbar region because of their small cross-sectional area [28].

- CL: These ligaments attach just beyond the margin of the articular processes and encapsulate the facet joint. The fibers are oriented in a direction perpendicular to the plane of the facet joints to prevent extreme distraction [28].

In order to better understand the mechanical properties and functional role of the ligaments the quantitative anatomy such as length and cross-sectional area are important. Table 1 summarizes these values found in the literature [28, 44-52]. The methods used to obtain these values are reviewed later in this chapter.

Table 1. Lumbar spinal ligament dimensions found in the literature

Ligament	X-sec area (mm^2)	Width (mm)	Thickness (mm)	Length(mm)	Source
ALL	56	16	3.5	13	W&P
	74				Goel
	65.6 +/- 12.76			12.3 +/- .76	Chazal 1985
	38.2 +/- 3.5				Neumann 1992
	32.4 +/- 10.9			37.1 +/- 5	Pintar 1992
	37.5	23	1.63		Tkaczuk 1968
	24				Shirazi-Adl 1986
PLL	16.2	9	1.8	11	W&P
	14.4				Goel
	24.71 +/- 6.78			11.29 +/- 1.15	Chazal 1985
	5.2 +/- 2.4			33.2 +/- 2.3	Pintar 1992
	12.2	10.2	1.2		Tkaczuk 1968
	14.4				Shirazi-Adl 1986
LF	68	20	3.4	19	W&P
	40				Goel
	39			19	Chazal 1985
	84.2 +/- 17.9			15.2 +/- 1.3	Pintar 1992
ISL	26.52	7.8	3.4	na	W&P
	40				Goel
	30.33 +/- 14.75			11.22 +/- 1.91	Chazal 1985
	35.1 +/- 15			16 +/- 3.2	Pintar 1992
SSL	23.8	7	3.4	11	W&P
	30				Goel
	30.33 +/- 14.75			11.22 +/- 1.91	Chazal 1985
	25.2 +/- 14			25.2 +/- 5.6	Pintar 1992
TL	1.8				Goel

2.2 Spinal Ligaments – Form, Function, and Characterization:

2.2.1 Ligamentous Composition and Microstructure:

The ligaments are composed of about 20% cellular material (fibroblasts) and 80% extracelluar matrix. Of the extracellular matrix 70% is water and 30% are solids. The majority of these solids are made up of collagen (Type I), elastin, and ground substance (consisting of proteoglycans and other small proteins and molecules) [53]. The Type I collagen gives the ligaments their tensile strength and makes up 70% of the dry weight of the spinal ligaments [54]. The elastin in the ligaments gives them their extensibility and is composed of rubber-like protein proline and alamine. Elastin fibers can stretch several times their original length (~500% strains). The LF in particular has a very high concentration (2 to 1 ratio) of elastin [40].

The collagen microstructure consists of triple helices of coiled polypeptide chains that are synthesized and secreted by the fibroblasts. These peptide (alpha) chains are made up primarily of three amino acids (glycine, proline, and hydroxyproline) [53]. The chains are bonded together with hydrogen bonds and crosslinks are formed between the collagen molecules giving the tissue its strength. The collagen molecules aggregate in a parallel arrangement to form microfibrils and then fibrils that appear banded under an electron microscope. These fibrils aggregate further into fibers that eventually form into densely packed ligamentous bundles (Figure 5).

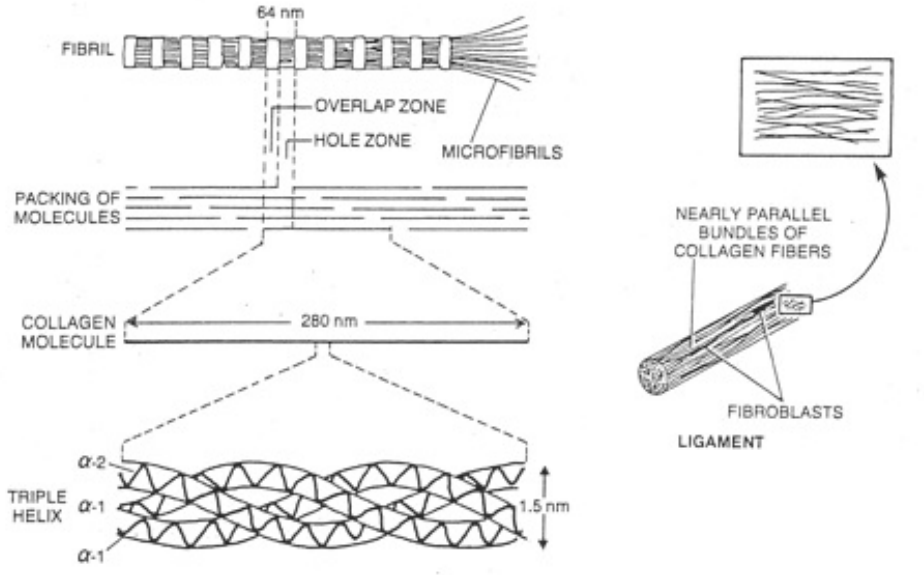

Figure 5. Microstructure of collagen fibers in spinal ligaments (Nordin, M. and F. VH, Basic Biomechanics of the Musculoskeletal System. ed. 2 ed. 1989, Philadelphia, PA: Lea and Febiger.)

2.2.2 Ligament function (Sensory):

Many human and animal studies have provided evidence of the idea that ligaments serve a sensory function in terms of proprioception, motor control, and joint stability. The ligaments have been found to contribute to joint stability through mechanical restraint as well as through sensory-motor control properties (Figure 6) [55]. The presence of a ligamento-muscular reflex has been proposed for the automatic control of the motion segment [42, 55-60]. Ligament afferents may contribute to joint stability, muscle co-activation, and proprioception through direct polysynaptic reflex effects onto ascending pathways and skeltomotoneurones, and/or indirectly via reflex actions on the gamma-muscle spindle system [55]. When conditions that challenge spinal stability are detected in the ligaments, the control unit activates the appropriate muscles in order to protect, restore, or avoid instability via contraction of the surrounding muscles, which typically favors unloading of the stimulated ligament [59, 61]. The ligamento-muscular reflex also acts as a protective reflex when unexpected movement occurs, eliciting a sudden increase in ligament tension. This increase in ligament tension may provide a fast dose of joint stiffness/stability. In order for protective reflexes to be helpful they must be fast acting. Solomonow's studies have shown that this reflex has a response time (or latency) ranging from 2.5 ms to 5 ms in human extremity joints [60].

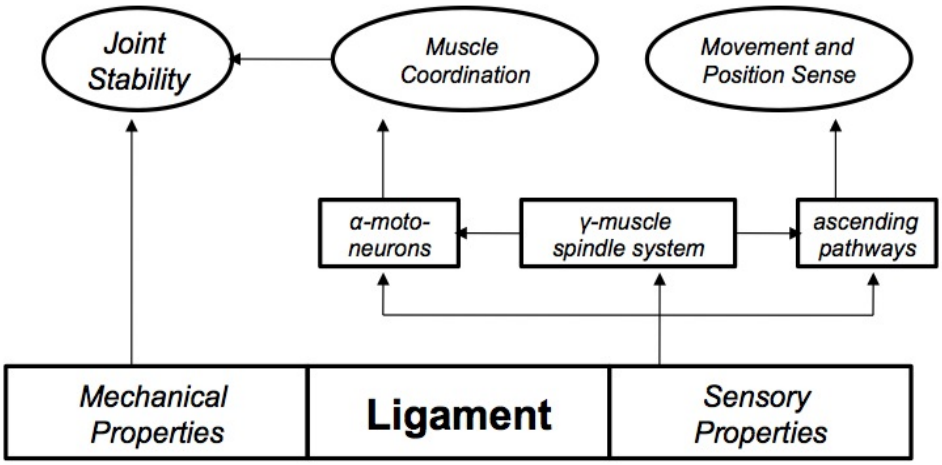

Figure 6. Sjolander et al. have proposed that the spinal ligaments provide joint stability via mechanical restraint as well as through sensory-motor control properties. (figure adapted from Sjolander, P., Johansson, H., and Djupsjobacka, M., 2002, "Spinal and supraspinal effects of activity in ligament afferents," J Electromyogr Kinesiol, 12(3), pp. 167-176.)

2.2.3 Ligament Function (Mechanical):

Unlike muscles, the spinal ligaments themselves are passive mechanical structures that along with the muscles play the role of providing stability to the spinal column within the physiologic ranges of motion. Clinical stability of the spine is defined as [28] "…the ability of the spine under physiologic loads to limit patterns of displacement so as not to damage or irritate the spinal cord or nerve roots and, in addition, to prevent incapacitating deformity of pain due to structural changes." **These soft tissues along with the intervertebral disc control the biomechanical response of the spine in terms of spine kinematics and load transfer.** The ligaments help protect the spinal cord by restricting the vertebrae motions within well-defined limits. Since the ligaments are passive structures they help to maintain spinal stability and limit motion with minimum energy expenditure or neuromuscular response. The viscoelastic and bilinear stiffness properties of the ligaments help

perform this function during normal loading as well as in traumatic situations. In high dynamic situations, such as a sudden impact, the viscoelasticity of the ligaments allows a large amount of energy to be absorbed. More information on these properties will be discussed later.

The location and orientation of the ligaments also affects their overall functional properties. For example, the anterior longitudinal ligament's function is determined not only by its microstructure and thus its mechanical properties but also its distance (moment arm) from the instantaneous axis of rotation of the function spinal unit (FSU). As stated before, the anterior longitudinal ligament's primary function is to resist movement and provide stability in extension since it acts in tension during this motion. During flexion, the ALL goes into compression and provides little resistance to motion. The in vitro physiologic strains in the ligaments were examined in a study by Panjabi et al [39]. Three-dimensional physiologic intervertebral motions were recorded along with the attachment points of each ligament. One interesting finding of the study was the significant amount of increase in the sagittal and horizontal plane neutral zones due to disc degeneration. Therefore, an aged or degenerated spine may be at a higher risk for increased ligament strains during physiologic motions. A lower stiffness ligament may provide less stability for the spinal column.

2.2.4 Ligament Mechanical Characterization:

Because the spinal column must be allowed to move freely within physiological limits yet be restrained from extreme motions, the spinal ligament's

nonlinear load-displacement or stress-strain behavior is one of their most important mechanical characteristics. This function is a direct effect of the wavy shape or coiling of the collagen fibers in the ligaments [52]. Reflected light microscopy showed that the ALL and PLL have a wavy appearance [38]. A typical sigmoid shaped load-displacement or stress-strain curve for a ligament in tension is shown in Figure 7. To quantify this behavior three main values are determined. The initial linear stiffness or neutral zone (NZ) where the ligament is elongated without large increases in load, the secondary stiffness or elastic zone (EZ) where the load increases linearly with displacement, and the deformation or strain at toe can be determined for each curve. The deformation or strain at toe is defined as being the displacement or strain where the two linear stiffness lines intersect.

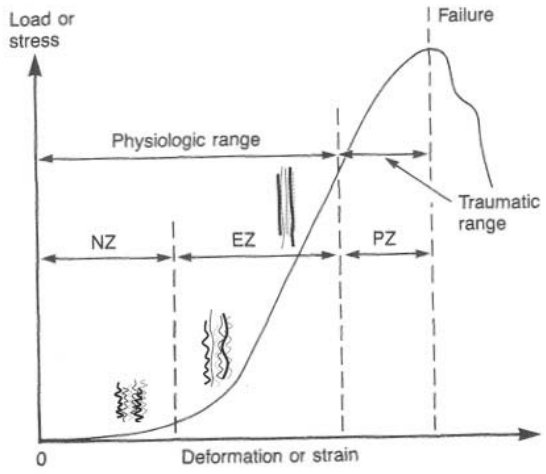

Figure 7. Typical load-displacement or stress-strain curve for a ligament in tension. The neutral zone (NZ) is a region of low stiffness where the collagen fibers are still straightening or uncoiling. The elastic zone (EZ) is a region of higher stiffness where the collagen fibers are straight and under load. The plastic zone (PZ) is a region where the ligament starts to fail. The deformation at toe or strain at toe is the area in between the NZ and EZ and is defined as deformation or strain at the point where the slope of the NZ intersects the slope of the EZ. During every day activities, soft tissues such as ligaments normally undergo deformation only within the elastic (physiologic) region. (White, A. and M. Panjabi, Clinical Biomechanics of the Spine 2nd Edition. ed. 2 ed. 1990, Philadelphia: J.B. Lippincott Company.)

The uncrimping of the collagen fiber waves or coils contributes to the nonlinearity of the ligaments [62, 63]. Interactions between the collagen fibers and the proteoglycan matrix as well as cross linking between the collagen fibers may also contribute to the ligament tissue's nonlinear behavior [64]. Inspection of the collagen fibers under a scanning electron microscope in Figure 8 shows how the fibers in a ligament are crimped when unloaded or relaxed and the then are straightened when loaded. Also, note how the fibers are primarily oriented in one direction parallel to each other.

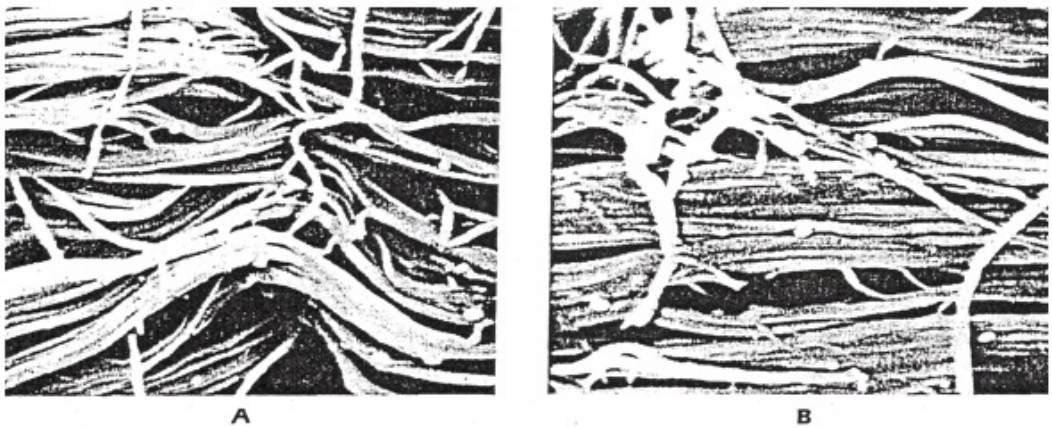

Figure 8. Collagen fibers under a scanning electron microscope in the unloaded state (A) and the loaded state (B). (Kennedy, J.C., et al., Tension studies of human knee ligaments. Yield point, ultimate failure, and disruption of the cruciate and tibial collateral ligaments. J Bone Joint Surg Am, 1976. 58(3): p. 350-5.) Copyright of image is owned by The Journal of Bone and Joint Surgery, Inc.

The viscoelastic properties of the ligaments such as stress-relaxation, creep, strain rate dependence, and hysteresis have been shown to result not only in mechanical functional degradation, but also in the development of sensory-motor disorders with short and long term implications on function and disability [65].

When the ligament is stretched isometrically to a fixed length, it develops a certain amount of initial tension. As time passes, the tension decreases exponentially to a finite minimum while the length remains constant (Figure 9A). This decrease in tension over time at a constant length is termed stress-relaxation [65]. When a ligament is stretched isotonically it will stretch to an initial length. If held at this constant load, it will continue to elongate over time in an exponential fashion up to a finite maximum (Figure 9B). This elongation over time with a constant load is termed creep. With rest the creep does not always fully recover immediately and will result in a laxity in the ligament. High frequency repetitive motion induces a larger amount of creep and requires a longer amount of time to fully recover [65].

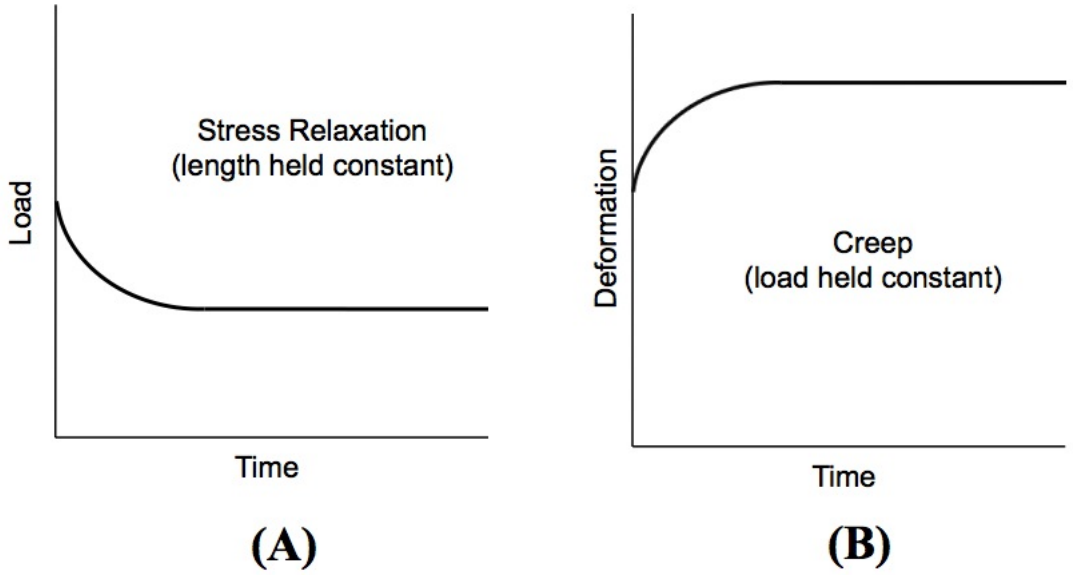

Figure 9. Viscoelastic behavior of spinal ligaments. Stress relaxation under displacement control (A) and Creep phenomenon under load control (B).

The amount of tension developed in a ligament is dependent on the rate at which it is elongated. Slow rates of elongation are associated with the development

of relatively low tension, whereas higher rates of elongation develop high tension (Figure 10A). Fast stretch of ligaments, such as high frequency repetitive motion or in certain sports activities are known to result in high incidents of ligamentous damage or rupture (i.e. sprained ankle). Fast rates of elongation may exceed the physiological loads that can be sustained by a ligament safely, but may still be within the physiological length range [65].

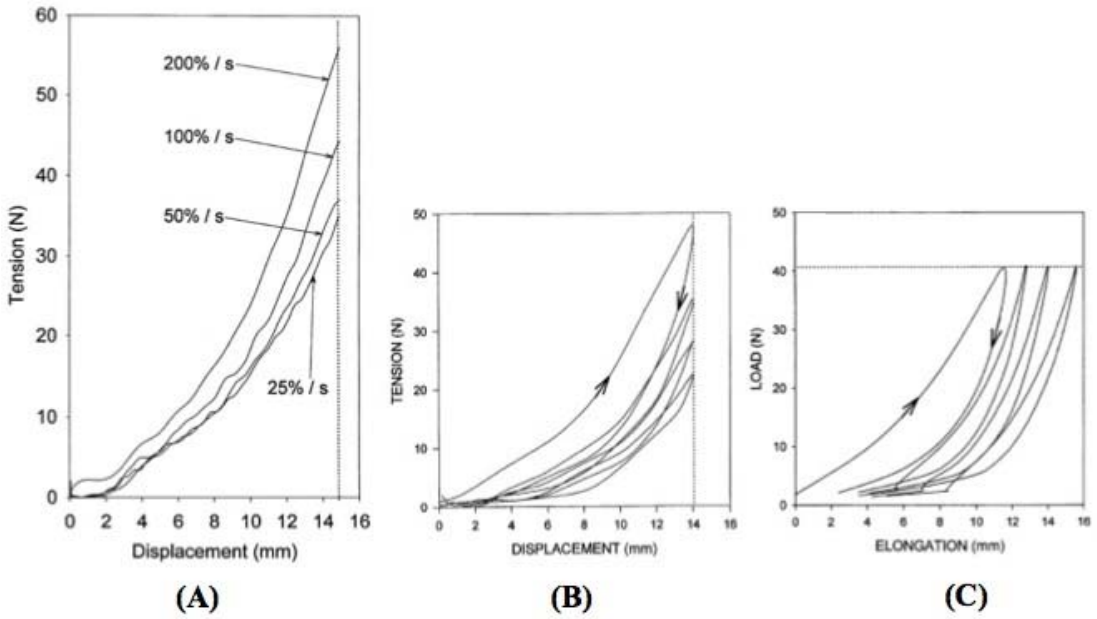

Figure 10. (A) The length-tension relation of a ligament when stretched at different rates. Increasing the rate of stretch from 25%/s to 200%/s develops nearly 50% more tension in the SSL. (B) The hysteresis associated with cyclic stretch of the same peak magnitude. (C) The hysteresis developed in a ligament when subjected to cyclic load of the same peak magnitude. (Solomonow, M., Ligaments: a source of work-related musculoskeletal disorders. J Electromyogr Kinesiol, 2004. 14(1): p. 49-60.)

Hysteresis is the inability to track the same stress-strain curve when subjected to a single stretch release or cyclic load-unload. The effect of hysteresis can be seen as related to the creep and tension-relaxation phenomena. Repetitive load cycles with a constant displacement will develop hysteresis along the tension axis due to tension-

relaxation (Figure 10B). Repetitive load cycles with a constant peak load will develop hysteresis along the length axis due to creep (Figure 10C). The impact of hysteresis is similar to that of creep and tension-relaxation. It produces decreased tension, joint laxity, reduced joint stability, and increased risk of injury [65].

2.3 Mechanical Properties of Human Spinal Ligaments:

Very little tensile stiffness data is available concerning such characteristics of the spinal ligaments. White and Panjabi [39, 66] found the load-displacement for the various ligaments as shown in Figure 11. The longitudinal ligaments (ALL and PLL) are structurally the largest and stiffest ligaments and provide a larger amount of resistance and stability than the other ligaments. For this reason they will be discussed in more detail than the other spinal ligaments. Tkaczuk et al. [52] did an extensive study of the tensile characteristics of the ALL and PLL. He found that the PLL is approximately twice as stiff in load-deformation as the ALL. The ALL, however is the stronger and wider of the two longitudinal ligaments and has failure load of between 330N and 510N while the failure load of the PLL ranges between 264N and 384N [28, 49]. The ALL is strongly attached to the vertebral body bones and also contains some collagen fiber interweaving with the AF. The PLL is smaller than the ALL and is only attached to the intervertebral discs. Due to the PLL's closer proximity to the axis of rotation the, it must be much stiffer than the other posterior ligaments (i.e. LF, ISL, SSL). The restoring force exerted by the stretched PLL will be less than that exerted by the much broader ALL. Therefore, the PLL is expected to be less important for resisting flexion than the ALL is for resisting extension.

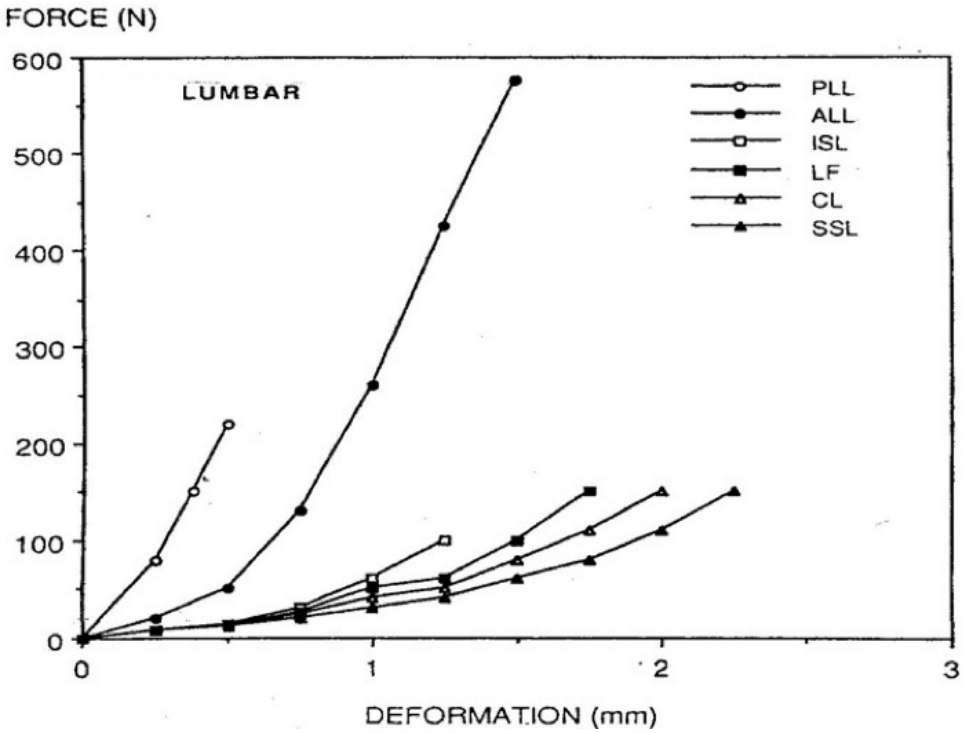

Figure 11. Load deformation behavior of spinal ligaments in tension (White, A. and M. Panjabi, Clinical Biomechanics of the Spine 2nd Edition. ed. 2 ed. 1990, Philadelphia: J.B. Lippincott Company)

A table of all soft tissue mechanical property ranges found in literature [28, 40, 44-50, 67, 68] can be seen in Table 2. More specifically, several studies [44-48, 50, 51] have attempted to characterize the mechanical properties of the longitudinal ligaments (Table 3). The methods used to obtain these values as well as the quantitative anatomy values in Table 1 are reviewed in the next section of this chapter. **There has, however, been a very large amount of variability in the results due to age, difficulties in identifying boundaries, variations in experimental techniques, and the inherent inter-specimen variability.** While one group (Neumann et al., 1992 [49]) found the elastic zone stiffness of the ALL to be very high at 759 ± 336 MPa, another group (Shirazi-Adl et al., 1986 [69]) found the

elastic zone stiffness of the ALL to be around 130 MPa. None of these studies, however, have compared ligament behaviors to overall segment behaviors. Gillespie and Dickey [70] compared the effect of lumbar spine ligaments on flexion-extension behavior in a parallel linkage robot model and a porcine model. **While general influences of the various components were noted, the effect of different soft tissue stiffness on flexibility and motion were not noted.**

Table 2. Soft tissue mechanical property ranges found in literature

Soft Tissue	NZ Stiffness	EZ Stiffness	Toe	X-Sec. Area (mm^2)
ALL	7.8 - 45 MPa	20 - 759 MPa	0.031 - .120 strain	22 - 74
PLL	10 - 502 MPa	20 - 937 MPa	0.0098 - .110 strain	2.8 - 16.2
LF	3 - 15 MPa	3.24 - 67 MPa	0.044 - .097 strain	40 - 102.1
ISL	10 - 27 MPa	2.23 - 132 MPa	0.028 - .020 strain	20.1 - 50.1
SSL	8 - 27 MPa	8.8 - 115 MPa	0.048 - .200 strain	11.2 - 39.2
CL	15 - 34 MPa	8.48 - 137 MPa	0.047 - 0.099 strain	15.5 - 72.1
IVD	357 - 737 N/mm	652 - 2380 N/mm	0.419 - .499 mm	N/A

Table 3. ALL and PLL mechanical properties from literature. The shaded properties were calculated from values found in many of Goel et al's FEA papers.

Ligament	NZ stiffness (MPa)	NZ stiffness (N/mm)	EZ Stiffness (MPa)	EZ Stiffness (N/mm)	Toe (strain)	Toe (mm)	X-Sec. Area (mm^2)	Initial Length (mm)
ALL				133.33 (Shirazi-Adl et al 1986)			24 (Shirazi-Adl et al 1986)	
	7.8 (Goel FEM)	19.87 - 55.21 (Goel FEM) 45.17	20 (Goel FEM)	50.96 - 141.56 (Goel FEM) 115.82	0.12 (Goel FEM)		63.7 (Goel FEM)	11 (Goel FEM)
	21 - 45 (White & Panjabi 1990)	78.64 (White & Pajabi 1990)	162 - 469 (White & Panjabi 1990)	632.36 (White & Pajabi 1990)	0.031 - 0.072 (White & Panjabi 1990)	0.681 (White & Pajabi 1990)	56 (White & Panjabi 1990)	11.5 - 25.4 (varied length to get stiffness ranges)
			24.88 (Chazal et al 1985)	115.89 (Chazal et al 1985)			53 - 78.4 (Chazal et al 1985)	11.3 - 13.3 (Chazal et al 1985)
			20 -56 (Pintar et al 1992)	17.3 - 48.7 (Pintar et al 1992)			10.6 - 52.5 (Pintar et al 1992)	32.1 - 42.1 (Pintar et al 1992)
PLL				133.33 (Shirazi-Adl et al 1986)			14.4 (Shirazi-Adl et al 1986)	
	10 (Goel FEM)	9.52 - 40 (Goel FEM) 22.22	20 (Goel FEM)	19.05 - 80 (Goel FEM) 44.44	0.11 (Goel FEM)		20 (Goel FEM)	9 (Goel FEM)
	227 - 502 (White & Panjabi 1990)	296.57 (White & Panjabi 1990)	411 - 920 (White & Panjabi 1990)	573.33 (White & Panjabi 1990)	0.0098 - 0.0217 (White & Panjabi 1990)	.257 (White & Panjabi 1990)	16.2 (White & Panjabi 1990)	11.5 - 25.4 (varied length to get stiffness ranges)
			61.56 (Chazal et al 1985)	124.1 (Chazal et al 1985)			18 - 31.4 (Chazal et al 1985)	10.29 - 12.29 (Chazal et al 1985)
			54 - 207 (Pintar et al 1992)	8.5 - 33.3 (Pintar et al 1992)			1.6 - 8 (Pintar et al 1992)	31 - 35.6 (Pintar et al 1992)

Similar to the intervertebral disc the mechanical properties of the spinal ligaments may be affected by age, gender, body weight, physical fitness, gender influences, and many other factors like the preparation of a specimen for a study. At maturation the number of crosslinks and cross sectional area of the collagen fibers is greatest. As the human body ages, the collagen content and crosslink quality decreases [53]. Injury or age degeneration in the spinal ligaments lead to spinal instability and may alter the overall biomechanics of the spine. This may open up the possibility of other problems such as disc degeneration and facet arthritis. In an age related study by Neumann et al. the ALL was found to fail at midsubstance in the younger population and at the bone insertion site in the older population [71]. In addition, the ultimate tensile strength of these ALLs significantly decreased as age increased. The spinal ligaments are also subject to injury when the spine is bent too extreme or too fast. This often times leads to joint instability and a decrease in strength and stiffness of the injured ligament as well as altered joint kinematics. Due to the low blood and nutrient supply to the ligaments it may take 12+ months to fully heal in some situations [53].

It has been shown that the longitudinal ligaments degenerate with age [40, 52, 66, 71, 72]. Tkaczuk [52] did an extensive study of the tensile characteristics of the longitudinal ligaments of the lumbar spine with the purpose of examining the influence of degeneration and age on biomechanical properties. **All biomechanical parameters of the spinal ligaments were found to decrease with age.** Panjabi et al. [39] found that the neutral zones were larger in degenerated spines. This could be

due to ligament degeneration and the decreased ability for the ligaments to limit spinal motion and provide spinal stability.

2.4 Spinal Ligament Test Methods:

Many researchers have performed studies on isolated human spinal ligaments to better determine their geometric and mechanical properties, however, their methods have varied greatly.

In a classic study, Nachemson and Evans [40] tested the LF of 10 spinal segments in an Instron material test system using an optical extensometer to measure displacement. Each specimen was dissected from the vertebral bodies keeping the ligament to bone attachment intact. Holes were drilled in the vertebral laminae and steel wires were passed through and attached to the cross head of the Instron. This study was one of the first to show nonlinear tensile behavior in a spinal ligament as well as an overall decrease in mechanical properties as age increased.

In Tkaczuk's study of the longitudinal ligaments [52], they dissected the entire ligament from the spinal column with the aid of a dissection microscope under 15x magnification. The ligaments were then cut into sections corresponding to the different spinal levels and were clamped in clamps that close using a butterfly screw on the side. The analysis of the load deformation data did not show any slippage and when loaded to rupture, the failure occurred in the free space between the edges of the clamps.

In a widely referenced study by Panjabi and colleagues in 1982 [39], the physiologic strains of the lumbar ligaments in-situ were looked at using optical

measurement techniques. The procedure included getting the 3D flexibility data of fully intact FSUs, tracking the spatial coordinates of the ligament attachment points, and then using a mathematical model to combine the stiffness and spatial data to compute ligament length changes and strains as functions of various spinal movements. In the study, three L3-L4 human FSUs and nine L4-L5 human FSUs (age 23-88) were loaded with a pure moment of ± 15 Nm. Many of the graphs that were presented in this study are of ligament strain (y-axis) vs. angle of rotation (x-axis). Length change of the various ligaments vs. applied moment and subsequent FSU rotation were also presented. **They found that the ALL showed the most strain during extension.**

Pintar and colleagues in 1992 [50] used the raw data from Myklebust's study in 1988 [73] to calculate additional mechanical properties (stiffness, energy to failure, stress and strain at failure) of 132 ligament samples from 41 fresh frozen male human cadavers. Geometric measurements of length and area were determined using cryomicrotomy techniques with an additional 8 cadavers (age 31-80) being used by Pintar. They defined ligament length as being from the mid-height of the inferior vertebral body to the mid-height of the superior vertebral body. The cross sectional area was obtained from axial anatomic images. Myklebust and associates tested the ligaments in-situ by sectioning all elements except the one under study. They fixed the vertebrae above and below the ligament in a M.T.S. (Minneapolis, MN) electrohydraulic test system frame with Steinman pins. With the exception of the SSL, a minimum of 3 specimens was tested for each ligament at each spinal segment

level from C2 to S1. The ligaments were aligned to be pulled in direct axial tension at a rate of 1 cm/sec. A slide potentiometer was fastened to the two adjacent vertebral bodies to measure displacement. The ALL failed at the highest average force of 676 N with the PLL failing at an average of 160 N. They found that the deflection at failure tended to increase with distance from the vertebral center of rotation and that there was a general increase in strength moving from cervical to lumbar levels due to increase cross-sectional areas.

Dumas et al. in 1987 [74] attempted to calculate the in-situ mechanical behavior of the posterior spinal ligament using 25 FSU's from 14 human cadaveric lumbar spines aging from 57 to 79 years. A conventional tensile testing machine (JJ Lyod, Model T22k) outfitted with load and elongation sensors was used. The vertebrae were potted in cups using bone cement with the tension axis located in at the mid-length of the spinous process. After potting, the disc and longitudinal ligament were excised leaving only the posterior ligament complex (LF, CL, ISL, SSL) intact. The specimen was tested in tension at a rate of 8mm/min and then the ligaments were progressively dissected in an anterior to posterior order with repeated testing between each cut. Rigidities were obtained for the LF, CL, ISL, and SLL by the difference between the corresponding curves. This type of method does not produce raw data for a single ligament instead it relies on calculating a difference in varying the ligament complex. They concluded that the rigidity of the ligaments tends to decrease with distance from nucleus center and that the linear zone of all posterior ligaments may start at the same angle of flexion.

Chazal et al. [44] in 1985 tested 43 spinal ligaments from various levels and types from 18 fresh human cadavers (age 30-80) using an original testing machine. The elongation of the ligament was measured using a comparator with an accuracy of 0.01 mm. The load values were obtained from electrical strain gauges and extensometer bridge system. After dissecting all soft tissues other than the ligament being tested, the vertebral bodies were fixed to the testing machine with clamps attached to universal joints. The cross-section of each ligament was measured with a palpator, resulting in a tracing on graph paper. The length was measured at rest with a micrometer between vertebral endplates. The tensile test was performed at a rate of 1 mm/min. Failure mostly occurred in the mid-substance of the ligament and not at its bony attachment. They found that all ligaments produced a sigmoidal shaped load-deformation curve and that the ligaments exhibited a hysteresis thus demonstrating their viscoelastic properties.

In 1992, Neumann et al. [49] developed a new ligament testing technique using a motion capturing system and a materials testing machine to investigate the regional differences in tensile properties of the ALL. Specimens were prepared by excising the intervertebral disc and all posterior elements before clamping the vertebral bodies into the testing apparatus using Steinmann pins. Measurements of the ligament thickness and width over the disc space were obtained using dial calipers. The bone-ALL-bone preparations were distracted to failure at a displacement rate of 2.5 mm/sec. Twelve plastic beads were sewn into the ligament using a 5-0 nylon suture to create a grid so that strain could be assessed at multiple

sites along the ligament. The location of the 12 plastic beads was monitored using a noninterlaced, 60 Hz CCD camera (NEC TI-23A, Tokyo, Japan). The grid allowed displacement measurements along the length of the ligament at the midsubstance of and at both bony insertion sites. Using only three fresh cadaveric specimens (age 21, 29, and 43), which produced six specimens, resulted in relatively high mechanical properties. The average failure load was 1060 N and the stiffness in the elastic zone ranged from 464-1367 MPa.

2.5 Spinal Segment Test Methods:

Many researchers have attempted to perform mechanical tests and evaluations of the lumbar spine with the use of Functional Spine Units (FSUs) [28, 39, 75]. Since the FSU is a 3D structure, one vertebra is allowed to move with respect to the other in any direction in space (six degrees of freedom = three translations and three rotations) under the application of a given force or moment (Figure 12). Typically in biomechanical studies, right handed coordinate systems are set up to be aligned with the body's anatomical planes. This allows the physiologically relevant rotations and translations of the vertebral bodies to be evaluated.

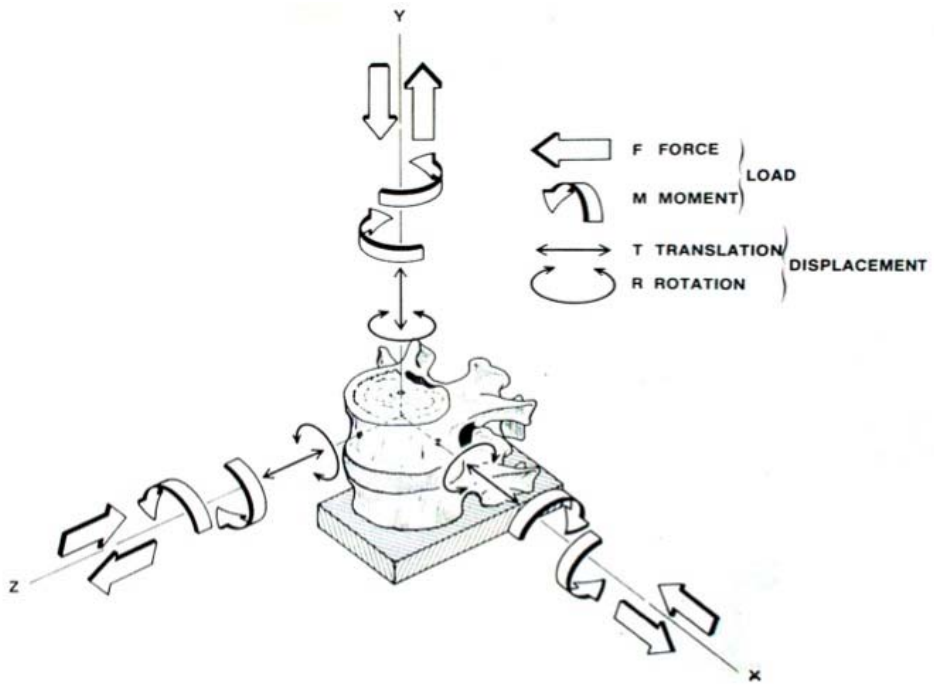

Figure 12. A Functional Spinal Unit (FSU) consists of two vertebral bodies, their accompanying intervertebral disc, and the intact spinal ligaments at that level. With one vertebrae fixed, the other vertebrae is allowed to move in 6 degrees of freedom when subjected to a load or moment. (White, A. and M. Panjabi, Clinical Biomechanics of the Spine 2nd Edition. ed. 2 ed. 1990, Philadelphia: J.B. Lippincott Company)

Because only two vertebral bodies are involved, the effects of induced injury or stabilization on adjacent spinal segment levels cannot be studied in an FSU model. Use of multilevel spine units is necessary for a more comprehensive and realistic investigation. Testing of multilevel spine units is not only fundamental to the understanding of the biomechanical properties (rigidity, range of motion, etc.) of intact spines, but also to that of fused or stabilized spines [76]. Over the years, investigators have developed a variety of multilevel spine unit testing protocols and loading conditions, but presently there is not a definitive standard. In 1998, Wilke [77] reported recommended loading methods, specimen conditions, and analysis parameters resulting from a series of workshops with spine experts. Although these

combined loading regimes may be more realistic, they have not yet been standardized.

The way multilevel spine segments are tested is one of the most debated and controversial issues facing the research community [78]. Some tests apply a known displacement at a free end of the spine and then quantify the resulting loads and motions across the various spinal segments (displacement control or stiffness protocol). Other methods measure the motion as a result of a known applied load (load control or flexibility protocol). Since the motion of the spinal segment typically changes dramatically with different treatment simulations (decompression, fusion, arthroplasty, etc.), applying pure moments before and after treatment is becoming the common consensus among investigators [21, 79]. The axial compressive forces used by investigators in testing the lumbar spine typically range from 400 -1000 N. The applied moments typically range from 6 to 10 Nm in the lumbar region and may be applied in a quasistatic manner with three load-unload cycles. The data from the third cycle is then recorded.

Goel [21, 75, 80-82] and coworkers used fresh frozen ligamentous human cadaveric lumbar spine segments with varying numbers of levels for the evaluation of the spine's mechanical properties and effect of various spinal treatments. The sacrum of the specimens was potted in a rigid base while the superior most vertebra was likewise secured to a loading frame with six degrees of freedom. To capture the kinematics of the vertebral bodies, a set of 3 light-emitting diodes (LEDs) were attached to each vertebra as well as the base and anatomic coordinate systems were

established. An Optotrak motion capture system (Northern Digital Inc., Waterloo, Ontario, Canada) was used to track the spatial coordinates of each rigidly attached active LED marker during the loading sequences. Pure moments that produced the anatomic motions (flexion/extension, right/left lateral bending, right/left axial rotation) were applied to the specimen via a system of weights, cables, and pulleys attached to the loading frame. For each loading modality, the specimen was loaded in steps typically to a maximum of ± 9 or ±10 Nm. For some of Goel's studies, the use of a 400 N compressive follower load was employed during flexion/extension only. The spatial data from the LEDs was then used to determine the load displacement curves and range of motion (ROM) for each spinal segment level. This procedure was performed once with the specimen intact and then repeated after the application of spinal instrumentation or a surgical procedure. In addition, Goel et al. often compares the results of their in-vitro cadaveric testing to their validated finite element models. They refer to this compilation of methods as the hybrid testing protocol. This method is, perhaps, the most widely accepted in the industry.

Similar to Goel's hybrid testing protocol, Panjabi and associates have developed a hybrid testing protocol as well [20, 83, 84]. Fresh human cadaveric lumbar spines were prepared for testing by potting the T12 and S1 in quick setting epoxy mounts with the L3-L4 disc oriented horizontally. Follower load rods were attached on the lateral sides of the vertebral bodies so that the cables used to apply the compression passed through the assumed center of rotation of each FSU. Motion capturing LEDs were rigidly attached to the vertebrae and epoxy mounts using

Plexiglas plates. A custom built test machine was then used to apply a continuous pure moment around each of the 3 traditional anatomic axes, without constraining the remaining five degrees of freedom. This was achieved by using three linear bearings and 3 circular bearings located at the base of each specimen. A single pneumatic torque motor attached to the upper mount was used to apply the pure moments. When the pneumatic motor was positioned to apply a pure moment around the flexion/extension axis, this degree of freedom was constrained at the lower end so that the moment could be transferred through the specimen. The 3D motion of each vertebrae was captured using an Optotrak motion capturing system. A maximum moment of ± 10 Nm was applied with and without a 400 N preload to ensure the preload did not apply any unwanted moments to the spine. Two preconditioning cycles were applied with data being taken from the third cycle. Range of motion was calculated for the overall spinal segment as well as at each intersegmental level at the maximum moment of 10 Nm. Panjabi's hybrid testing protocol is based on the idea that patients will attempt to move their spines the same ways after spinal surgery as they did before surgery. This hybrid testing protocol consists of four steps: 1) choose the lumbar spine specimen; 2) apply pure moments and measure the ranges of motion of the intact specimen; 3) apply pure moments that will allow the implanted spine to reach the intact overall range of motion; 4) compute and compare the differences in ranges of motion at each level.

Cheng et al. in 2007 [85], used 12 fresh frozen human cadaveric spines (L1-L5) to evaluate the effect of a posterior dynamic stabilization device on the spinal

kinematics. They used a 6-axis spine testing machine with three rotary motors mounted to two sets of guide rails on the superior aspect of the spine tester. The inferior base of the spine tester used to secure the inferior vertebrae, included a ball spine that allowed vertical translations. The rotary motors allowed application of loads in the three common anatomical planes. The specimens were aligned in the simulator and a ± 6 Nm moment was applied at 1°/sec with no follower load. The relative intervertebral motions were recorded using an Optotrak 3020 measurement system and LED markers rigidly attached to each vertebra. The motions of the superior vertebra with respect to the inferior vertebra were quantified using Euler angle transformations calculated using the included Optotrak software.

Patwardhan et al. in 2003 [86], tested the effect of a compressive preload on the stability of an anterior lumbar interbody fusion construct. Fourteen human L1 to S1 cadaveric spine segments were anchored in cups using bone cement and pins. The sacrum of the spine was fixed to the testing apparatus and the superior end of the spine was free to move in any plane. The specimens were tested intact and after insertion of two cylindrical cages at the L5-S1 motion segment. A moment was then applied by pouring water into bags attached to loading arms hanging from the L1 potted cup. The apparatus allowed the spine to be cycled back and forth in flexion and extension between maximum moments or 8 Nm and 6 Nm respectively. The motion of the L5 vertebrae was measured using Optotrak and biaxial angle sensors were attached to each of the other vertebrae. A multi axis load cell was attached to the fixed base to measure the reaction loads and moments. Several different

increasing compressive preloads of ≤ 1200 N were applied along a path that followed the lordotic curve of the spine. In this particular study they found that the effectiveness of the cages in decreasing range of motion at the fused level was significantly improved following greater compressive preload.

Similarly, Gardner-Morse and Stokes [87] noted the influence of preload on motion and flexibility parameters of the lumbar spine. They varied preload on motion segments from zero to 500 N. They found that physiological axial compressive preload can increase stiffness by a factor of two or more and may reduce the amount of load-displacement nonlinearity.

As mentioned previously in the text, Gillespe and Dickey [70] have developed a displacement controlled parallel linkage testing machine or robot that controls all six degrees of freedom. They have done this so that they can repeat the exact kinematics for an FSU between each testing condition. The robotic manipulator used six legs composed of linear stepper motors that control the motion. A six degree of freedom load cell was attached to the base of the spine fixture to measure the induced loads. The robotic manipulator was designed to work within a pure moment testing machine so that a pure moment could first be applied and the robot could "learn" the unconstrained in vitro motion profile of the spine. The robot was then removed from the pure moment testing apparatus and the motion path could then be replayed for all subsequent testing configurations.

Wilke and associates [88, 89] have built a custom spine tester that consists of a base mount that is allowed to move horizontally in two directions. The upper mount is attached to a specially designed gimbal joint. The gimbal allows rotation around all three axes and can move vertically. This configuration allows the spine to move in all six degrees of freedom. Each degree of freedom can be constrained individually or in combination. All displacements are applied using stepper motors and a pneumatic system. Pure moments in flexion/extension, right/left bending, and axial rotation are applied via integrated motors in the gimbal. A six degree of freedom load cell measures the induced loads and moments. Their system even allows muscle forces to be introduced by using cables attached with screws to the insertions points. This test machine was employed in a study to evaluate the effect of various interspinous spacers on flexibility and intradiscal pressure [89]. Twenty-four fresh frozen FSUs were used and a ± 7.5 Nm pure moment was applied with no preload in all three directions of rotation at a rate of 0.5°/sec. Range of motion at the maximum applied moments was determined in the third cycle of rotation for each trial.

Other researchers have resorted to much simpler methods of testing using widely available standard material testing equipment. Rousseau et al. [90] simply used a servo-hydraulic apparatus (Bionix 858, MTS Systems, Eden Meadow, MN) with a linear actuator and a 40° wedge to simulate a compressive load and an anterior shear load. An L5-S1 FSU was mounted in the testing apparatus and the motions of the vertebrae were captured along with other measurement transducers. Glazer and

coworkers [91] harvested 12 lumbar spines from fresh human female cadavers (age range 42-69). L1-L5 was mounted in an aluminum jig for nondestructive testing in axial compression, torsion, flexion/extension and lateral bending using a biaxial material testing machine.

2.6 Effect of Spinal Elements on Segmental Biomechanics:

The kinematic behavior of the spinal motion segment(s) is highly related to ligament function. Many researchers have attempted to assess the effect of individual contributions of the soft tissue components on the overall biomechanical response of certain regions of the spine. Much of this research has been done with the use of FEA models because of the ability to vary one parameter, such as ligament stiffness, while holding all other parameters constant. This allows the researcher to study the effect of this one parameter on the biomechanics of the spinal segment being tested. The in vitro cadaveric studies that have been performed to determine individual soft tissue contribution usually involve stepwise reduction of a series of spinal components followed by repeated testing. The major limitation to these types of studies is that once a ligament has been cut it cannot be reattached to measure another ligament's influence with all other ligaments intact.

Little is known about the effect of changing a parameter of a single ligament while keeping all other spinal components intact. In 2007, Heuer et al. [92], used eight human cadaveric L4-L5 FSUs (median age 52) to quantify the function of anatomical components for different loading magnitudes. Pure moments from 1 to 10 Nm were applied in all three anatomical planes at a loading rate of 1°/sec in a custom

built spine tester based on Wilke et al.'s spine tester. The specimens were tested intact and then tested again between the dissection of the spinal components in the following order: SSL, ISL, LF, CL, vertebral arches, PLL, ALL, NP. The range of motion (°), neutral zone (°), and change in lordosis angle at unloaded posture were calculated for each condition. They found that transection of the posterior ligaments increased flexion ROM and that the ALL slightly contributed to the resistance of axial rotation, but strongly resisted extension. One limitation is that the results presented are only valid in the specific order of stepwise reduction performed. If a different order would have been followed the FSU may have behaved differently. The author suggests that the results of this study could be useful in FEA model calibration.

Zander et al. [93, 94] used a nonlinear finite element model of the L3-L4 FSU to determine the influence of ligament stiffness on intersegmental rotation and forces in the ligaments. The lowest "soft" and highest "stiff" values for ligament stiffness found in the literature were used in two separate sets of calculations. Their review of the literature also resulted in a wide range of ligament stiffness values. The FE model was loaded with pure moments of 7.5 Nm and 15 Nm in the three anatomical planes. Forces and strains in the ligaments and intersegmental rotation were calculated for each condition. Their results showed that the ALL was the only ligament that was loaded during extension and was completely unloaded during flexion. The ALL also showed a small loading in lateral bending and torsion, but only when the model was in the "stiff" ligament configuration. The intersegmental rotation was strongly

influenced by the stiffness in the ligaments, especially during extension. With a bending moment of 7.5 Nm the "soft" and "stiff" ligament model allowed 5.1° and 1.5° of rotation in extension, respectively. With a 15 Nm the difference in the "soft" and "stiff" ligament model was even more pronounced at 8.5° and 2.4°, respectively. They concluded that due to the wide variation of ligament stiffness data found in the literature, quantitative results of finite element studies involving the spine are not completely reliable and should be validated using experimental data.

Another ligament stepwise reduction study by Adams et al. [95] characterizes the resistance of flexion by the posterior elements of 27 human cadaveric lumbar FSUs. The FSUs were tested intact first and then repeated after cutting the ISL/SSL complex, then cutting the LF, and then finally cutting the CL. They found that the LF plays a small roll in full flexion but contributes to a large amount of the initial segment stiffness in flexion. In full flexion, the CL provides approximately 39% of the joint resistance, while the IVD provides approximately 29%. Gillespie et al. [70] performed a similar study using porcine FSUs and their parallel linkage robot spine tester. They found similar results in terms of contributions of posterior elements in resisting joint motion.

As an alternative to the experimental methods of stepwise reduction of spinal components, Lee et al. [96] conducted a FE material sensitivity study on the L2-L3 motion segment under sagittal plane loading. They used a probabilistic method to account for the biologic variation. The probabilistic method provided a sensitivity plot for output parameters to determine which spinal components are most important.

A 400 N preload was applied and a 15 Nm flexion/extension moment was applied incrementally in five steps. The model was validated against experimental results with and without posterior elements. When the posterior elements were not intact, the results of the FE model deviated from the experimental results at high extension loadings. The relative importance of each input variable (material properties of bone, ligaments, and disc) on the response of the FE model was determined. The CL, NP, annulus poisson ratio, ALL, and NP poisson significantly influenced the extension angular rotation (elements listed in order of influence). Since the soft tissues primarily control the complex response during flexion/extension rotations, this study reinforces the need to accurately determine these material properties to better understand the biomechanical behavior of the human spine. The variations in material properties of hard tissues (cortical and cancellous bone) were found to have negligible influence on the predicted response.

Brolin et al. [97] also developed a FE model of the upper cervical spine in order to analyze the effect of ligament material properties on spinal kinematics. They stated that an injury that changes the mechanical response of the spinal ligaments will influence the structural behavior of the spine and could lead to further degeneration of the other spinal elements. In the study, the effect of variations in elastic stiffness, neutral zone, and pretension were studied. The changes from "average" were as follows: stiffness was increased by 50% from "average", the length of neutral zone (deformation at toe equivalent) was decreased by 45%, and pretension was increased by shifting the entire ligament load-deformation curve in the negative x direction by

15%. The model was then subjected to axial rotation, flexion/extension, and right/left bending. They found that a change in the neutral zone of the ligaments had a larger effect on spinal kinematics than a change in the elastic stiffness. One thing to note in this study is that they only applied 1.5 Nm so the ligaments most likely didn't even have a chance to get into their elastic stiffness zone. This is possibly why the results did not show a large effect from changing the elastic stiffness of the ligaments. All ligaments influence the kinematics to some extent. Even a small ligament injury that affects the material characteristics of one spinal ligament will change the overall structural behavior of the spine.

2.7 The Synthetic Analogue Spine Model vs. Other Types of Spine Models:

In order to better understand the reasons for developing a synthetic mechanical analogue of the lumbar spine, an overview of current spine model testing and their disadvantages and limitations will be of value. One of the most realistic and commonly accepted representations of the lumbar spine, or any spinal region, is that of in-vitro cadaveric samples. These segments, removed from sheep, cattle, and human donors, are used extensively to test and evaluate newly developed spinal fusion, arthroplasty, and surgical instrument devices. Despite the widespread use of these testing methods, there are many limitations that can be found in cadaveric specimen testing.

2.7.1 Biologic models:

There are severe limitations in the use of biological models in testing. A substantial amount of biomechanical testing has been performed on fresh frozen

human cadaveric spines. The mechanical properties of these specimen's soft and hard tissues change over time and with exposure to air. This alters the rigidity and kinematic response of the spine segment. Wilke et al. [98] quantified the effect of exposure and time after thaw to biomechanical response of the spine segment. They determined that the most critical factor that affects the response of the spine is the length of exposure. They found that within 2-3 days of testing and cooling, the specimens begin to change in terms of smell, color, and moisture level.

Many researchers wish to measure the in-situ loads, pressures, and strains of the various spinal components. It can be very difficult to introduce or fixate many of these transducers onto the biologic spinal components without disrupting the tissue or spinal segment response being targeted. The application of spine instrumentation such as fusion or arthroplasty devices and/or various transducers such as strain gauges can be very time consuming. There is a high risk of degenerative changes due to exposure time while implementing these items.

Several complex test methods requires staged preparation and testing which in turn requires multiple freeze/thaw cycles over multiple days of testing. Hongo et al. [27] found that the initial freezing of porcine spine specimens resulted decrease neutral zone range of motion and increased stiffness in the neutral zone in all directions of loading. Subsequent freezing up to two more freeze-thaw cycles did not seem to have an additional significant effect on the measured parameters. The soft tissues have also been show to be affected by the freezing. Freezing reduces the stress at which ligaments may fail for in-vitro testing due to the formation of ice

crystals [38]. Another factor that is often not accounted for in biomechanical testing of biologic spine models is the amount of time between expiration of donor and freezing. This uncontrolled and variable factor in human cadaveric specimens undoubtedly affects the mechanical properties.

One of the great things in life is that we are all different. This plays a large role when trying to use a human cadaveric model to investigate spinal properties or evaluating the effect of a change. Biologic models, especially human cadaveric, display a significant inherent interspecimen variability. This makes direct comparison of results between cadaveric models difficult. Investigators have found up to 500% variation in normal disc pressures between different human cadaveric specimens [26]. Variation in the size of the specimens and the quality of the bone stock and soft tissues can also be tremendous. These variations make statistical comparison of clinically relevant parameters as well as surgical and device variations difficult with a reasonable sample size.

The availability of quality cadaveric spines can be difficult since a majority of cadaveric specimens are from elderly donors and are often osteoporotic and have variable states of degeneration in the soft tissues. Also, many elderly specimens contain bone spurs, which can dramatically alter the natural biomechanics of the spine. This is unfortunate from a mechanical testing and comparative analysis viewpoint. In addition, the cost of human cadaveric specimens has increased dramatically over the last several years.

Many researchers have used non-human biological models for testing of spines. Wilke et al. [99] showed similar mechanical properties, such as range of motion and stiffness in certain segments, between human and calf FSUs. Kettler and associates [100] concluded that FSUs and polysegmental spines had qualitatively similar mechanical properties. Researchers have used the calf spine model in evaluating the effect of spinal instrumentation. Wilke et al. tested sheep spine segments and showed similarity to human cadaveric spines [101]. These animal models have severe restrictions in terms of size and angle of lordosis.

2.7.2 Computer Models:

Finite Element Analysis (FEA) models have been developed, but effects such as slight variation in surgical technique are difficult to model. In addition, validation of FEA models of the spine is very difficult because of the complex geometries and mechanical interactions of the spinal elements. Most geometries used in finite element modeling are obtained from CT or MRI images of the spinal column. Some of these imaging methods cannot distinguish between surrounding soft tissues and other bones. For these reasons, the results of FE studies are strongly case dependent and should be regarded as qualitative rather than quantitative data. As a result, many FE models are based on assumptions about the material properties and how the different components interact. For instance, Zander et al. [93, 94] assumed in their FE model that since friction in the facet joints is negligible, they were modeled to only transmit compressive forces. The ligaments, in turn, were only assumed to transmit tensile loads.

Detailed examination of the convergence and accuracy of the FEA spine models is very rarely undertaken; instead the models are validated by comparison with experimentally measured deflections. While this invariably shows that the overall characteristics of the model may be reasonable, it does not ensure convergence and accuracy of the stresses within the model. Indeed, because of the relatively coarse meshing in the great majority of current spine models, the absolute values of stress that they predict should be considered with great caution. Validation of any spinal finite element analysis model is essential but extremely difficult, due to the unavoidable and often significant physiological variation among individuals and specimens. Comparison with experimental data needs careful interpretation and analysis, because validation with the simplistic loading conditions invariably applied in a laboratory setting does not necessarily mean that the model will function correctly with all the complex loading regimes experienced in-vivo. Many of the investigations use models that are simplified and idealized because of the unparalleled complexity and uncertainty in the geometry, material properties, and boundary conditions of these problems [102].

As seen by the large variation in mechanical properties of spinal ligaments found in the current literature review, the material property inputs for the FEA spinal models is not clear cut. This results in the possibility for a wide range of results that can be obtained without transgressing the limits of literature values [93]. In fact, in Goel and Gilbertson's FEA model [46, 103], they state that if the material properties cannot be found from published experimental data then they can be, "assigned

arbitrary values such that the model responds realistically to a set of imposed loads and displacements (boundary conditions)." Essentially this mean the FEA spine model is "tuned" to behave a desired way. This poses a major limitation to using FEA models, because in unpredicted or combined modes of loading or displacement, the spine may not behave like an in-vivo spine. Also, this results in the stresses and strains found in the FEA models to not be clinically relevant values.

2.7.3 Other Synthetic Models:

Other synthetic spine models have been used in quasistatic testing but have mostly been in the form of testing jigs in material testing machines. None of the models to date provide correct spinal anatomy, rigidity, and kinematics. An ASTM Standard F1717 dictates that two polyethylene blocks with a space in between be used for the static and fatigue testing of spinal implant constructs in a full vertebrectomy model. This standard is thought to represent a worst-case scenario for testing of implants, but gives no information about the effect of the instrumentation on the spine and its components. Dick et al. [104] evaluated different brands of cross-link spinal instrumentation to determine which design characteristics were most desirable mechanically. The model he used was a pair of polyurethane foam vertebrae L3 and L4. A primary advantage of using the polyurethane vertebrae over human cadaveric vertebrae is that there is no specimen degradation or inter-specimen variability during testing. The testing model used by Dick et al. was similar to the commonly used ASTM Standard F1717, but has a more physiological alignment of the pedicle screws. Neither of these synthetic models have ligamentous

representation and again represent a worst case testing scenario without the capability of assessing the effect of the instrumentation on the biomechanical response of the spine itself.

Wilke et al. [105] has developed a mechanical model which attempts to improve upon the existing simplified standard of independent polyethylene blocks. One motion segment of the model consists of circular metal plates joined by a complex of silicone studs and accessory hardware including a ball-and-socket joint, which together all determine the segmental stiffness. This model was validated against an in-vitro human cadaveric spinal segment. The main limitation of this model, as stated in the manuscript is that, "…it does not represent the morphology of real anatomical structures." Due to the way this model operates and is constructed, it would be difficult if not impossible to evaluate the effect of spinal instrumentation or surgical procedures on the biomechanical properties of the spine. This model may, however, serve as a standard to accurately compare the differences in the various testing techniques used by researchers.

2.7.4 Mechanical Analogue Spine Model:

The mechanical analogue lumbar spine model would essentially be a melding together of both in-vitro human cadaveric spine testing and FEA methods. The analogue spine model takes the advantages of FEA and human cadaveric testing and mixes them together while simultaneously not succumbing to many of their disadvantages.

Use of a validated, anatomically correct mechanical analogue spine in spinal instrumentation testing would provide consistent, repeatable and comparable results while maintaining accuracy. Development and validation of the anatomically correct mechanical analogue spine for quasistatic loading would open the doors for researchers and manufacturers in examining a multitude of clinical questions and implant design issues. Surgical procedures such as laminectomy and discectomy can easily be performed on the analogue spine that incorporate the subtle but important nuances of variation in surgical technique (i.e., pedicle screw angle placement). An anatomically relevant and mechanically accurate analogue spine model could also help to investigate the role that specific spinal elements play on overall spinal biomechanics. Because of the ability to manufacture a physical spine in a consistent manner, one specific parameter can be evaluated while holding all other parameters constant.

2.8 Previous Soft Tissue Development in the KU Structural Biomaterials Lab

Much work has been done by Friis et al. on the development of the mechanical analogue spine model prior to this study [106]. This includes mechanical characterization and validation of the epoxy used by PRL to manufacture the vertebral bodies and development of the facet joint capsule and articular surfaces. Funding from the NIH SBIR Phase I proposal for the present study allowed for two graduate students to work on the development of the components for the mechanical analogue spine model. It was determined that one student would lead the development and characterization of the synthetic ligaments and one student would

lead the development and characterization of the synthetic intervertebral disc (IVD). Past and present synthetic ligament development details are discussed in more detail in Chapter 3 since ligament development and characterization are the primary focuses of this study.

The intervertebral discs used on the analogue spine model were made from molds created to mimic the shape of the individual disc for the specified level. The AF was composed of a F42 ShoreA polyurethane (PU) embedded with polyester fibers oriented at ± 30° to the horizontal plane. The NP was made up of significantly lower durometer of PU. Many different techniques were used to embed different volume fractions (VFs) of polyester fiber into various numbers of layers in the AF. Ultimately it was decided to place a single full wrap (like a tube sock) around the outside of each IVD. This allowed the polyester fibers of the wrap to be attached directly to the vertebrae 360° around the disc. By attaching the fibers directly to the vertebrae it allowed the AF to be pulled in tension on one side during bending as well as provide a more durable bond between each vertebra. The development of the intervertebral discs used in the analogue spine model was led by a fellow graduate student, therefore the details of this development will not be covered in this study.

Phase II funding from the NIH SBIR grant was secured while the work in this study was being performed and development of the analogue spine model will continue between Pacific Research Laboratories, Inc. and KU. Phase II funding allows for further development of a cancellous bone core and vertebral endplates of the analogue vertebrae. This will allow the vertebrae to better mimic the structure of

the human vertebrae and will allow for better interaction with spinal implant devices such as pedicle fixation, subsidence testing, and vertebroplasty. In addition to this, the development, implementation, and qualification of techniques to measure disc pressure and facet joint loads will be performed. An instrumented mechanical analogue spine model manufactured at PRL would serve as a valuable tool in evaluating adjacent level effects in the disc and facet joints due to spinal implants or surgical procedures.

2.9 Objectives of Study:

I. Demonstrate that non-linear mechanical properties of the spinal ligaments can be simulated with advanced composite synthetic ligaments. (Chapter 3)

II. Demonstrate that the mechanical properties of the synthetic ligaments can be controlled by changing the properties of the ALL. (Chapter 3)

III. Show that the "average" analogue spine model rigidity fits within the same order of magnitude of human cadaveric spinal rigidities. (Chapter 4)

IV. Quantify the effect of changing ALL stiffness on the overall stiffness of the T12-S1 synthetic lumbar analogue spine model. (Chapter 4)

V. Attempt a first run at implementing a spinal kinematic recording method in the University of Kansas Structural Biomaterials Lab and associate changes in ligament stiffness to the kinematics of the spine (ROM). (Chapter 4)

Chapter 3 – Synthetic Ligament Design, Control, and Repeatability

3.1 Synthetic Ligament Development:

In order to mimic the non-linear tensile properties of human lumbar spinal ligaments, several iterations of synthetic ligament designs were developed and tested. Prior designs of the synthetic lumbar ligaments used layers of fabric and wire mesh at a 45 degree bias at various pre-strains embedded in a silicone matrix to control the nonlinear load-deformation properties of the ligaments [106]. The mesh at a 45 degree bias was easy to deform initially until the individual wires came into alignment. As the wires aligned, more force was required to stretch the material, resulting in a higher secondary stiffness. These versions of ligaments were developed before the author was involved on the project. In order to allow for better control over mechanical properties in the ligaments a drastically different design for the synthetic ligaments was developed by the author and colleagues using polyester fibers and a linear elastic polyurethane (PU) matrix.

Polyester fibers were embedded in a linear elastic polyurethane (PU) matrix in various 3-dimensional wave patterns. The nonlinear load-deformation behavior was achievable by creating a depth-oriented sinusoidal wave pattern in the longitudinally aligned polyester fibers, thus mimicking the crimped and coiled collagen fibers in human spinal ligaments. The waved polyester fibers are easy to deform initially while the waves are straightening and as the fibers become straight, more force is required to stretch the composite; therefore the composite ligament exhibits a higher secondary stiffness. **Initial stiffness (NZ) is controlled primarily by the choice of**

matrix material while secondary stiffness (EZ) is primarily controlled by the volume fraction of fibers. Deformation at toe in the analogue ligament is controlled by the amplitude and frequency of the fiber waves.

A sine wave can be mapped by rotating a point on a circle while translating the entire circle along a line Figure 13. One cycle of a sine wave equals 2π radians and the distance along the path of one wavelength of a sine wave depends on the wave's amplitude, A, and thus equals 2πA. The thickness of the ligament being designed constrains the amplitude, the gauge length can be determined based on literature values and intervertebral disc heights, and the desired strain at toe was determined from literature values.

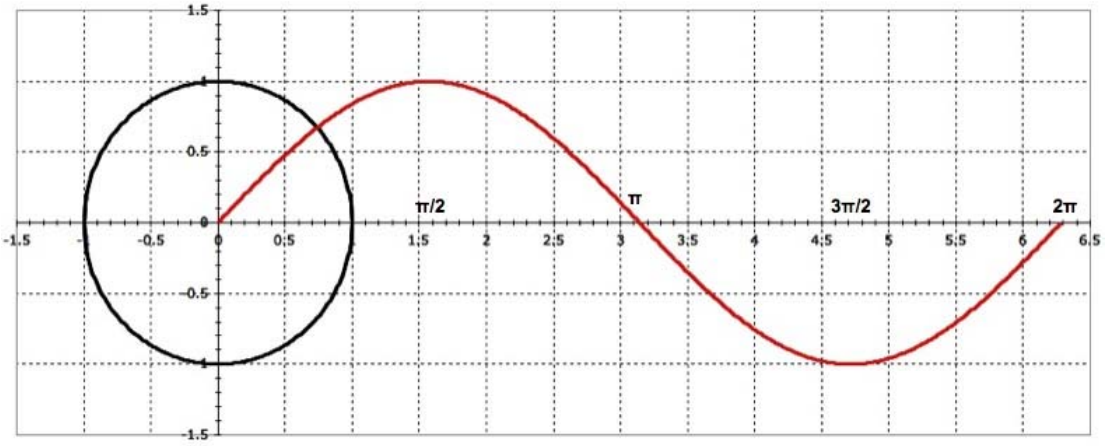

Figure 13. Mapping of a sinusoidal waveform

$$\varepsilon = \Delta l/l = (l_f - l_i) / l_i \qquad \text{Eqn. (1)}$$

$$l_f = 2*\pi*A*N = \varepsilon(l_i) + l_i \qquad \text{Eqn. (2)}$$

Where:

ε = desired strain at full extension of matrix/fibers (strain at toe)

l_i = gauge length (initial ligament length)

l_f = final ligament length of matrix/fibers

A = Waveform Amplitude

N = # of cycles in gauge length

Using Equations 1 and 2 above, the dimensions for the ALL and PLL, and the desired strain at toes (strain at which the two linear stiffness lines intersect), two different waveform frequencies were determined for each ligament (Table 4). The amplitude for the ALL and PLL waveforms was chosen to be 90% of the thickness of each ligament. Polyethylene (PE) molds were made for each profile using the Computer Numerical Control (CNC) machine in The University of Kansas Mechanical Engineering Machine Shop.

Table 4. Synthetic ALL and PLL dimensions and polyester fiber waveform profiles tested in the KU Structural Biomaterials Lab prior to transfer of soft tissue technology to PRL.

Ligament	Thickness (mm)	Width (mm)	Gauge Length (mm)	Desired strain at toe	Amplitude (mm)	Frequency (cycles/cm)
ALL - Type 1	3.5	16	22.10	5-8%	1.575	1
ALL - Type 2	3.5	16	22.10	5-8%	1.575	1.5
PLL - Type 1	1.8	9	13.32	2-3%	0.81	2
PLL - Type 2	1.8	9	13.32	2-3%	0.81	2.5

Creation of the ligaments in the lab consisted of two stages. Stage 1 involved wetting out mesh or straight polyester fibers with PU and forming it into a waveform by clamping together the two-sided PE molds (Figure 14). Each waveform mold was

cut to the width of the desired ligament and tongue depressors were taped to the sides to help contain the liquid PU and allow for a more uniform distribution of fibers throughout the matrix. The PU must be allowed to cure for 12-24 hours before removing from the waveform molds. Dry portions of the mesh or fibers should stick out the ends of the mold in order to control fibers in the waveform mold and keep them aligned in the longitudinal direction while the PU cured. Stage 2 involved placing the formed fiber waves into a PE compression mold and filling with PU. Each PE compression mold has a thickness similar to the desired ligament thickness. This must be allowed to cure for an additional 24 hours before removing ligaments from molds.

Figure 14. Polyethylene waveform mold used in stage 1 of the synthetic ligament creation at KU

In order to be able to calculate volume fraction (Vf) of fibers in the composite ligament the cross section of a single grouping of fibers was estimated. To do this, several tows of fiber, 10 cm in length, were weighed on a scale with an accuracy of 0.01 grams. A tow of fiber is defined as a grouping of individual fibers (like a tiny rope) that is a result of the braiding or twisting process of the polyester rope. Tows of fiber were chosen to quantify the Vf of the fiber in the synthetic ligaments because of the ease in identifying the boundary between each tow of fiber. The material density found on the material data sheet, a sample length of fiber weighed, and the fiber's

weight (sample length) were all used to determine a single tow's cross-sectional area to be 0.27 mm^2. The following equation was used :

(material density)$^{-1}$ ***[mm^3/g]*** *x (weight of sample length of fiber* ***[g]*** */ sample length of fiber tow* ***[mm]****) = cross sectional area of a single tow of fiber* ***[mm^2]*** Eqn. (3)

A polyurethane matrix was chosen for its superior properties over silicone rubber in forming and adhering the synthetic soft tissues. Control over matrix quality was much higher when using polyurethane and there are many different durometers of polyurethane that allow for more control over the load-deformation properties of the ligament, more specifically the neutral zone stiffness of the ligament's tensile load-deformation curve.

3.2 Preliminary Materials and Methods:

Pacific Research Laboratories, Inc. (PRL) or Sawbones was chosen to collaborate on the development and manufacturing of the mechanical analogue spine model. A NIH SBIR grant was awarded to KU and PRL to further the development of the mechanical analogue spine model and its components. This relationship between KU and PRL was established from previous work done on the development of mechanical analogue femur bones. Before transferring the technology of the synthetic ligament construction techniques and ligament characteristics to PRL, preliminary ligament creation and tensile testing was performed using custom designed ligament clamping jigs. The tensile clamping jigs used were comprised of two plates with corrugations, 3.35 mm thick and 3.35 mm deep on the inner surface to hold the synthetic ligaments and try and prevent them from slipping out during testing (Figure 15). An aluminum alignment jig was used to help ensure that the ligament

was clamped longitudinally in the jigs. Representative ligaments, created in the KU Structural Biomaterials Lab using the two-stage molding process described above are shown in (Figure 16).

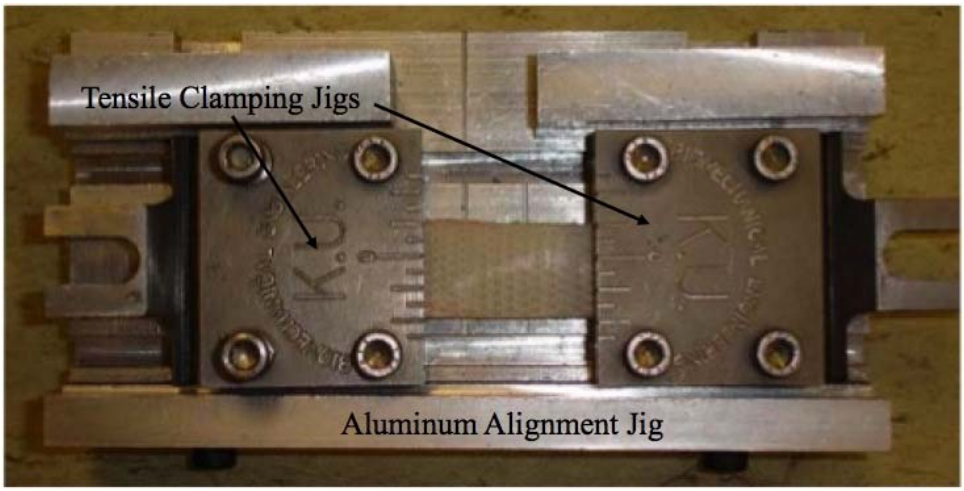

Figure 15. Top view of the corrugated tensile clamping jigs and the tensile ligament alignment jig. The corrugations are not visible in this image.

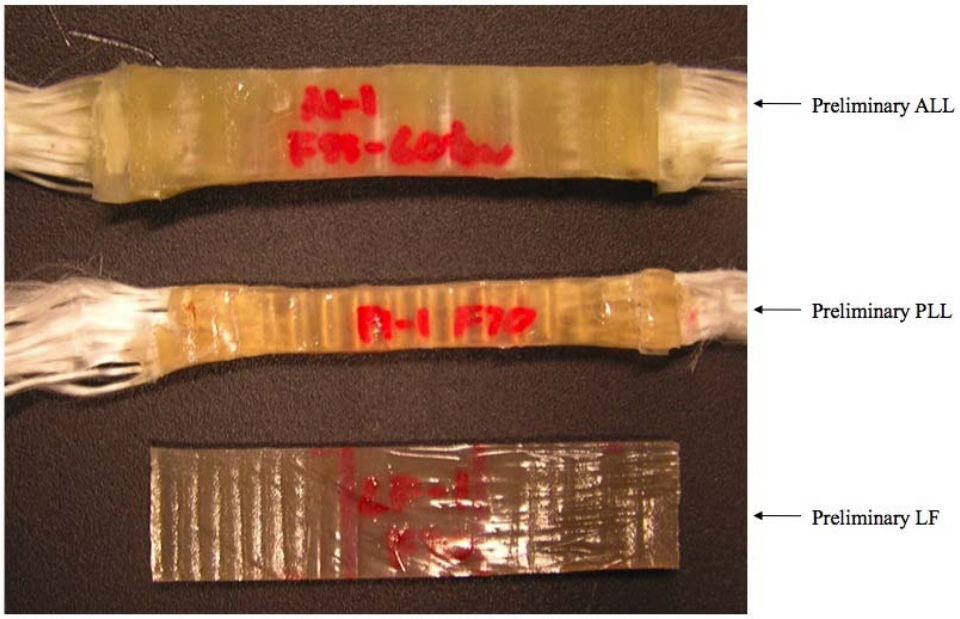

Figure 16. Example of ALL, PLL, and LF synthetic ligaments made in The University of Kansas Structural Biomaterials Lab.

Before testing each ligament section in tension, the thickness and width of the ligament was measured six times using digital calipers and the ligament cross-sectional area was calculated. Each specimen was then placed in the clamping jigs so that there was a 20 mm gauge length between the clamps. Within the clamps, sandpaper was wrapped around each ligament end to help prevent slipping. After zeroing the load cell, the clamps were placed into the MTS MiniBionix 858 machine using pins and the ball joint attachments. A preload of 4 or 5 N was applied, the displacement was zeroed, and then the ligament was stretched at a constant rate of 0.0423 mm/sec until failure. The load-displacement data was then normalized by converting it to stress-strain data using the gauge length and cross-sectional area. This allows for calculation and comparison of the neutral zone stiffness, elastic zone stiffness, and strain at toe. These parameters are defined in section 2.2.4.

For the ALL and PLL, the different waveform profiles listed in Table 1 were tested along with varying the number of tows of fiber (or Vf) and varying the durometer of the PU matrix material. Shore A F55 and F70 polyurethanes from BJB Enterprises, Inc. (Tustin, CA) were used and a range of 10 to 60 polyester tows were evaluated for the different waveform profiles. Due to the relatively lower stiffness of the LF found in the literature review, pure PU was tested to determine the best material to represent this ligament.

3.2.1 Problems With Testing:

The corrugated jigs that were being used for testing presented some problems. First of all, the stress-strain curves for the composite ligaments were not showing

very distinct nonlinear properties. Secondly, the stiffness was relatively low compared to what was expected. One tow of fiber was tested to determine the material properties of the polyester used in the synthetic ligament fibers and it showed a higher stiffness than some of the ligaments with several tows of the same fiber. It was believed that the ligaments were either slipping or the corrugations/teeth in the clamps were so tight that the fibers were being cut, especially where the corrugation came together. Also, it appeared as though the fibers were not getting directly pulled on and instead were shearing out of the PU matrix. This could explain why the nonlinear behavior was not as pronounced and the elastic zone was not as stiff as expected.

A short term solution to these problems was to wrap the extra length of the ligament that extruded out the back of the clamps around a flat steel bar that was also clamped down using the same tightening bolts. This altered clamping method pulled on the fibers more because they were wrapped around the back of the clamping plate and the extra flat plate provided additional clamping surface area. Also, the corrugated plates were flipped so that the corrugations/teeth were in direct contact with each other instead of alternating. Using this method, the desired ligament properties were able to be determined and were transferred to PRL for them to develop a repeatable manufacturing technique.

In order to address the clamping problems with a more permanent solution, a new set of clamping jigs were developed that eliminated the corrugations/teeth, and instead, the gripping surface was comprised of a coarse knurled surface (Figure 17).

By removing teeth, stress concentrations on the ligaments that were cutting into the ligament were eliminated. The new flat grip clamping jigs had a feature for removable tightening nuts because the bolts in the previous jigs tightened directly into threads in the jig clamping faces and stripping was occurring. This may have also caused a loose grip on the specimens. The jigs were designed so that the extra length of the ligament being tested could extrude out the back and be snaked around additional clamping bars to help pull on the fibers more exclusively after the fiber waveform had straightened out. The back part of the clamping plate where the ligament extrudes out was curved to reduce the stress concentration on the ligament when it was wrapped around the back plate.

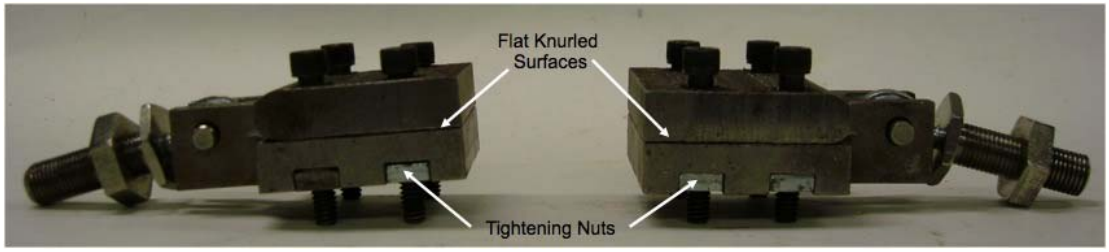

Figure 17. Newly developed tensile testing jigs with a flat knurled clamping surface and the ability to replace the tightening nut to prevent stripping of the jigs

3.2.2 Transfer of Ligament Technology to PRL:

Based on the preliminary testing, Table 5 shows ligament properties that were transferred to PRL in order for them to apply their expertise in manufacturing with these materials. The ligaments were made to run the entire length of the spine with the fiber waveform throughout.

Table 5. Initial ligament properties transferred to PRL

	ALL	PLL	ISL/SSL	LF	TL
Waveform Amplitude (mm)	1.575	0.81	1.575	N/A	N/A
Waveform Frequency (wavelength/cm)	1	2	1	N/A	N/A
# of tows	60	30	15	N/A	N/A
PU Type	F55 ShoreA	F70 ShoreA	F55 ShoreA	F70 ShoreA	F42 ShoreA
Width (mm)	16	9	7.5	20	No data
Thickness (mm)	3.5	1.8	3.4	3.4	No data

At first, the ISL/SSL ligament complex was approximated to use the same waveform profile as the ALL, only it would have a smaller cross sectional area and less tows of fiber. This was determined based on the mechanical properties seen in White and Panjabi [28] only. After testing a preliminary full segmented analogue spine model, it was determined that the posterior ligaments (ISL/SSL) were causing the spine to be too stiff in flexion.

Ultimately it was decided that the ISL/SSL complex, the TL, and the LF would be made purely out of F42 ShoreA polyurethane to reduce the stiffness of the spine model in flexion. This was also decided for simplicity in the model and because these ligaments do not have a large effect on the biomechanics of the spine in the normal range of motion compared to the ALL and PLL. Molds for the ISL/SSL complex and TLs were created that fit the specific anatomy of the spinous and transverse processes, respectively. These ligaments were created mainly for aesthetic appeal as input from Dr. Vijay Goel showed that these ligaments do not have a large biomechanical contribution to the spinal behavior, but needed to be present. The ligaments were attached to the various processes using cyanoacrylate (super-glue) and featured a fibrous pattern molded into the surface of the ligaments.

Controllability and Repeatability Study

3.3 Materials and Methods:

All preliminary ligaments prior to transferring the ligament technology to PRL, had been made with the waveform profiles along the entire length of the ligament and the dry fibers were only attached at the T12 and S1 vertebrae. Through collaboration with PRL, it was determined that this was not properly mimicking the way the ligament was loaded in the human body. It was decided that the ligament needed to be segmented so that the fiber waveform was only present over the disc space and the straight portion of fiber over the vertebral body needed to be somehow directly attached to the vertebrae. Unless the fiber was directly attached to the vertebrae, as it is in the human body [49, 107], the fiber was going to continue shearing out of the PU thus not providing the level of stiffness desired. After a few iterations, a manufacturing technique and molds for a dry fiber-wave-dry fiber segmented ligament was developed by PRL. This allowed the dry fiber sections of the ligament to be directly attached to each vertebra along the spine (Figure 18). This also led to a redesign of how the ligament specimens were being tested in tension. In order to better mimic the boundary conditions of the ligaments on the synthetic model a new ligament attachment and clamping method was developed.

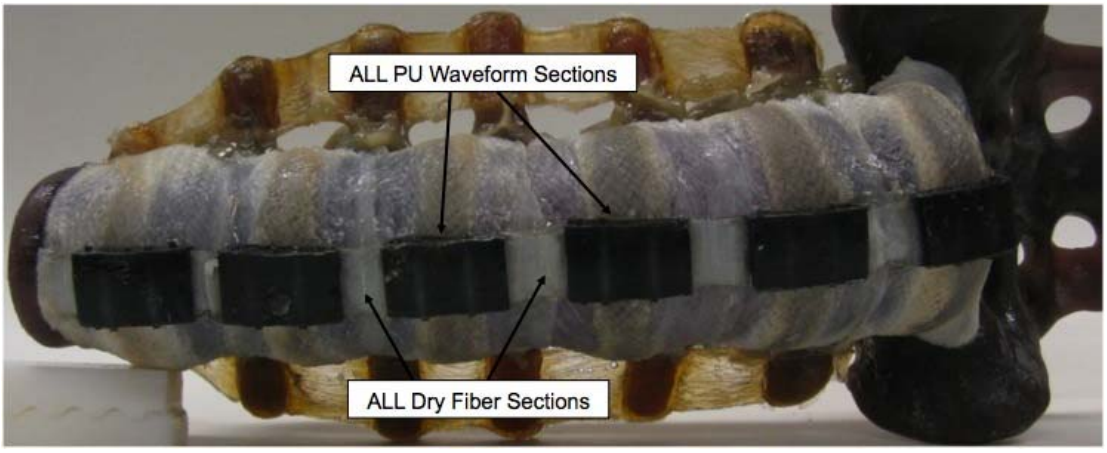

Figure 18. Segmented ALL with dry fiber-PU waveform-dry fiber sections attached to the synthetic analogue spine model. The dry fiber sections are attached to each vertebral body using quick dry epoxy.

3.3.1 Segmental Ligament Preparation

Epoxy bone slabs (the same epoxy used in the analogue vertebral bodies) were cut into identical sizes and shapes that allowed easy clamping in the newer knurled testing clamps. The analogue spine model disc-vertebrae-disc pattern was digitized to collect the correct spacing of the dry fiber sections for each full-length ligament. PRL sent each ligament as a full multi segmented ligament with a total of six PU wave sections. Three of these segments with dry polyester fibers on both sides were cut from each full ligament. Both dry fiber portions of the ligament segment were attached to the two bone slabs using a 5-minute quick dry epoxy glue (Figure 19). UHMWPE alignment forms were used to make sure that the ligament was being held straight on the bone slabs while the epoxy was curing and that the gauge length for each segment was constant. Small cut portions of wooden tongue depressors were used to compress the epoxy glue onto the dry fibers while curing. This best simulated the loading condition and how the ligaments would attach to the synthetic spine

model. The epoxy glue was allowed to dry overnight before measuring the thickness, width, and gauge length of each ligament segment using digital calipers.

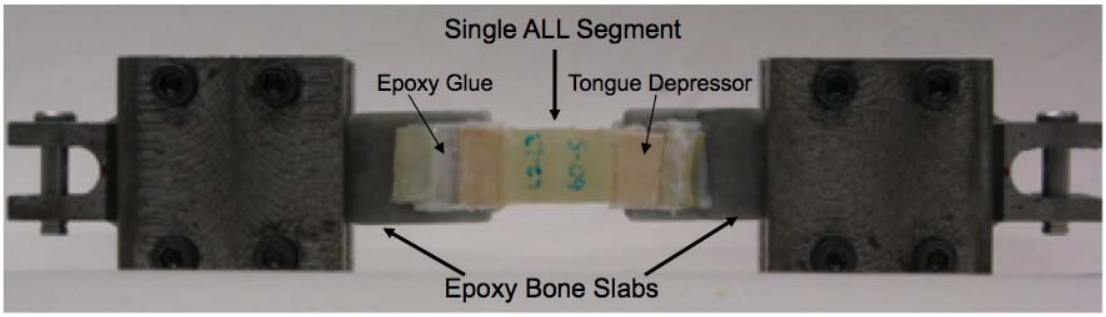

Figure 19. Segmented ligament attached to epoxy bone slabs with quick dry epoxy glue. The bone slabs are clamped in the flat testing grips and is ready to be mounted in the MTS for testing.

The epoxy bone slabs were then securely clamped in the new flat grip clamping jigs and attached to the servohydraulic test system (MTS MiniBionix 858, Minneapolis, MN) using pinned ball joints that allowed free rotation in all three directions. All synthetic ligaments attached to epoxy bone slabs were tested in tension to failure at a constant displacement rate of 0.0423 mm/sec in flat grip clamping jigs. The load-displacement data was then normalized by converting it to stress-strain data using the measured gauge length and cross-sectional area. This allows for calculation and comparison of the neutral zone stiffness, elastic zone stiffness, and deformation/strain at toe.

3.3.2 Fiber Type Differences (Single Tow):

Single tows of two different fiber types were tested in tension using the MTS MiniBionix 858 test system. Since the cross sectional area of a single tow was not known, force-displacement data was compared between the two types of fibers (Table 6). In order to make sure data could be compared, the same gauge length was used

for all specimens tested. Each toe of fiber was glued to the same epoxy bone slabs used for ligament testing using a 5-minute quick dry epoxy. Three specimens of each fiber type were tested to failure and the linear stiffness and failure load was averaged. Failure for each specimen occurred within the gauge length of the fiber and not at the epoxy glue interface. The fibers were also tested by a simple hand-pulling test in an attempt to break the fiber. The F2 fiber could be pulled apart with moderate effort while the F1 fiber was very difficult to break without hurting your fingers.

Table 6. Elastic modulus and failure load for a single tow of polyester fibers used in the synthetic ligament advanced composites

	Average Linear Stiffness (N/mm)	Failure Load (N)
F1 fiber (fiber from preliminary study w/ PE coating)	20.69	84.49
F2 fiber (newer fiber)	5.28	26.49

There was approximately a factor of 4 difference in the linear stiffness of the two fiber types with the F1 fiber being stiffer and thus failing at higher loads. There was also approximately a factor of 3.2 difference in the failure load between the two fiber types.

When examining the fibers under the digital stereoscopic microscope the F1 fibers appeared to have a larger diameter and a much smoother surface finish (like fishing wire). The F2 fiber appeared to have a smaller diameter and was crinkled in appearance (Figure 20). The reason for the F2 fiber being less stiff and less strong is

most likely due to the smaller diameter and bends which may act as small stress concentrations.

Figure 20. Stereoscopic microscope pictures used to examine the variations in polyester fibers used for the synthetic ligaments. F1 fiber on the left and F2 fiber on the right IN EACH PICTURE

3.3.3 Ligament Specimens Tested

In order to focus effort, the ALL was chosen to perform a controllability and repeatability study on. This ligament was chosen because of its easy accessibility on the anterior portion of the spinal column and its relatively high mechanical properties compared to the other spinal ligaments. The line of thought was that the findings from this study can easily be transferred to the PLL and any other synthetic ligament to be modeled. In order to study the controllability and repeatability, the type of polyester fiber (F1 or F2) and number of tows of fiber were varied in several different ligament segments. The volume fractions tested for the F1 fiber were as follows: 3.5% Vf (10 tows), 7% Vf (20 tows), 14% Vf (40 tows), and 21% Vf (60 tows). The volume fractions tested for the F2 fiber were 4.9% Vf (14 tows), 11.2% Vf (32 tows), and 21% Vf (60 tows). The PU matrix used was a ShoreA F42 durometer and was held constant. F42 PU was chosen because of its availability from its use in the other

surrounding spinal ligaments and intervertebral disc. Also, it was determined that the modulus of elasticity did not vary enough between other similar PU durometers to make a significant difference to the ligament's overall mechanical properties. The waveform profile was held constant due to the available molds at PRL and had an amplitude of approximately 1.5 mm and a frequency of approximately 1 wavelength/cm.

3.4 Results:

The anterior longitudinal ligaments have by far been the most tested synthetic ligament at KU. Below is a comparison of the initial (NZ) stiffness, secondary (EZ) stiffness, and deformation/strain at toe for ALL's with both F1 and F2 fiber types (Table 7). The types of ligament in Table 7's rows are ordered first by fiber type and second by Vf or number of tows of fiber. The F2 fiber ligament values are listed first due to the F2 fiber type being relatively lower in stiffness.

Table 7. Synthetic ALL tensile mechanical property results for controllability and repeatability study

INITIAL (NZ) STIFFNESS

# of Tows	Fiber Type	1st Region(MPa)	std(%)	1st Region(N/mm)	std(%)	(# of segments tested)
14	F2	5.35	5	13.02	11	n=18
32	F2	5.75	6	15.71	8	n=6
60	F2	6.68	8	18.56	6	n=6
10	F1	30.12	12	66.73	13	n=3
20	F1	32.22	14	74.36	20	n=3
40	F1	29.41	18	72.17	14	n=3
60	F1	34.31	10	77.96	7	n=3

SECONDARY (EZ) STIFFNESS

# of Tows	Fiber Type	2nd Region(MPa)	std(%)	2nd Region(N/mm)	std(%)	(# of segments tested)
14	F2	32.08	16	77.09	9	n=18
32	F2	57.10	15	154.66	7	n=6
60	F2	99.49	17	274.40	10	n=6
10	F1	92.95	11	205.53	10	n=3
20	F1	161.52	7	370.24	8	n=3
40	F1	246.84	15	606.13	11	n=3
60	F1	400.42	3	911.03	2	n=3

DEFORMATION/STRAIN AT TOE

# of Tows	Fiber Type	Strain at toe(ε)	std(%)	Disp. at toe(mm)	std(%)	(# of segments tested)
14	F2	0.0822	8	2.30	9	n=18
32	F2	0.1108	15	3.08	11	n=6
60	F2	0.1395	6	3.92	6	n=6
10	F1	0.0215	18	0.58	18	n=3
20	F1	0.0177	17	0.48	16	n=3
40	F1	0.0217	2	0.59	2	n=3
60	F1	0.0329	3	0.88	3	n=3

It is realized that using three specimens to calculate a standard deviation is not statistically legitimate and it should be noted that these values are given in Table 7 and Figures 21-25 purely for comparison purposes. The only specimens with n=3 are specimens with the F1 fiber type. There were less F1 fiber specimens because PRL ran into a supply chain issue with the manufacturer of the F1 fiber type. In order to ensure a limitless supply of fiber, the type of fiber being used in the ligaments was switched to the more abundant F2 fiber. This explains why only three specimens of each volume fraction were tested using the F1 fiber type.

Note that the standard deviations are smaller in the non-normalized (N/mm) secondary stiffness and are smaller in the normalized (MPa) initial stiffness region.

Also, the standard deviations in general are smaller for the F2 fiber ligaments (especially the initial stiffness). Figure 21 and Figure 22 show the average stiffness values analyzed from the non-normalized data and the normalized stress-strain data, respectively.

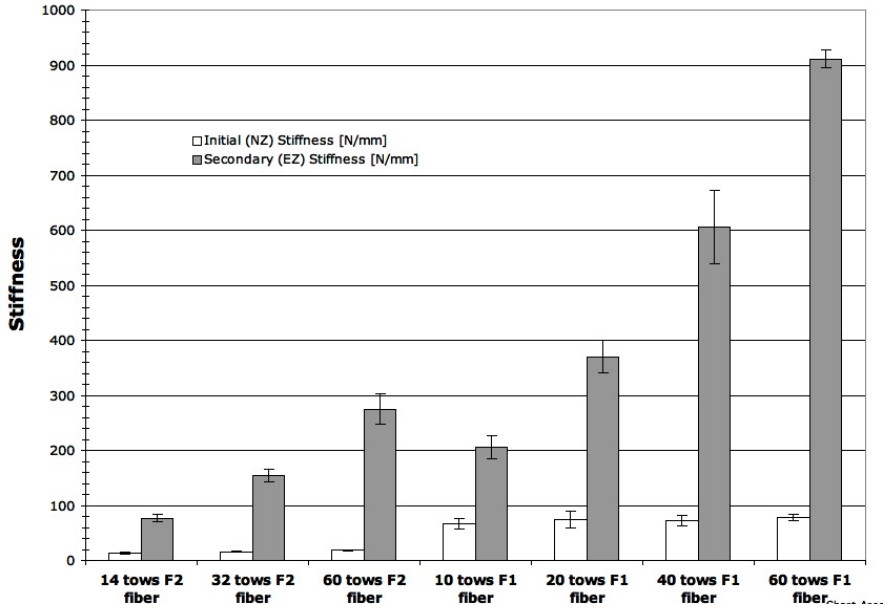

Figure 21. Non-normalized [N/mm] initial (NZ) stiffness and secondary (EZ) stiffness average values for anterior longitudinal ligaments analyzed.

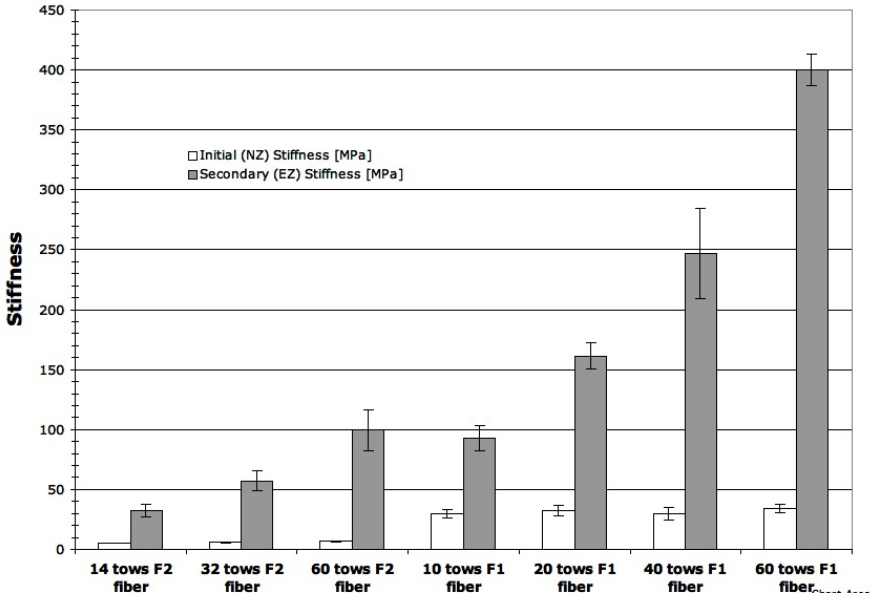

Figure 22. Normalized [MPa] initial (NZ) stiffness and secondary (EZ) stiffness average values for anterior longitudinal ligaments analyzed.

The deformation at toe and strain at toe can also be seen in Figure 23 and Figure 24, respectively. The error bars in all bar graph figures represent ± 1 standard deviation of the value presented.

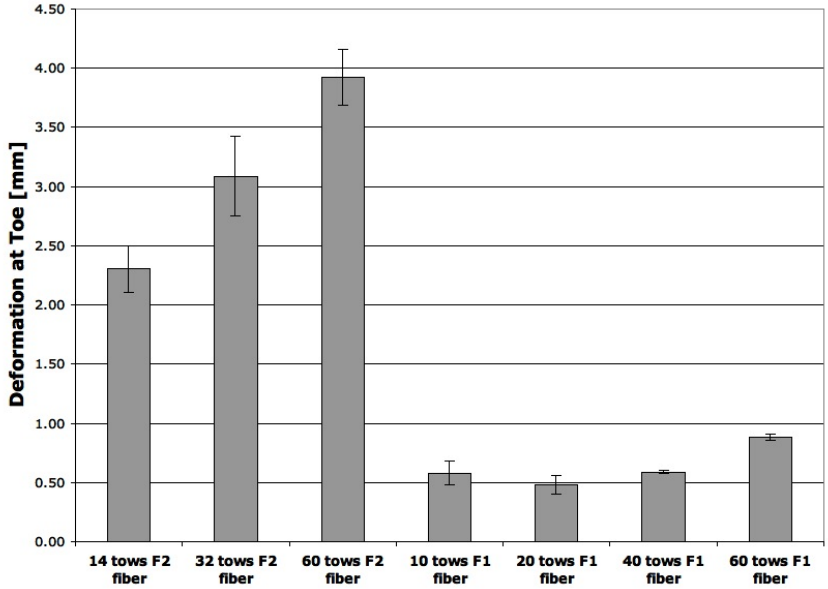

Figure 23. Deformation at toe [mm] average values for anterior longitudinal ligaments analyzed.

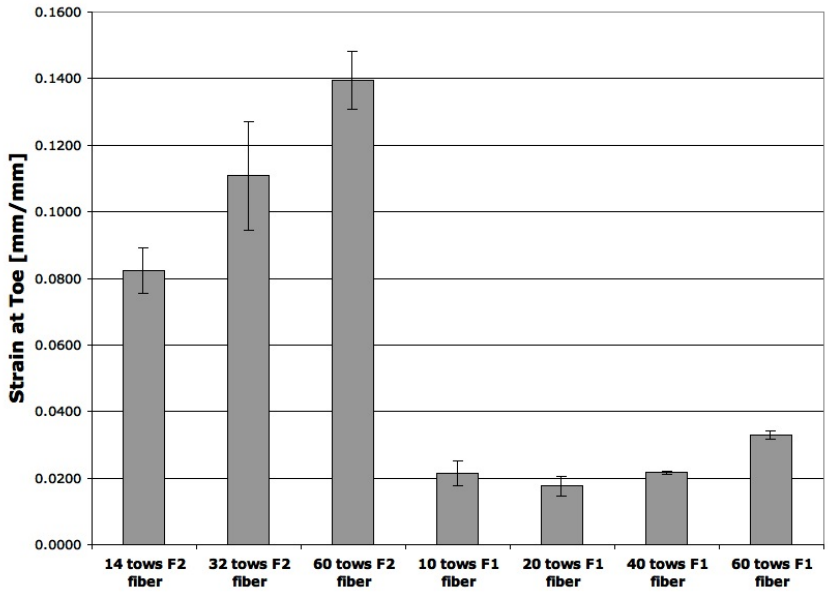

Figure 24. Strain at toe [mm/mm] average values for anterior longitudinal ligaments analyzed.

The secondary stiffness was the property that was focused on the most since it is primarily controlled by the number of tows present and is reported in the literature more than the initial stiffness. Also, the ligament's primary function of resisting extreme spinal motion occurs when the ligament is in its secondary stiffness zone. It was found that for each fiber type there is a linear relationship between the number of tows and the non-normalized (N/mm) secondary stiffness. This can be seen in Figure 25.

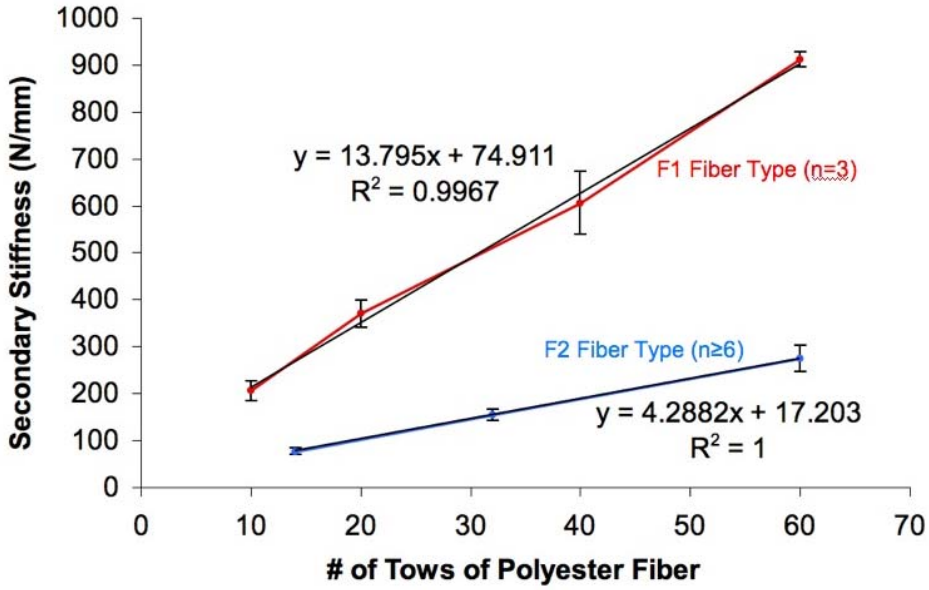

Figure 25. Number of Tows vs. Secondary Stiffness (N/mm). Both types of polyester fibers (F1 and F2) used in testing ALL segments are represented here.

These linear relationships can be used to estimate the non-normalized secondary stiffness value of a synthetic ALL by changing the number of tows. Once again, there was approximately a factor of 3.2 difference between the slope of the F2 fiber line and the slope of the F1 fiber line. This may be a coincidence but it matches up nicely with the single tow fiber tensile testing results.

3.5 Discussion:

The stiffness values for each ligament segment were analyzed two ways. The stiffness value for each ligament was recorded from both the normalized stress-strain curve [MPa] and the non-normalized load-displacement curve [N/mm]. There was a large standard deviation especially in the secondary stiffness region when looking only at the normalized stress-strain values. It was hypothesized that the large

deviation was due to the variation in cross section of each ligament segment. There seemed to be a trend that the cross sectional area increased inferiorly in the individual segments of the full ligament (mainly in the thickness dimension). To alleviate this issue, the secondary stiffness (EZ stiffness) of the non-normalized load-displacement curve was examined. Analyzing the load-displacement data was deemed acceptable considering many investigators present their ligament data this way in order to allow for a more direct comparison and to eliminate anatomical differences in ligament cross-section. This was possible due to all ligaments having the same initial gauge length because of the potting jigs used when epoxying the ligament segments to the bone slabs and it was assumed the same number of tows equally carried the load in all similar segment types. Since the fibers are primarily carrying the load in the secondary region, the cross sectional area of the matrix (PU) part of the ligament had a very small effect on stiffness. This was done for both the initial (NZ) and secondary stiffness (EZ) regions, but the initial region had smaller standard deviations when using the normalized (MPa) stiffness. This makes sense because in this region, both the fibers and PU matrix are sharing the load. As PRL's manufacturing techniques are standardized and perfected it is expected that the standard deviations in the non-normalized and normalized data will decrease and will become closer to the same.

Both the non-normalized deformation at toe [mm] and the normalized strain at toe [mm/mm] were determined as well. Since the initial gauge length was kept very

consistent, there was not a major difference in standard deviations or trends between the non-normalized and normalized values.

After testing the specimens with the F1 fiber type, large variations between specimens of the same type especially with the initial stiffness and deformation at toe were observed. This was evident by comparing the standard deviations of the F1 fiber ligaments to the F2 fiber ligaments. Keep in mind the number of F1 specimens tested was never greater than n=3 making proper standard deviations impossible to calculate. Never the less, the standard deviations were still calculated purely for comparison purposes between the two fiber types. It was speculated that it was possible that the fiber waveform was not being repeated consistently in each ligament segment while being molded. In order to address this problem, PRL developed a new nail-in-board peg manufacturing method to hold a more uniform waveform while the ligament was being vacuum-sealed in the rectangular PU matrix segment.

After improving the manufacturing technique, all non-normalized parameters of the different volume fractions of F2 fiber ALL segments had a standard deviation less than ±11%. In fact, only two of these parameters (as seen in Table 7) had a standard deviation greater than ±10%. The parameters that had standard deviations less than or equal to ±10% showed repeatability within the defined range of success for phase I of the SBIR grant between KU and PRL. This was a dramatic increase in repeatability over the F1 fiber ALL segments, which had standard deviations for the initial stiffness and deformation/strain at toe as large as ±20%. For this same group

of F2 fiber ligaments, the standard deviation for the initial stiffness decreased even more when looking at the normalized values. This is because the cross section of the ligament has a larger effect on the mechanical response of the initial stiffness region.

Controllability of the mechanical properties in the synthetic ligaments is clearly demonstrated in Figure 25. The secondary (EZ) stiffness increases linearly as the volume fraction (number of tows) of fibers increases in the synthetic ALL specimens. Interpolation of this graph allows an ALL to be designed with a specific EZ stiffness by simply choosing a fiber type and number of tows. An appropriate secondary stiffness value can be determined from the literature and a synthetic ligament can then be constructed to mimic a human spinal ligament's secondary stiffness. In Figure 21 and Figure 22, it can be seen that while the secondary (EZ) stiffness increases, the initial (NZ) stiffness remains relatively the same within each type of fiber (F1 or F2). This confirms that the initial stiffness is primarily controlled by the stiffness of the PU matrix and the fiber waveform profile. Since a ShoreA F42 PU matrix was used for all ligaments, the initial stiffness did not vary dramatically. However, the type of fiber used did have an effect on the initial stiffness. The initial stiffness was higher for the F1 fiber type but still did not vary greatly with a change in number of tows of fiber.

It was hypothesized that the fiber waveform profile primarily controls the deformation/strain at toe. For the F1 fiber type the deformation/strain at toe did not vary greatly with a change in number of tows of fiber. The strain at toe was expected to be in the same range since the sinusoidal wave amplitude and wavelength was the

same for each specimen. However, for the F2 fiber, the deformation/strain at toe tended to increase as the number of tows of fiber increased. This is difficult to explain and further investigation into the new method of constructing the waveform profile at PRL may be needed. It is worth noting that, despite this trend of increasing deformation/strain at toe, the new peg method of creating the waveform profile seemed to produce a better interspecimen repeatability (lower standard deviation) than the method used with the F1 fiber ligaments.

Ligaments with a low Vf failed by the fibers tearing at the end of the waveform just at the edge of the PU matrix or at the peak of the waveform in the middle of the segment (Figure 26A). These failure points may be due to crimping at the peaks of the waveform, which may have caused a weakening of in the fibers. Most of these failures occurred around 12-14 mm of extension, which is around 50% strain in the ligament segments being tested and is well within the physiologic strain experienced in-situ [28, 39]. The ligaments with high Vfs tended to not fail by the fibers tearing but from the epoxy glue on the bone slabs popping off due to shear stress (Figure 26B). The failure loads in literature were also compared to the current data from the synthetic ALLs. The ALL segments tested with the lowest Vfs failed around 400 N while it has been reported in the literature that the human ALL somewhere in a range of 330 N - 510 N [28, 49]. It is very likely that the synthetic ALLs will satisfy the failure loads reported in the literature and will remain intact under all physiological loads experienced in the lumbar spinal column.

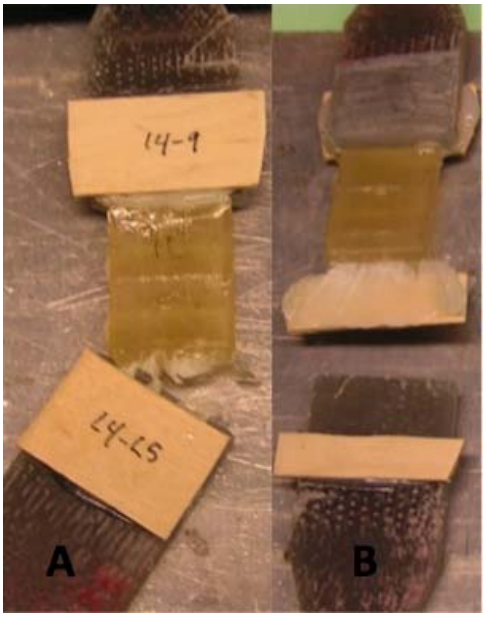

Figure 26. (A) Failure of the synthetic ALL segment by way of the fibers breaking. This usually occured in segments with a low Vf and the fibers typically broke at the epoxy glue interface or at a peak of the fiber waveform. (B) Failure of higher Vf ALL segments by way of the epoxy glue "popping" off of the epoxy bone slab.

One of the major difficulties in choosing the manufacturing properties (Vf of fiber, waveform profile, PU matrix) for the synthetic ligaments comes from the large variations in mechanical properties found in the literature for lumbar spinal ligaments. The data presented in White and Panjabi [28] is widely references as a target for ligament mechanical properties, but the methods used to obtain those values vary drastically from the methods used in this study and other ligament studies (i.e. Pintar 1992 [50], Chazal 1985 [44], Shirazi-Adl 1986 [51], and Goel [21]). White and Panjabi's in-situ method of testing ligament tensile characteristics may be the reason that their stiffness values are much higher. Because of this, the ligament can be made less stiff than the original values transferred to PRL. For this reason, 24 tows of the F2 fiber were chosen for use in the ALL. This should give the ALL an approximate secondary stiffness of 120 N/mm, which compares nicely to the secondary stiffness

values found using similar testing methods. Based on the values found in the literature for the PLL and comparing the ALL and PLL relative values in each study the PLL was chosen to have 14 tows of F2 fiber. This should produce a secondary stiffness of approximately 77 N/mm and is in line with the non-normalized values reported in the literature cited above. Even though there are fewer tows of fiber in the PLL, due to the smaller cross sectional area, the Vf of fiber is still higher than in the ALL, thus producing a higher normalized stiffness in the PLL. Using F2 fiber will be very convenient since the F2 fiber type is less stiff, easier to work with (not twisted in a rope), and more readily available for the long term.

A better comparison may be of the non-normalized results to the non-normalized stiffness values found in the literature because these values represent the mechanical loading characteristics across an individual motion segment. Many of the values for ligament mechanical properties are presented in non-normalized values and represent the mechanical response over one segment of the lumbar spine. Due to the segmented design of the ligament specimens, if mechanical properties of these ligament segments were designed to match the load-displacement literature data then there should be a good fit when implemented in the overall analogue spine model.

This control over soft tissue mechanical response allows for easy adjustment of soft tissue parameters in order to control the overall model response as needed in order to match the human cadaveric segment response. Figure 27 shows how simply changing the number of F2 fiber tows in the ligament alters the tensile mechanical response of the synthetic ALL. The control also gives greater flexibility to design

different types of synthetic spine models, such as scoliotic models and varying ages or laxities of spine models for future research. As stated earlier, the combination of the waved polyester fibers and the PU matrix allows for excellent control of the three desirable measures for tensile ligament characterization: Initial linear region stiffness, secondary linear region stiffness, and deformation at toe.

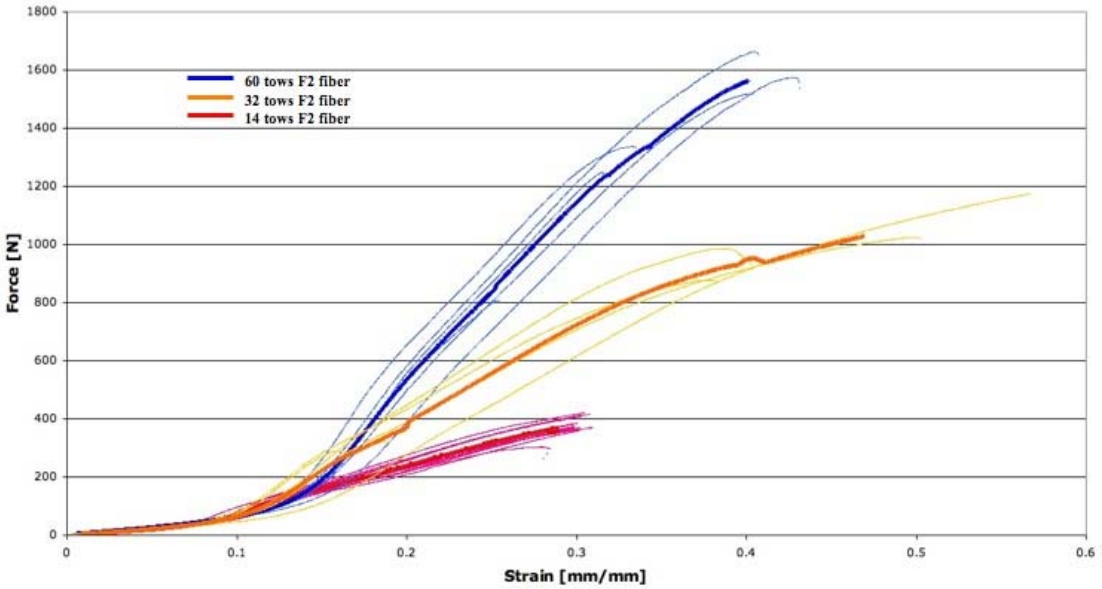

Figure 27. Strain vs. Force graph for anterior longitudinal ligaments with varying number of tows of F2 fiber. The bold lines in each grouping of data represents the average of all individual test runs.

3.6 Conclusions:

The current ligament tensile study demonstrated the ability to successfully control the nonlinear mechanical properties of the synthetic soft tissue ligaments of the spine in a repeatable fashion. The parameters of the synthetic spinal ligaments can be altered in order to achieve any non-linear load-deformation response desired. This same approach can be applied to the PLL and other minor ligaments yielding similar results. The ALL and PLL manufacturing properties that were chosen for the first

generation commercial analogue spine model used in Chapter 4 are as follows. These values were chosen based on the results of this study and the human ligament mechanical properties discussed in Chapter 2.

3.6.1 Anterior Longitudinal Ligament:

- Average ALL - 24 tows of F2 fiber (120.12 N/mm secondary stiffness based on Figure 25)
- *Stiff ALL in Chapter 4 will contain 60 tows of F2 fiber (300.30 N/mm secondary stiffness based on Figure 25)
- F42 PU matrix
- Dimensions (16 mm x 3.5 mm for all segment levels)
- Length of PU matrix segment: Approximately 28 mm
- Wave Properties: 1.575 mm amplitude and 1 wavelength/cm
- Strain at toe target is 5% - 10%

3.6.2 Posterior Longitudinal Ligament:

- 14 tows of F2 fiber (77.24 N/mm secondary stiffness based on (Figure 25))
- F42 PU matrix
- Dimensions (9 mm x 1.8 mm for all segment levels)
- Length: Approximately 18 mm
- Wave Properties: 0.81 mm amplitude
- Strain at toe target is 2% - 4%

Characterizing the control of the other parameters such as waveform profile and PU matrix stiffness would help to form a more complete understanding of the synthetic ligament control. More testing is also needed for the other synthetic spinal ligaments, especially the PLL. It would be beneficial to produce a parameterization graph similar to Figure 25 for the PLL.

Chapter 4 – Effect of ALL Stiffness on the Synthetic Analogue Lumbar Spine Model

4.1 Introduction:

Control over the mechanical properties of the synthetic spinal ligaments has been demonstrated in Chapter 3. It was of interest to examine the effect that different spinal ligaments have on the overall biomechanics of the lumbar analogue spine model. For this purpose, the ALL stiffness was chosen as the ligament and mechanical parameter to vary because of its size, relative strength, and overall biomechanical effect seen in the literature. This is seen as the first step in designing different versions of clinically relevant synthetic analogue spine models. These include scoliotic models or models of varying ages and laxities. The opportunity for future research using these variations of the synthetic analogue spine model is seemingly endless. The goal is that the synthetic analogue spine model can become a common tool used by medical device companies and researchers to answer a multitude of clinical questions.

4.2 Materials and Methods:

Bending rigidity and compression testing was performed using a servo-hydraulic MTS 858 Mini Bionix II (Eden Prairie, MN) test system (Figure 28A). The MTS was outfitted with a 25 kN uniaxial load cell attached to its base to measure axial tensile and compressive loads. Single axis rotational MTS spine simulator jigs were mounted at the base on top of the uniaxial load cell and to the linear actuator of the cross-head. The rotational spine simulator jigs each have a round pot with four

transverse screws used to rigidly fix the inferior and superior vertebrae of the spinal segment(s) being tested.

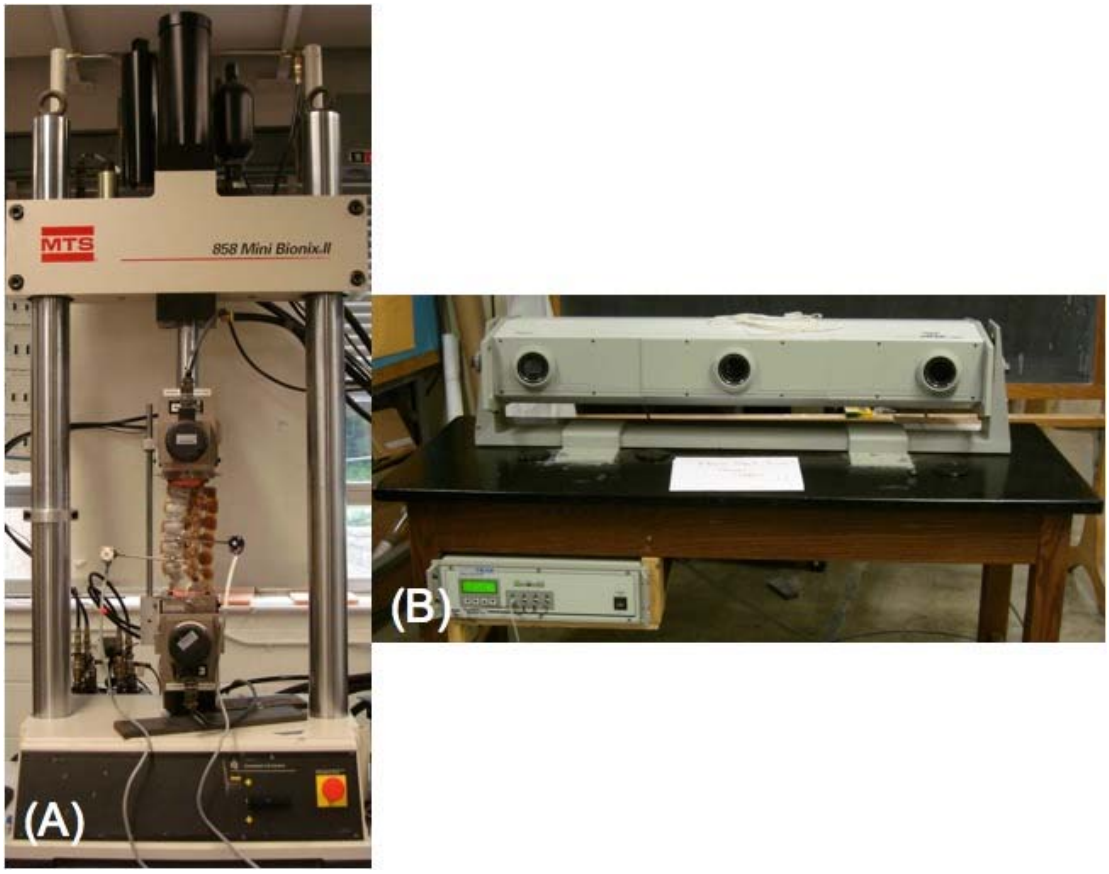

Figure 28. (A) MTS 858 Mini Bionix II (Eden Prairie, MN) test setup with inferior and superior rotational spine testing fixtures. The analogue spine model shown is set up for Flexion/Extension bending with the IRED rigid bodies attached to the L3 and L4 vertebrae. (B) Optotrak 3020 (Northern Digitial Inc., Waterloo, Ontario, Canada)

The L3-L4 segmental motion was recorded using an Optotrak 3020 (Northern Digitial Inc., Waterloo, Ontario, Canada) (Figure 28B) motion capture system during each trial of bending and compression tests performed in this study. The camera was pre-focused by the manufacturer for a distance of 2.25 m and was placed this distance from the MTS test frame. The L3 and L4 vertebrae were each outfitted with a series of four infrared light emitting diodes (IREDs) arranged onto a plastic rigid body.

These IRED rigid bodies were rigidly attached to each vertebral body using metal rods and a lockable universal joint. A metal rod with threads on one end was threaded into the vertebral bodies and was secured additionally with quick dry epoxy glue (Figure 29).

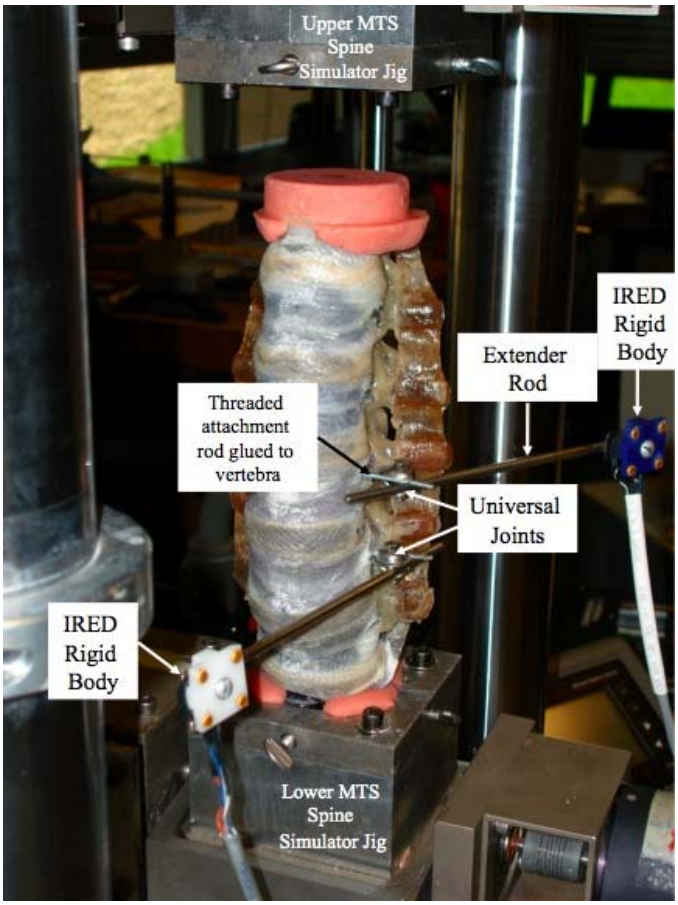

Figure 29. IRED rigid bodies attached to L3 and L4 vertebral bodies using metal rods and lockable universal joints.

4.2.1 Materials:

Five synthetic mechanical analogue lumbar (T12-S1) spine segments were each tested in three different ligament configurations. In order to investigate the effect of ALL stiffness on the lumbar spine model biomechanics, three different ALL

configurations were tested: No ALL intact (referred to as NONE), an average ALL comprised of 24 tows of polyester fiber and a F42 PU matrix (referred to as AVG), and a stiff ALL comprised of 60 tows of polyester fiber and a F42 PU matrix (referred to as STIFF). Each T12-S1 lumbar spine specimen was sent from PRL with the STIFF ALL initially intact. The spine was fully tested as described in the following paragraphs. After testing with the STIFF ALL configuration, the stiff ligament was fully transected and testing was repeated with the NONE ALL configuration. An AVG ALL, sent from PRL, was then attached to the spine using 5-minute quick dry epoxy. Special elastic bands with rubber tubing were used to keep the ligament aligned and tight to the anterior portion of the spinal column while the epoxy glue cured (Figure 30). Once the epoxy fully cured, the spine was repotted as necessary and testing was once again repeated with the spine in the AVG ALL configuration.

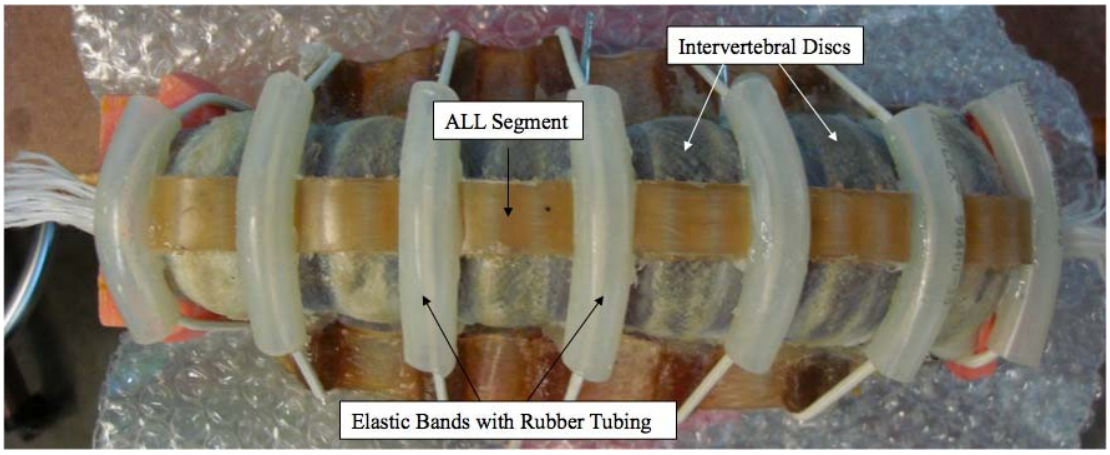

Figure 30. Elastic bands with silicone tubing used to apply pressure to the dry fiber sections of the AVG ALL ligament while gluing it to the analogue spine model using a 5-minute quick dry epoxy glue.

4.2.2 Specimen Preparation and Potting:

In order to prepare the T12-S1 analogue lumbar spine model for testing the full sacrum must be cut down in order to fit in the custom made testing jigs. Three cuts were made on the sacrum and the rough corners were sanded down using a rotating power sander. Three holes are pre-drilled on the superior endplate of T12 and the bottom of the cut down sacrum or S1. The center drill hole was placed symmetrically in the frontal plane and 1/3 of the total A/P distance back from the anterior most point in the sagittal plane. The other two drill holes are to be placed skewed from the center at an angle. Screws (¼" D x ¾" L) were placed in the pre-drilled holes on each end of the lumbar segment. Figure 31 shows the cut and sanded sacrum with the three screws in place. These screws are intended to give more purchase to the PMMA bone cement used to pot the spine in the custom testing jigs. When potting the spine, the testing jigs must be prepared using masking tape to block the tightening screw holes from PMMA and petroleum jelly to prevent adhesion to the jigs. The spinal segment was oriented so that the center screw on the superior and inferior vertebrae line up in the center of the top and bottom pots. The L3-L4 disc level was assumed to be the peak of the lordotic curve and thus was oriented so that this level's disc was horizontal. The PMMA was allowed to cure for approximately 20-30 minutes before testing began.

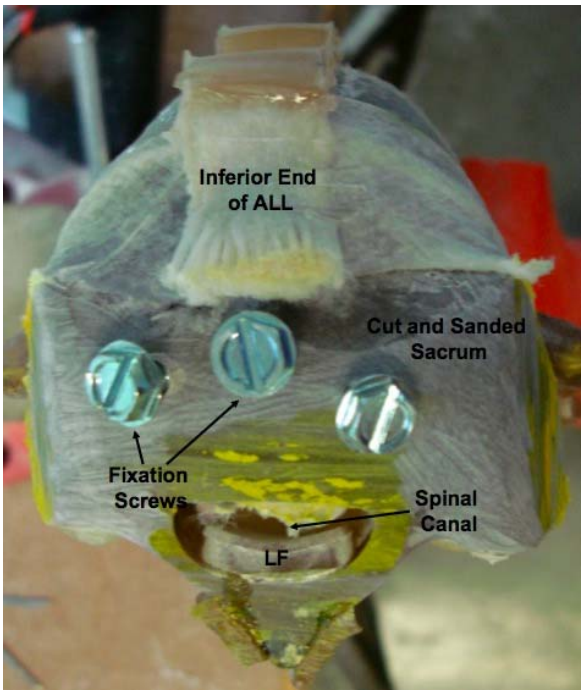

Figure 31. Inferior end of S1 vertebrae. The full sacrum has been cut and sanded down so that it will fit in the MTS spine simulator testing jigs. The three screws will help the bone cement in the potting fixtures to rigidly fixate onto the spine model.

4.2.3 Bending Rigidity Testing:

The potted lumbar spine segments were each tested in flexion-extension (FE) and right-left lateral bending (RL) using the MTS 858 Mini Bionix II and spine simulator jigs. The specimens were tested to a minimum moment of ±6.0 Nm in angular displacement control at a rate of 0.46 degrees/second for bending. An initial axial compressive preload of -100 N was applied to the spine in order to simulate the weight of the upper body. Through a series of initial trials, the angular deformation required to reach ±6.0 Nm in bending was determined. Once these angles were determined, the specimen was preconditioned by cycling through the angles 50 times in order to help "break-in" the spine. The specimen was not preconditioned again through 50 cycles for the alternate NONE ALL or AVG ALL conditions. If after the

50 cycles, the peak moment was less than ±6.0 Nm, then the angles were increased to reach the ±6.0 Nm peak moment again before testing continued. One run of FE or RL bending consisted of three precondition cycles and data from the third cycle was used in the data analysis. Moment-angular deformation data was collected at 10 Hz, plotted, and then analyzed.

4.2.4 Compression Testing:

Using the same MTS axial load frame the specimens were tested in compression (C) at a rate of 0.25 mm/second using a minimum axial compressive preload of -40 N. The spine was manually displaced until -1200 N of axial compressive load was reached and the displacement at this load was noted. The load was then reduced to -40 N and the displacement was zeroed. One run of compression consisted of three cycles between -0.1 mm and the displacement required to reach -1200 N. Once again, load-displacement data from the third cycle was used in the analysis.

4.2.5 Spinal Kinematic Testing:

Kinematic data from the Optotrak was collected at 100 Hz simultaneously with the MTS bending and compression procedures. During each bending or compression trial, the Optotrak recorded the spatial locations of the IREDs that were secured to the L3 and L4 vertebrae. These spatial locations were used to compute a rigid body coordinate system for each IRED rigid body (RB3 and RB4 in Figure 32). Before each trial, a one second static collection was performed in order to confirm that the IRED rigid bodies had not shifted during testing. In addition, the locations of

key anatomical landmarks on each vertebra were probed in their respective IRED rigid body coordinate systems according to Holt et al. 2005 [108]. These points included the two lateral most points (points X and X') and the most anterior point (point Y) of the vertebral body endplates (Figure 33). An anatomic coordinate system with origin, O, was constructed on the L3 and L4 vertebral body using these anatomic landmarks (ACS_L3 and ACS_L4 in Figure 32).

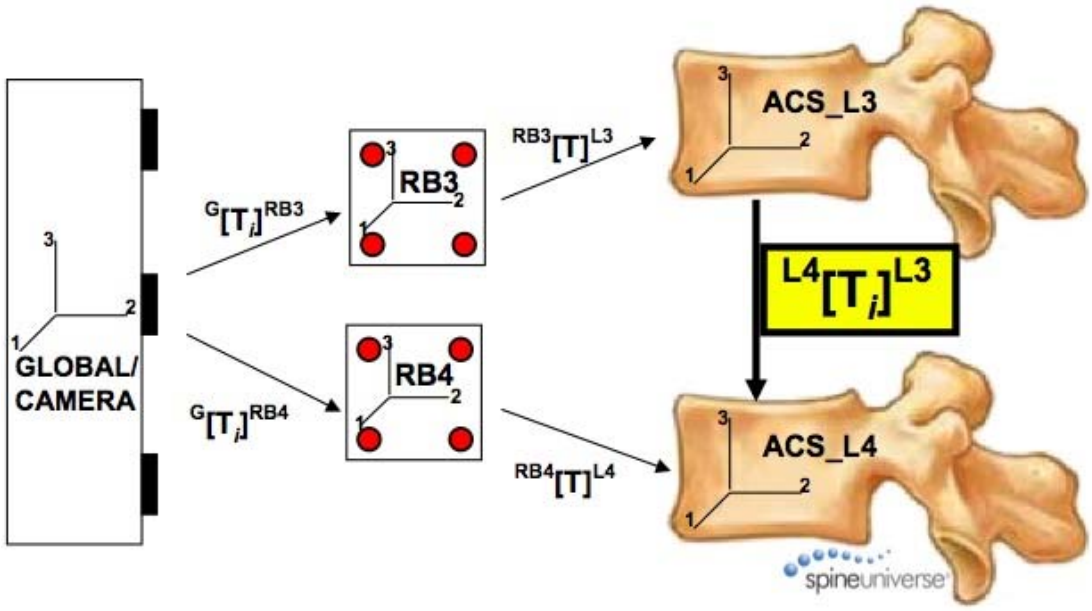

Figure 32. Coordinate systems and transformations used to calculate the L3-L4 motion segment's kinematics (vertebrae figures only courtesy of spineuniverse.com)

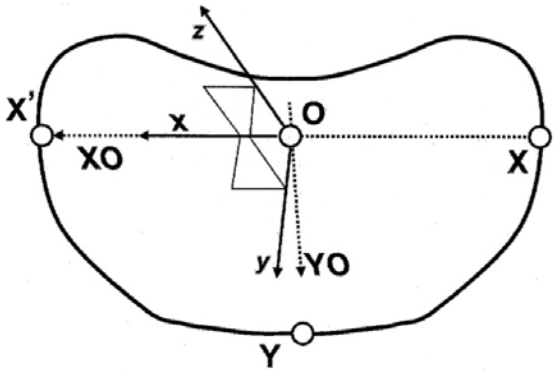

Figure 33. Diagram showing the setup of the Anatomical Coordinate System (ACS) looking down on the end plate of the vertebral body. The two most lateral points (X and X') and the most anterior points (Y) are probed. The origin of the ACS (O) is defined as the mid-point of the XX' line connecting the most lateral points of the endplate. The x-axis is defined by the unit vector x along OX. The vector along OY is the calculated and, and z is defined by the cross of this vector and x. y is then defined by the cross of the unit vectors x and z. (Holt, C.A., et al., Three-dimensional measurement of intervertebral kinematics in vitro using optical motion analysis. Proc Inst Mech Eng [H], 2005. 219(6): p. 393-9.)

All trials of bending and compression were performed in a randomized order to allow for viscoelastic recovery. At least 5 trials for each spine model in each ALL configuration were obtained. Once the testing for the STIFF ALL configuration was complete, the same angles and compressive displacements were applied in the repeated testing of the NONE and AVG ALL configurations.

4.3 Analysis:

4.3.1 Bending Rigidity Analysis:

In order to analyze the bending rigidity data, the third cycle of the angular displacement-moment curves were plotted. The neutral zone (NZ) and elastic zone (EZ) stiffness were calculated for flexion, extension, right bending, and left bending trials. The NZ stiffness for flexion and extension were averaged to get the NZ stiffness for the overall FE bending. This was also done for the overall RL bending. The ROM was also measured two different ways. The first (ROM), was by looking

at the angle at which the linear part of the neutral zone started to become non-linear. The second (±6ROM), was by finding the bending angles at ±6.0 Nm and taking the absolute difference in angles. Figure 34 illustrates how these parameters will be reduced on a typical moment-angular displacement curve. The peak moment in flexion, extension, right bending, and left bending was also determined for each trial. The peak moment was determined at the same bending angle for each analogue spine model. The non-linear load-displacement compression data was analyzed very similar to the ligament analysis in Chapter 3. The compressive response consists of an initial (NZ) stiffness, a secondary (EZ) stiffness, and a displacement at toe.

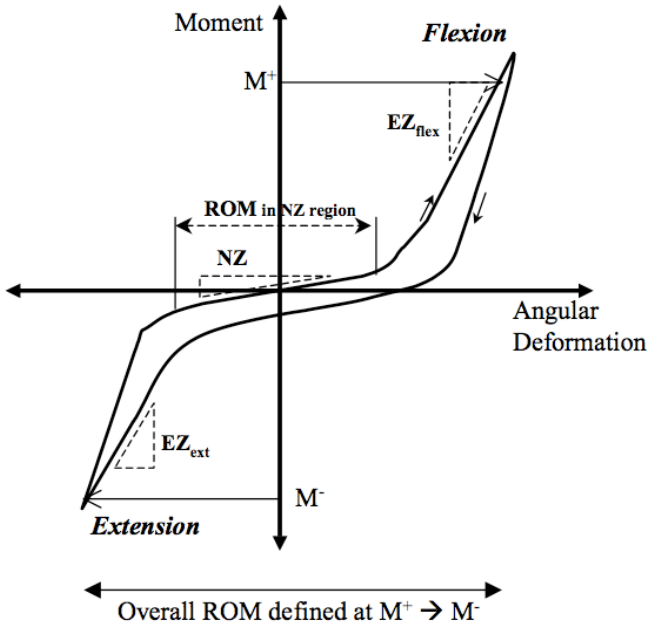

Figure 34. Typical loading pattern of KU spine segment testing. Data reduction includes measurement of the five illustrated parameters (EZext, EZflex, NZ, ROM, and +/-6ROM).

4.3.2 Optotrak Kinematic Analysis:

For each trial, the NDI First Principles Software (Eden Prairie, MN) outputs the IRED rigid body kinematics (rotation matrices and translations) for each time

step. These are recorded in the global or camera reference frame and put into transformation matrices ($^{G}\mathbf{[T_i]}^{RB3}$ and $^{G}\mathbf{[T_i]}^{RB4}$). For example, this is spoken, "*transformation of RB3 in the Global coordinate system.*" From the probe points, anatomical coordinate systems were established and put into transformation matrices ($^{RB3}\mathbf{[T]}^{L3}$ and $^{RB4}\mathbf{[T]}^{L4}$). These transformation matrices were constant for all time steps since the IRED rigid bodies were assumed to be rigidly attached the vertebral bodies throughout testing. Through a series of matrix multiplications (Equations 4-7), the transformation matrix was calculated for the L3 vertebral body relative to the L4 rigid body ($^{L4}\mathbf{[T_i]}^{L3}$).

$$^{G}\mathbf{[T_i]}^{L4} = {}^{G}\mathbf{[T_i]}^{RB4} * {}^{RB4}\mathbf{[T]}^{L4} \quad \text{Eqn. (4)}$$

$$^{L4}\mathbf{[T_i]}^{G} = (^{G}\mathbf{[T_i]}^{L4})^{-1} \quad \text{Eqn. (5)}$$

$$^{G}\mathbf{[T_i]}^{L3} = {}^{G}\mathbf{[T_i]}^{RB3} * {}^{RB3}\mathbf{[T]}^{L3} \quad \text{Eqn. (6)}$$

$$^{L4}\mathbf{[T_i]}^{L3} = {}^{L4}\mathbf{[T_i]}^{G} * {}^{G}\mathbf{[T_i]}^{L3} \quad \text{Eqn. (7)}$$

The transformation matrix at each time step for the bending and compression trials represents the difference in angle and translation between the two anatomic coordinate systems. Because the L3 vertebrae is allowed to move in 6 degrees of freedom relative to the L4 vertebrae, its position can be described by three angular rotations and three translations. The transformation matrix contains a 3x3 direction cosine matrix (rotation matrix) that can be decomposed as a product of three simple rotations about the coordinate system's axes. This order dependent sequence of three rotations describes the body's orientation. The anatomic probe points were chosen so

that the resultant coordinate systems are oriented so that the calculated rotations and translations about their axes are biomechanically and clinically relevant. A rotation about the x-axis represents flexion/extension, a rotation about the y-axis represents right/left lateral bending, and a rotation about the z-axis represents right/left axial rotation.

There are several established joint coordinate systems for calculating the three rotations that describe the rigid body's orientation. Two of the more common methods are the tilt/twist method [109] based on an Euler ZXZ transformation and the Grood and Suntay method [110] which is used as a staple in analyzing knee kinematics. A separate study was performed for a research project that investigated which of these methods was more robust to anatomic probe point variability. It was determined that the Grood and Suntay method was more robust to anatomic probe point variability when calculating the angular rotations, and was thus chosen for the analysis in this study. The Grood and Suntay coordinate system method specifies the relative position between two bodies, each with a defined origin. Two non-orthogonal axes are embedded in the bodies and are the fixed axes. A third axes is defined by the cross product of the two fixed axes, this is the floating axis because it is not fixed in either body, and moves in relation to both. Please refer to Grood and Suntay et al. for a more detailed description of this method [110].

The Grood and Suntay rotation matrix equations developed in this method can be seen in Equation 8 and are used to solve for the rotations between the bodies. The angles α, β, and γ are angular coordinates: α and γ are the angles formed between the

floating axis and the reference line embedded in each body, and β is the angle between the two fixed axes. The C and S represent cosine and sine, respectively. Using a custom written Matlab code, the three angles were solved for using the nine equations in the rotation matrix at each time step. Solving for α represents the angle for flexion/extension, solving for β represents angle for right/left lateral bending, and solving for γ represents the angle for right/left axial rotation.

$$\begin{bmatrix} C\gamma S\beta & -C\alpha S\gamma - C\gamma S\alpha C\beta & S\alpha S\gamma - C\gamma C\alpha C\beta \\ S\gamma S\beta & C\alpha C\gamma - S\gamma S\alpha C\beta & -S\gamma S\alpha - C\alpha C\beta S\gamma \\ C\beta & S\beta S\alpha & C\alpha S\beta \end{bmatrix} = {}^{L4}[\mathbf{T}_i]^{L3} \quad \text{Eqn. (8)}$$

Once the three angles were determined for each time step in the third cycle of bending, the data was filtered using a 4th order Butterworth filter with a 1000 Hz cutoff frequency. The angular rotation at ±6 Nm was then determined for each trial. The angular ROM (aROM) in each direction is simply the absolute difference between these angles. The translation in all three directions of the L3 vertebral body in relation to the L4 vertebral body was also determined at ±6 Nm. These values were similarly used to calculate the translation ROM (tROM). Therefore, the kinematic analysis of the L3-L4 motion segment yielded six parameters that were determined for each bending or compression trial: aROM_FE, aROM_RL, aROM_AX, tROMx, tROMy, tROMz.

4.3.3 Statistical Analysis:

A multivariate general linear statistical analysis (MANOVA) was performed to determine if any statistical differences ($p<0.05$) exist between the parameters for

the three ligament configurations. This was performed for the MTS rigidity results as well as the Optotrak kinematic results. All analyses were performed with commercially available software (SPSS Inc, Version 16.0 for Mac OS X, Chicago, IL). Furthermore, to determine which specific ligament configuration was different, a LSD post-hoc analysis was performed to compare each of the three ligament configurations with the other two configurations. A significant difference was determined for p-values less than 0.05. Since a primary assumption for MANOVA is that the variance must be equal or similar, a homogeneity test was performed as a check. Another assumption was that the data was a normal distribution.

4.4 Results:

4.4.1 Bending and Compression Rigidity Results

A critical goal of the synthetic mechanical analogue spine model project has always been to demonstrate a similar mechanical response to that of in-vitro human cadaveric specimens. In order to do this the spine models tested in their AVG ALL configuration for this study were used to compare to the human cadaveric database tested in The University of Kansas Structural Biomaterials Lab from 2003 to present (n=7). The T12-S1 specimens were tested and analyzed using the same bending and compression protocols described previously for the mechanical analogue spine models. The moment-angular displacement curves in Figure 35 and Figure 36, and load-displacement compression curve (Figure 37) demonstrate how the five synthetic analogue spine models stack up to the widely varying dataset of human cadaveric results. The bold lines represent the synthetic analogue spine models and the light dashed lines represent the human cadaveric spines.

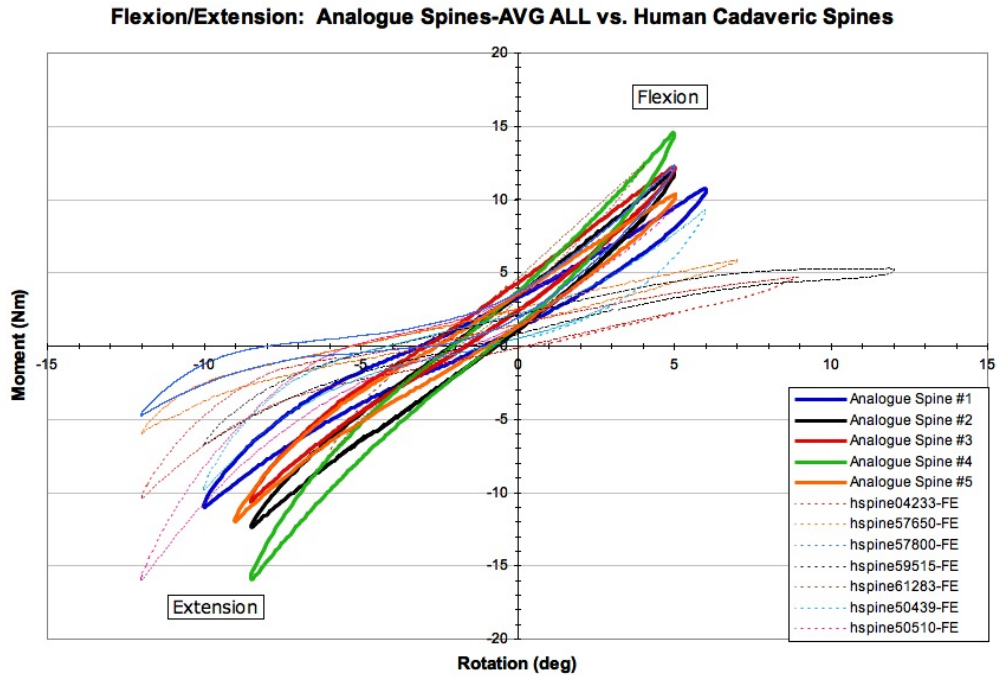

Figure 35. Flexion/Extension rigidity curves comparing the five synthetic analogue spine models to the human cadaveric spines tested in The University of Kansas Structural Biomaterials Lab.

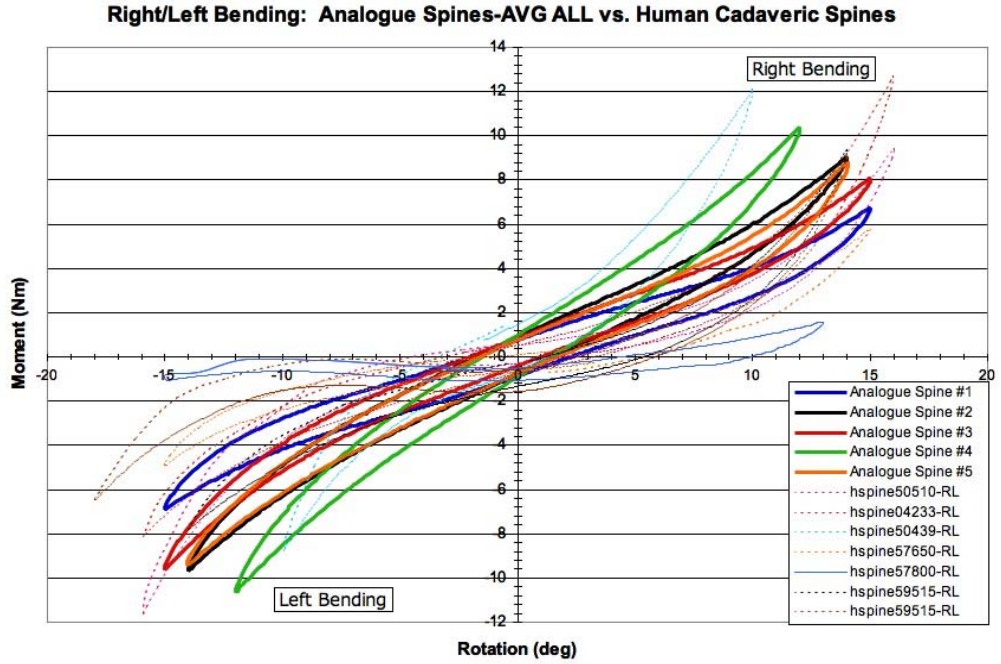

Figure 36. Right/Left Bending rigidity curves comparing the five synthetic analogue spine models to the human cadaveric spines tested in The University of Kansas Structural Biomaterials Lab.

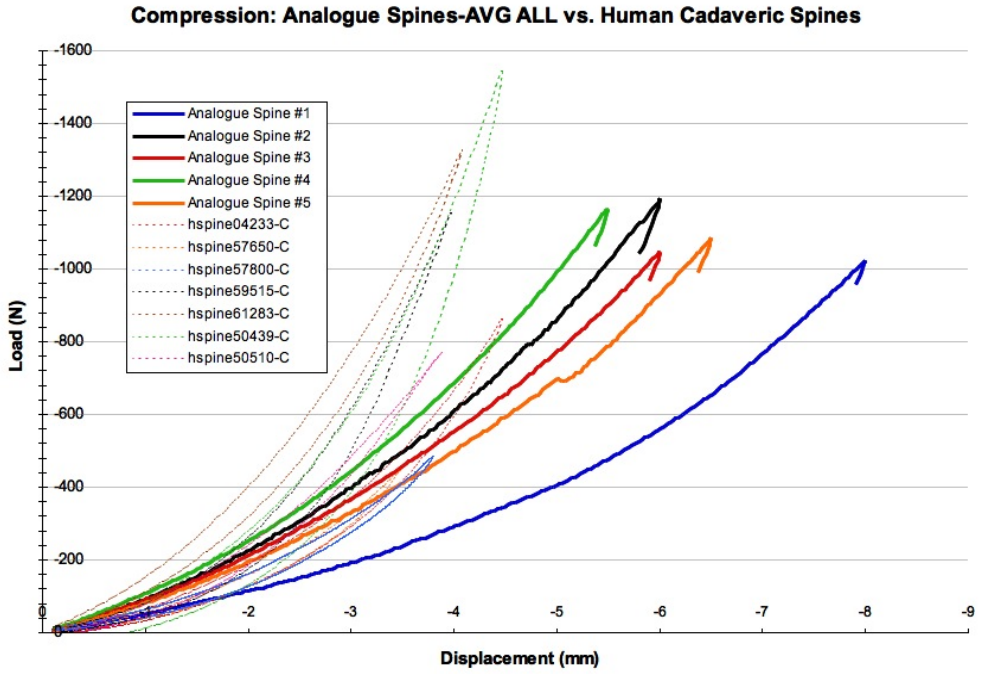

Figure 37. Load-displacement compression curves comparing the five synthetic analogue spine models to the human cadaveric spines tested in The University of Kansas Structural Biomaterials Lab.

One of the primary objectives of this study was to quantify the effect of changing the properties of a soft tissue component of the multi-segment synthetic mechanical analogue spine model. This will advance the ability to control the overall biomechanical response of the model. In order to quantify this effect the stiffness of the ALL was varied and the rigidity parameters were quantified and compared. These parameters were also compared to the human cadaveric dataset to better determine the ability of the analogue spine model in mimicking the biomechanics of the human lumbar spine. Figure 38, Figure 39, Figure 40, and Figure 41 quantify these parameters.

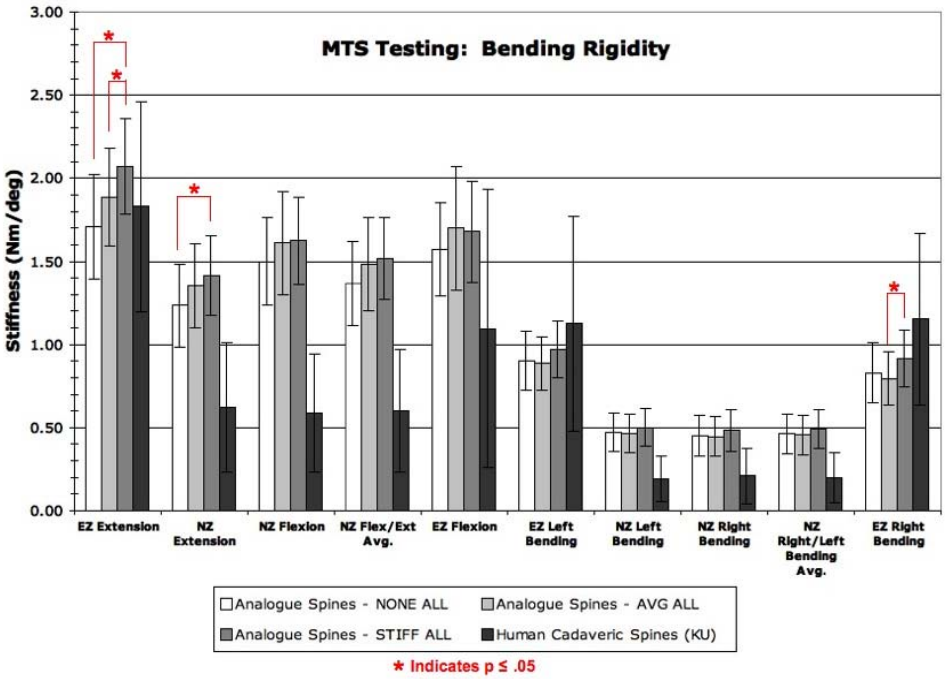

Figure 38. Bending stiffness parameters analyzed for the AVG ALL, NONE ALL, STIFF ALL configurations as well as the human cadaveric dataset collected in The University of Kansas Structural Biomaterials Lab.

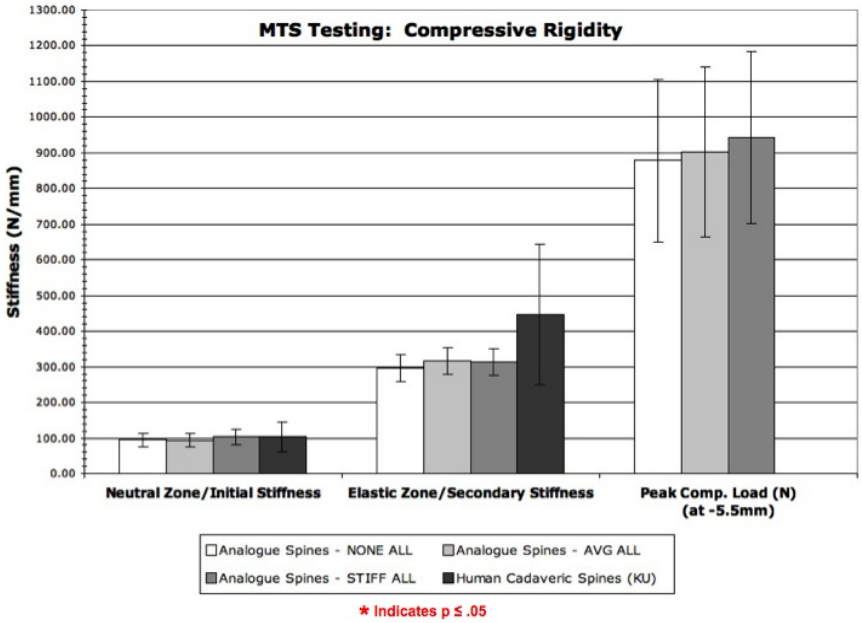

Figure 39. Compressive stiffness parameters analyzed for the AVG ALL, NONE ALL, STIFF ALL configurations as well as the human cadaveric dataset collected in The University of Kansas Structural Biomaterials Lab.

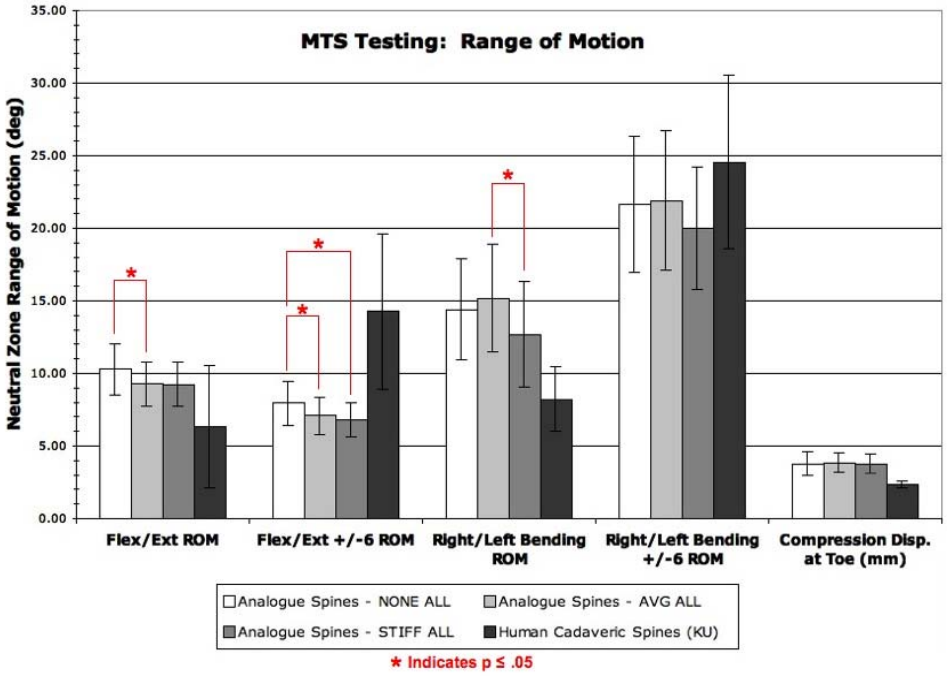

Figure 40. Range of Motion (ROM) and displacement at toe parameters analyzed from the MTS rigidity testing for the AVG ALL, NONE ALL, STIFF ALL configurations as well as the human cadaveric dataset collected in The University of Kansas Structural Biomaterials Lab.

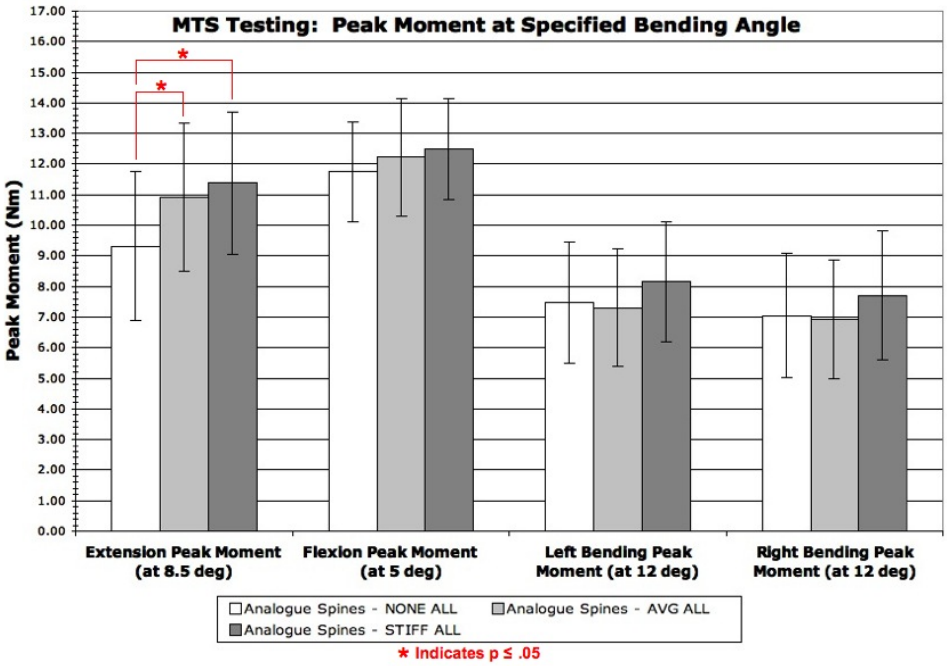

Figure 41. Peak moments (Nm) analyzed for the AVG ALL, NONE ALL, and STIFF ALL configurations at specified common angles for flexion, extension, right bending, and left bending.

The effect of the ALL can also be demonstrated graphically with the moment-angular displacement curves and load-displacement compressive curves. Figure 42, Figure 43, and Figure 44 demonstrate an example of a typical mechanical test. Due to the large amount of data collected, one representative run of analogue spine model 2 was used to compare the rigidity response of the AVG ALL, NONE ALL, and STIFF ALL configurations.

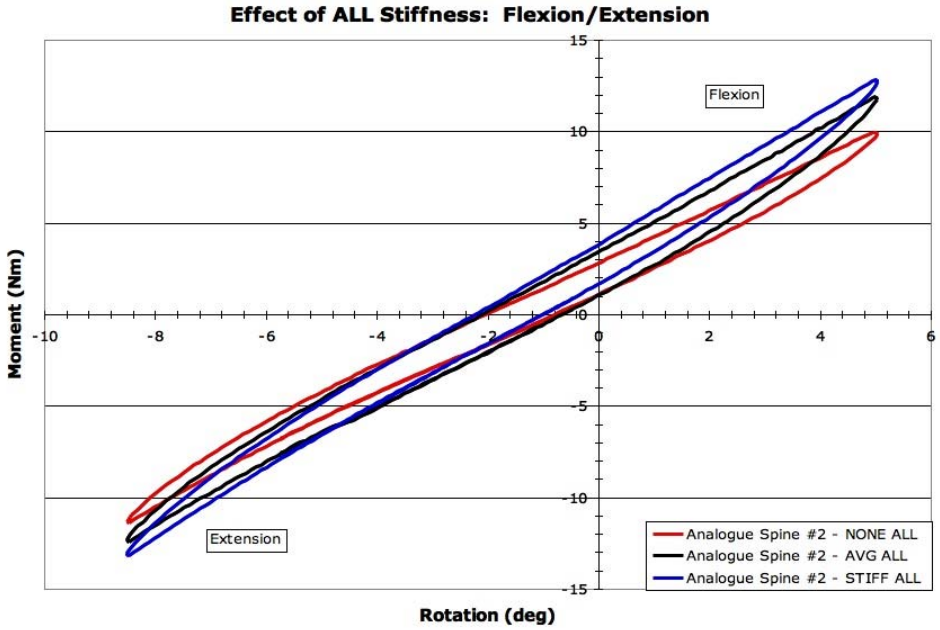

Figure 42. Graphical comparison of the different ALL configurations in flexion/extension rigidity testing.

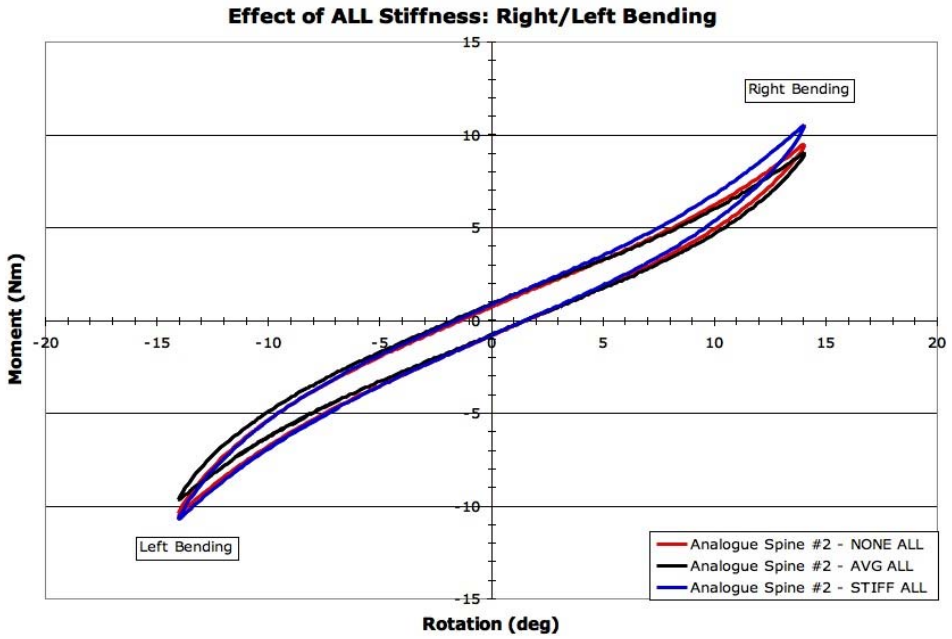

Figure 43. Graphical comparison of the different ALL configurations in right/left lateral bending rigidity testing.

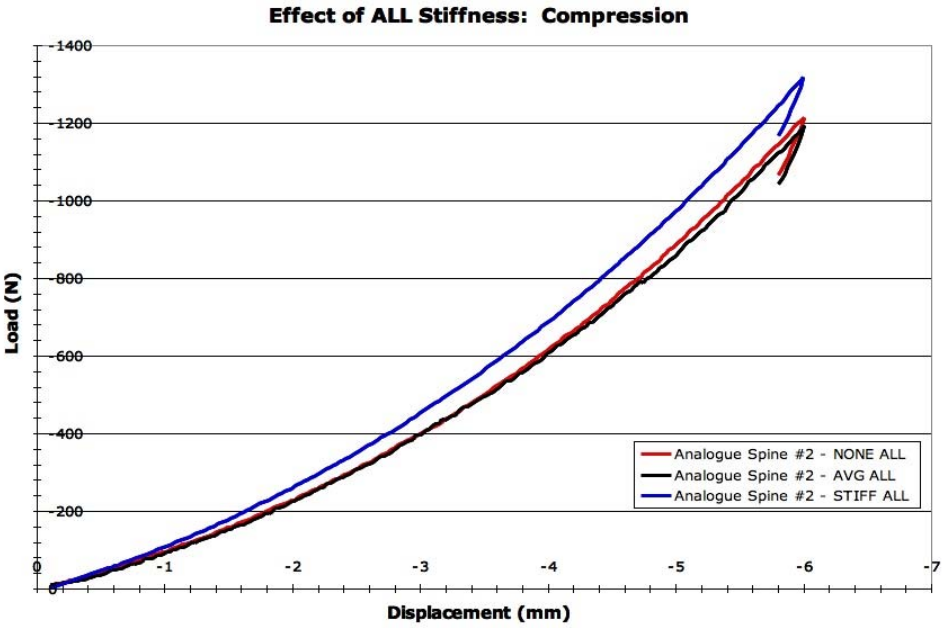

Figure 44. Graphical comparison of the different ALL configurations in compression testing.

4.4.2 Kinematic Results

The results of the kinematic analysis can be seen in Figures 45-47. The angular range of motion (aROM) and translational range of motion (tROM) were analyzed for each mode of testing (FE, RL, and C). The ranges of motion were found by calculating the change in angles and translations between the ±6 Nm moments in each mode of bending. Because of the six degrees of freedom of the L3-L4 spine segment tested, each testing mode has six output parameters (3 rotations and 3 translations). The three rotations correspond to rotations in the clinical planes of motion (FE=sagittal plane, RL=frontal plane, AX=transverse plane). The three translations correspond to the anatomical coordinate systems of the vertebral bodies which in turn correspond with anterior/posterior (A/P) translation, medial/lateral (M/L) translation, and axial translation. These parameters can be seen in Figure 45, Figure 46, and Figure 47.

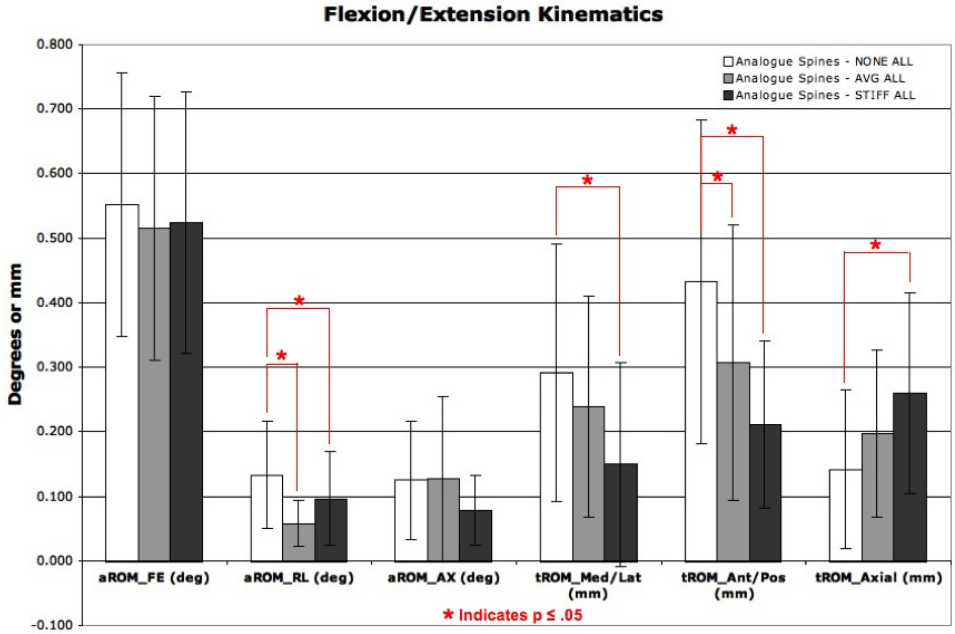

Figure 45. Flexion/Extension kinematic response of the L3-L4 motion segment on the synthetic mechanical analogue spine model. The ranges of motion were found by calculating the change in angles and translations between the ±6 Nm moments in each mode of bending.

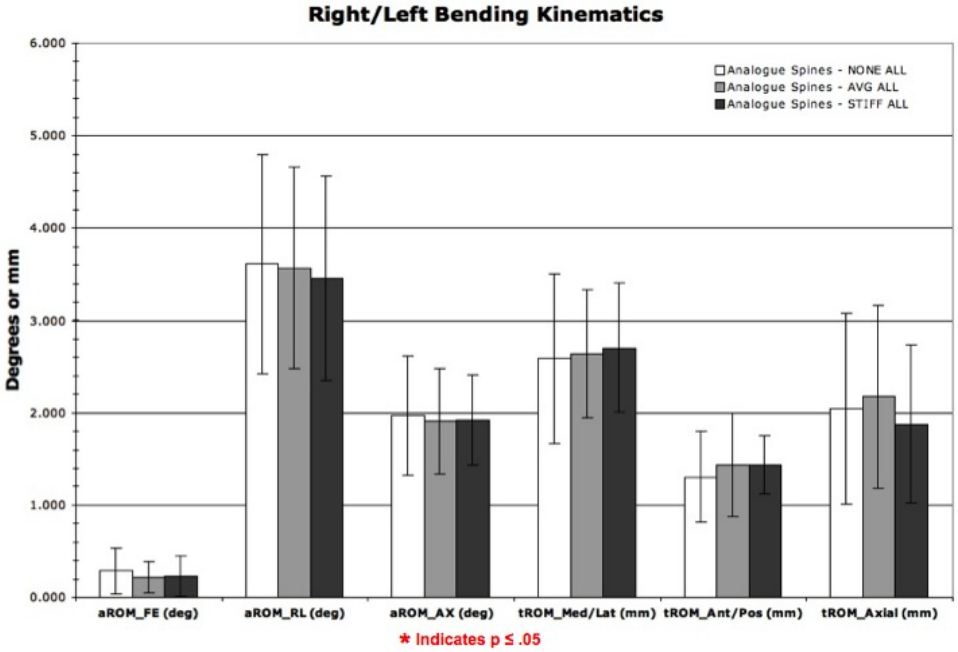

Figure 46. Right/Left lateral bending kinematic response of the L3-L4 motion segment on the synthetic mechanical analogue spine model. The ranges of motion were found by calculating the change in angles and translations between the ±6 Nm moments in each mode of bending.

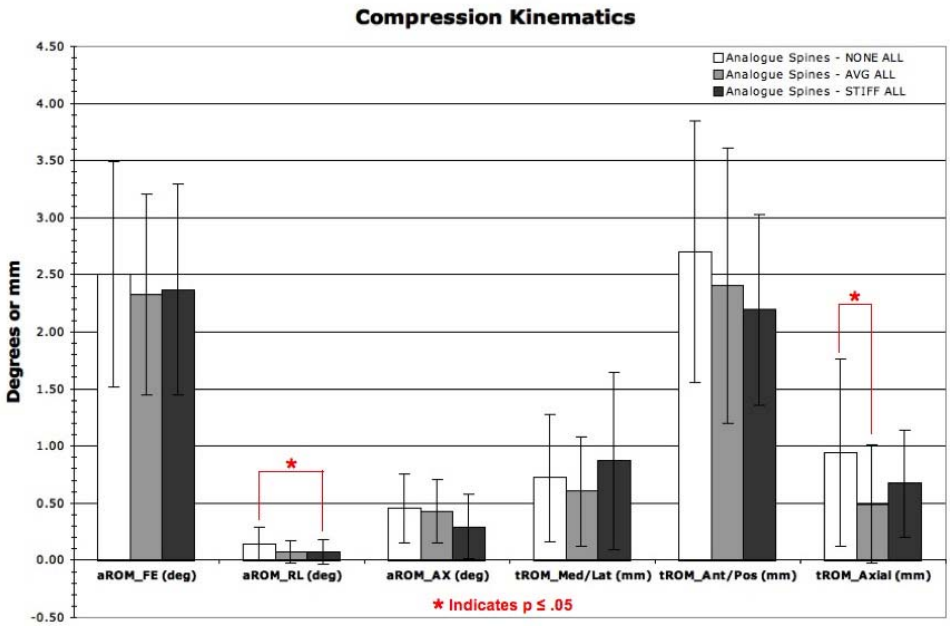

Figure 47. Compressive kinematic response of the L3-L4 motion segment on the synthetic mechanical analogue spine model. The ranges of motion were found by calculating the change in angles and translations between the ±6 Nm moments in each mode of bending.

4.4.3 Statistical Results

A MANOVA statistical analysis was performed for the MTS rigidity and Optotrak kinematic results. In order to determine if there were any outlying data points in the results a simple box plot was created for each parameter in each ALL configuration. These box plots showed if a data point was outside of the 75th percentile of the distribution. A table of the MTS rigidity box plot results can be seen in Table 8. The first group of columns (Rigidity Statistics 1) represents all five synthetic spine models. There were many more outliers, specifically in analogue spines 1 and 4. For this reason separate statistical analyses were performed once for excluding analogue spine 1, once for excluding analogue spine 4, and once excluding both 1 and 4. The same box plot analysis was done for the Optotrak kinematic parameters only, however only spine 1 appeared to be a repeating outlier.

Table 8. MTS rigidity box plot results. The first group of columns (Rigidity Statistics 1) includes all 5 synthetic analogue spine models, thus representing the current state of manufacturing at PRL. The second, third and fourth group of columns exclude one or more of the spine models from the statistical analysis based on the results of the fist group of columns.

	Rigidity Statistics 1			Rigidity Statistics 2			Rigidity Statistics 3			Rigidity Statistics 4		
	Analogue Spines 1-5			Analogue Spines 2-5			Analogue Spines 1, 2, 3, 5			Analogue Spines 2, 3, 5		
	none	avg	stiff	none	avg	stiff	none	avg	stiff	none	avg	stiff
EEZ	4(5)	4(5)	4(5)		4(5)			1(1)		3(1)		
ENZ								1(5)				
FNZ												
FENZ												
FEZ	4(5)	4(5)			4(4)		3(1)					
FEROM	1(1) 4(5)		4(3)	4(5)		4(5)	1(3)					2(2)
FE6ROM	1(4)							1(5) 2(1)				
EPKMOM	1(4) 4(5)	4(3)										
FPKMOM	4(1)	4(1)		4(1)	4(1)	4(1)						
CNZ	1(5) 4(2)	1(5)	1(4)									
CEZ										2(3)		
DEFTOE	1(5)	1(2)	1(4)									
PKLOAD												
LEZ												
LNZ	4(2)			4(1)								
RNZ	4(5)	4(5)	4(3)	4(4)								
RLNZ	4(5)	4(2)		4(4)								
REZ												
RLROM			5(1)			5(1)			5(1)			5(1)
RL6ROM				4(2)								
LPKMOM	4(1)	4(4)	1(3) 4(5)	4(4)					1(3)			
RPKMOM	4(5)	4(5)	4(1)	4(5)								

Outlyers
Analogue Spine 1
Analogue Spine 2
Analogue Spine 3
Analogue Spine 4
Analogue Spine 5

The MANOVA and LSD post hoc p-value results are shown in Table 9 and Table 10 for the MTS rigidity parameters and the Optotrak kinematic parameters respectively. Again the first group of columns represents all five synthetic spines being analyzed. The other groups of columns represent the analysis after throwing out a specific spine that was deemed an outlier. The parameters that were determined as significantly different are also labeled in the bar graphs above.

Table 9. MANOVA and LSD Post Hoc p-values for the MTS rigidity parameters analyzed. The gray shaded boxes represent a significant difference using MANOVA only. The yellow shaded boxes represent a significant difference between specific ALL configurations for a given parameter and were found using a LSD Post Hoc analysis. Each grouping of columns (Rigidity Statistics 1, 2, ...) represent different combinations of analogue spines analyzed.

		Rigidity Statistics 1		Rigidity Statistics 2		Rigidity Statistics 3		Rigidity Statistics 4	
		Analogue Spines 1-5		Analogue Spines 2-5		Analogue Spines 1, 2, 3, 5		Analogue Spines 2, 3, 5	
		stiff	avg	stiff	avg	stiff	avg	stiff	avg
EEZ	none	0.001	0.138	0.003	0.264	0	0.006	0	0.007
	avg	0.047	0.003	0.05	0.01	0	0	0	0
ENZ	none	0.023	0.128	0.004	0.04	0.007	0.107	0	0.006
	avg	0.442	0.07	0.384	0.013	0.259	0.026	0.068	0
FNZ	none	0.157	0.182	0.141	0.126	0.046	0.196	0.02	0.117
	avg	0.942	0.285	0.934	0.226	0.47	0.129	0.418	0.06
FENZ	none	0.065	0.149	0.036	0.075	0.016	0.135	0.001	0.028
	avg	0.686	0.154	0.753	0.08	0.34	0.052	0.191	0.003
FEZ	none	0.248	0.14	0.282	0.165	0.021	0.041	0.028	0.072
	avg	0.731	0.302	0.732	0.347	0.79	0.043	0.683	0.067
FEROM	none	0.068	0.044	0.305	0.333	0	0	0.002	0.001
	avg	0.831	0.087	0.961	0.517	0.327	0	0.593	0.001
FE6ROM	none	0.007	0.038	0.002	0.011	0.001	0.013	0	0
	avg	0.522	0.02	0.582	0.005	0.373	0.003	0.263	0
EPKMOM	none	0.009	0.041	0.008	0.047	0	0.006	0	0.001
	avg	0.558	0.024	0.487	0.023	0.237	0.001	0.034	0
FPKMOM	none	0.146	0.317	0.189	0.234	0.009	0.137	0.007	0.04
	avg	0.65	0.332	0.91	0.352	0.236	0.032	0.483	0.02
CNZ	none	0.135	0.932	0.014	0.77	0.109	0.925	0	0.96
	avg	0.111	0.199	0.006	0.01	0.126	0.189	0	0
CEZ	none	0.276	0.15	0.27	0.074	0.296	0.166	0.33	0.081
	avg	0.709	0.326	0.464	0.197	0.923	0.354	0.398	0.213
DEFTOE	none	0.703	0.985	0.567	0.838	0.581	0.923	0.303	0.942
	avg	0.685	0.9	0.43	0.713	0.645	0.836	0.329	0.501
PKLOAD	none	0.382	0.738	0.228	0.567	0.323	0.704	0.121	0.444
	avg	0.587	0.674	0.522	0.479	0.538	0.603	0.419	0.295
LEZ	none	0.279	0.589	0.177	0.239	0.228	0.984	0.111	0.357
	avg	0.102	0.247	0.012	0.04	0.214	0.253	0.012	0.038
LNZ	none	0.53	0.871	0.646	0.873	0.248	0.981	0.159	0.89
	avg	0.424	0.698	0.529	0.806	0.252	0.362	0.194	0.285
RNZ	none	0.601	0.866	0.68	0.837	0.236	0.999	0.171	0.927
	avg	0.483	0.764	0.53	0.813	0.23	0.407	0.192	0.295
RLNZ	none	0.565	0.868	0.664	0.853	0.077	0.557	0.162	0.908
	avg	0.453	0.732	0.529	0.81	0.018	0.381	0.19	0.285
REZ	none	0.188	0.424	0.24	0.418	0.112	0.399	0.104	0.653
	avg	0.034	0.099	0.046	0.131	0.015	0.047	0.036	0.086
RLROM	none	0.153	0.49	0.071	0.347	0.112	0.399	0.035	0.2
	avg	0.034	0.094	0.006	0.02	0.015	0.046	0.001	0.004
RL6ROM	none	0.343	0.858	0.398	0.843	0.133	0.92	0.051	0.957
	avg	0.255	0.471	0.291	0.529	0.105	0.19	0.042	0.068
LPKMOM	none	0.374	0.772	0.396	0.684	0.128	0.854	0.022	0.67
	avg	0.233	0.459	0.203	0.426	0.084	0.165	0.007	0.014
RPKMOM	none	0.447	0.785	0.523	0.769	0.106	0.948	0.056	0.961
	avg	0.296	0.554	0.344	0.622	0.088	0.154	0.058	0.086

MANOVA Significant Difference Between none, avg, OR stiff ALL configurations
LSD Post Hoc Significant Difference (p<0.05) Between ALL configurations

Table 10. MANOVA and LSD Post Hoc p-values for the Optotrak kinematic parameters analyzed. The gray shaded boxes represent a significant difference using MANOVA only. The yellow shaded boxes represent a significant difference between specific ALL configurations for a given parameter and were found using a LSD Post Hoc analysis. Each grouping of columns (Kinematic Statistics 1 and 2) represent different combinations of analogue spines analyzed.

		Kinematic Statistics 1		Kinematic Statistics 2	
		Analogue Spines 1-5		Analogue Spines 2-5	
		stiff	avg	stiff	avg
C aROM_FE	none	0.529	0.321	0.456	0.330
	avg	0.710	0.602	0.809	0.592
C aROM_RL	none	0.044	0.058	0.004	0.050
	avg	0.912	0.077	0.331	0.012
C aROM_AX	none	0.082	0.807	0.068	0.547
	avg	0.139	0.171	0.225	0.176
C tROM_Med/Lat	none	0.480	0.494	0.313	0.449
	avg	0.169	0.385	0.083	0.216
C tROM_Ant/Pos	none	0.123	0.296	0.075	0.236
	avg	0.623	0.287	0.558	0.192
C tROM_Axial	none	0.124	0.003	0.216	0.007
	avg	0.143	0.014	0.117	0.024
FE aROM_FE	none	0.545	0.435	0.675	0.601
	avg	0.856	0.713	0.913	0.856
FE aROM_RL	none	0.063	0.000	0.978	0.015
	avg	0.035	0.001	0.014	0.020
FE aROM_AX	none	0.103	0.834	0.009	0.004
	avg	0.069	0.135	0.763	0.007
FE tROM_Med/Lat	none	0.008	0.392	0.102	0.203
	avg	0.070	0.025	0.723	0.226
FE tROM_Ant/Pos	none	0.000	0.030	0.003	0.005
	avg	0.113	0.001	0.904	0.004
FE tROM_Axial	none	0.005	0.179	0.017	0.229
	avg	0.536	0.018	0.231	0.057
RL aROM_FE	none	0.336	0.263	0.365	0.310
	avg	0.865	0.477	0.903	0.534
RL aROM_RL	none	0.625	0.876	0.494	0.783
	avg	0.743	0.882	0.688	0.787
RL aROM_AX	none	0.754	0.641	0.552	0.631
	avg	0.876	0.892	0.287	0.563
RL tROM_Med/Lat	none	0.592	0.906	0.448	0.703
	avg	0.681	0.853	0.712	0.748
RL tROM_Ant/Pos	none	0.347	0.380	0.013	0.330
	avg	0.957	0.572	0.125	0.042
RL tROM_Axial	none	0.550	0.591	0.753	0.184
	avg	0.260	0.528	0.103	0.223

MANOVA Significant Difference Between none, avg, OR stiff ALL configuratiions
LSD Post Hoc Significant Difference ($p<0.05$) Between ALL configurations

4.5 Discussion:

4.5.1 Analogue Spine Models Compared to Human Cadaveric Spines:

When comparing the bending rigidity results of the AVG ALL synthetic analogue spines to the human cadaveric spines tested at KU, many observations can be made. For flexion/extension, the NZ stiffness appears to be higher in stiffness compared to the human cadaveric NZ stiffness as can be seen in Figure 35 and Figure 38. The neutral zone stiffness of the spinal column is primarily controlled by the mechanical properties of the intervertebral disc. In order to decrease the neutral zone stiffness in the analogue spine model during flexion/extension, the stiffness of the nucleus pulposus and the annulus fibrosis could be decreased to allow for easier bending in the neutral zone. One difficulty with this, is finding an attachment method for the intervertebral discs that will allow the disc to deform without failing at the interface. A high stiffness bond is needed (such as superglue or epoxy) to bond the disc to the endplate, but the disc itself must be significantly less stiff thus creating a large stress concentration at this interface. In preliminary analogue spine models this has been seen as an area of concern for interface failure. The ideal synthetic intervertebral disc would have a strong and durable attachment to the vertebral body endplates, but would still allow the disc to deform and the NP to act hydrostatically. This has proven to be a difficult endeavor and makes one appreciate the complexity of the human intervertebral joint interfaces. The ligaments come into play when the spine is bent outside of the neutral zone area, thus resulting in the increase in overall stiffness.

For right/left lateral bending the analogue spine moment-angular displacement data appears to fall into the range of human cadaveric data shown in Figure 36. The right bending and left bending elastic zone stiffness was very comparable to the human cadaveric stiffness (Figure 38). Similar to flexion/extension, the NZ stiffness for right/left lateral bending was also a little higher for the analogue spine models. For compression, the initial (NZ) stiffness was well within the range of human cadaveric spines, but the secondary (EZ) stiffness was less than the human values (Figure 39). This result seems odd since the neutral zone stiffness for FE and RL bending seems high. It would make more since if the secondary (EZ) stiffness in compression was more stiff than human spines because of the high stiffness neutral zones in FE and RL bending.

One of the most common parameters used to evaluate the biomechanical effectiveness of a spinal device (fusion or arthroplasty) is the physiologic range of motion (ROM) at the instrumented and adjacent levels [111]. This is defined as the amount of motion (translation or rotation) possible across the segment or segments at a pre-determined nondestructive moment or load, usually in the range of 6 to 10 Nm. The full T12-S1 segment ROM was determined using the bending rigidity data as described in the analysis. The bending angles at ±6 Nm in flexion, extension, right bending, and left bending were collected from the moment-angular displacement curves. The ±6 ROM was smaller than the human cadaveric ±6 ROM. This can also be attributed to the stiff neutral zones of the analogue spine models since the bending moment will reach ±6 Nm sooner with a stiffer spine.

Of the thirteen bending rigidity parameters analyzed, (EEZ, FENZ, FEZ, LEZ, RLNZ, REZ, CNZ, CEZ, DEFTOE, FEROM, FE6ROM, RLROM, and RL6ROM) eight of them were within one standard deviation of the KU human cadaveric dataset. Two of the other five parameters were within two standard deviations of the human dataset. The parameters that were least like the human dataset were the NZ stiffness or ROM parameters. This also included the displacement at toe for the compression testing. These results represent a very strong first attempt at mimicking the rigidity of human cadaveric spines. Decreasing the stiffness in the neutral zone, by allowing the spine to move more freely in the initial bending angles, will help the analogue spine to be even more in line with the results of human cadaveric dataset.

4.5.2 Repeatability of Analogue Spine Models:

One of the significant advantages in having a commercially manufactured synthetic spine model available is its ability to reproduce the same biomechanical response in each specimen. Due to the extremely large variation in human cadaveric specimens, a more repeatable physical test model could be a huge benefit to the research and development community. The standard deviation in the KU human cadaveric dataset was as high as ± 79% of the mean. Even though the standard deviations in many of the parameters of the analogue spine model were larger than desired, they were on average half to one third of the human cadaveric standard deviations. This shows a significant increase in the repeatability of using commercially manufactured synthetic analogue spine models vs. human cadaveric spines for a scientific investigation.

The standard deviations in the synthetic analogue spine models were still as high as 25% in some bending parameters. This was still much higher than expected and thus led to the investigation of which spine or spines in particular may have been causing the large variation. By looking at simple box plots for the rigidity parameters analyzed it was immediately apparent that analogue spine 1 and 4 had a large number of outlying data points (outside of the 75th percentile). This can be seen in Table 8 by the large amount of yellow (spine 1) and green (spine 4) shaded boxes in the Rigidity Statistics 1 group of columns.

When comparing the moment-angular displacement curves for the five analogue spines, (Figures 35-37) it appeared as though analogue spine 1 was generally less stiff than the other spine models and analogue spine 4 was generally higher in stiffness. These two models form upper and lower bounds of the analogue spine curves with analogue spine 2, 3, and 5 falling in between spines 1 and 4. After further visual inspection of the spine models, it appeared as though the polyester fibers in the annulus fibrosis of the intervertebral discs of spine 1 were not as rigidly glued to the vertebrae as the other spine models (Figure 48). This could explain the lower stiffness response of analogue spine 1. The higher stiffness in analogue spine 4 may be explained by the visual differences in the consistency of the PU used in the facet joint capsules (Figure 49). Compared to the other analogue spine models, the PU used for the facet joint capsules of spine 4 appears rough and "chunky." Even though the same durometer of PU was used in both spine models the ratios of the two part mixing compound may have been slightly different. This may have resulted in

stiffer material properties of the synthetic joint capsules of spine 4 and could alter the overall stiffness response of the spine.

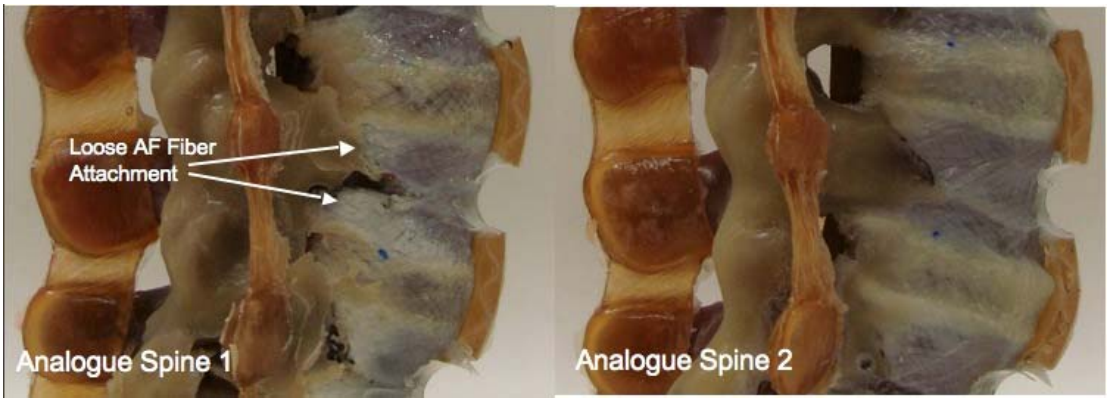

Figure 48. Difference in AF fiber attachment to analogue vertebral bodies. Notice the area that appears white in analogue spine 1 indicating a loose attachment. The AF fiber attachment of the other analogue spines appeared similar to analogue 2 in this picture. It is speculated that this is a reason for the low stiffness response of analogue spine 1 in bending rigidity testing.

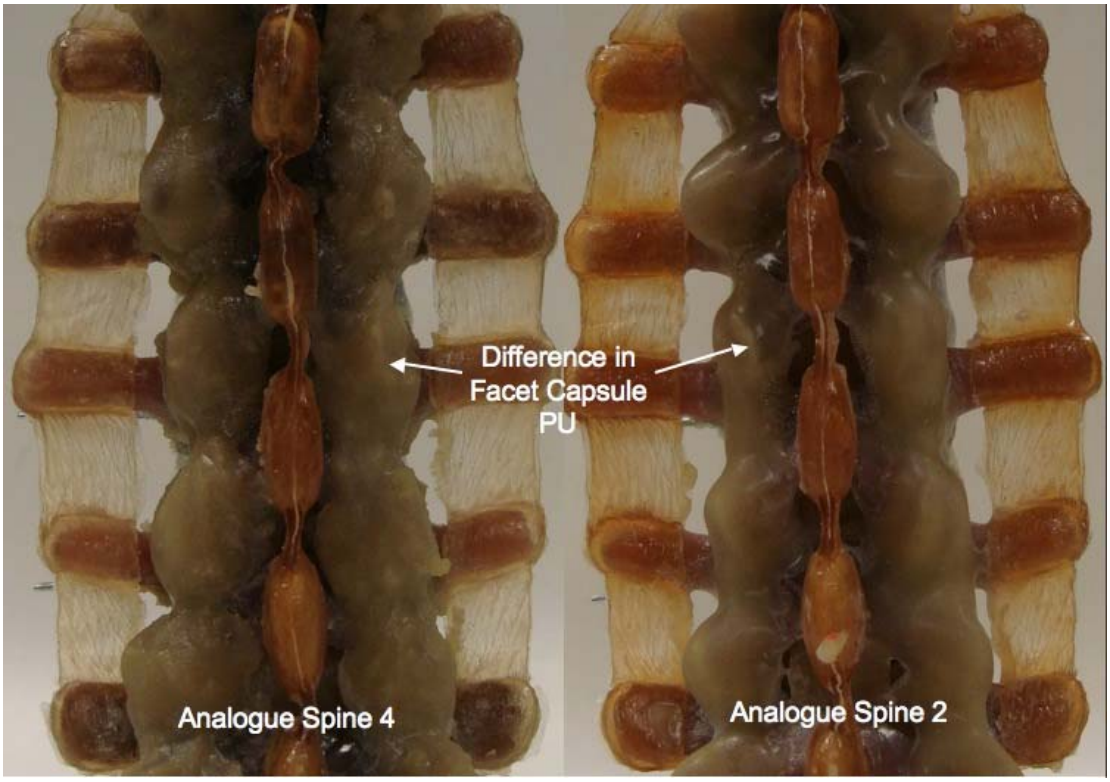

Figure 49. Difference in consistency of polyurethane used for the facet joint capsules. The PU covering the facet joints in analogue spine 4 appears rough and "chunky" and appears smooth in analogue spine 2 and other analogue spine models. It is speculated that this is a reason for the high stiffness response of analogue spine 4 in bending rigidity testing.

It is important to note, that all results shown in Figures 35-41 and 45-47 are the results using all five synthetic analogue spines in the dataset. This shows a true representation of the current state of manufacturing at PRL. The construction and assembly of each biomechanically accurate analogue spine model is a very involved and complicated process to ensure spinal alignment and component attachment. It is expected that as the methods for construction of the spine model are perfected and standardized, the amount of variation between the models will drop considerably. The additional statistical analyses performed after excluding analogue spine models 1 and 4 shown in Table 8-10 were performed purely as an academic exercise. This was done primarily to see how the dataset was affected by throwing out data from spines that could be viewed as outliers.

4.5.3 Effect of ALL stiffness on rigidity

It was hypothesized that changing the stiffness of the ALL would have the largest effect on extension bending related parameters such as the extension NZ, extension EZ, extension peak load, and FE ROM. In order to determine if there was a significant difference in the rigidity and kinematic parameters analyzed between the NONE, AVG, and STIFF ALL configuration a graphical and statistical method was employed.

Figures 42-44 show a graphical representation of how the MTS rigidity curves responded to the different ALL configurations. The representative curves are from analogue spine 2 which seemed to have an average response and did not show any significant outliers in the box plots of the statistical analysis. For this particular spine

model, the most noticeable difference between the three configurations was in the FE curves of Figure 42. In extension and flexion it was apparent that as the stiffness in the ALL is increased, the peak moment and EZ stiffness also increased. As a result of the flexion and extension stiffness increasing with ALL stiffness the ROM tended to decrease in FE bending as ALL stiffness increased (Figure 38 and Figure 40). In the right/left bending and compression curves of Figure 43 and Figure 44, there was not as obvious of a stepwise change with increasing ALL stiffness. It did, however, appear that the STIFF ALL configuration caused an increase in the compression EZ stiffness and compressive peak load in Figure 44. These results fall in line with the notion that the primary function of the ALL is to resist hyperextension and bulging of the disc [28, 38]. The stepwise increase in the flexion parameters could be due to the ALL resisting the bulging of the disc or the higher number of polyester fibers providing a resistance to compression in the ligament segments.

In order to evaluate, statistically, if any significant differences existed between the ALL configurations of all five analogue spines a MANOVA statistical analysis was performed. A MANOVA statistical analysis was chosen over ANOVA because there were multiple dependent variables (NONE, AVG, STIFF ALL configurations) that to be associated with the independent variables (EEZ, FENZ, FEZ, … etc.). The advantage with using MANOVA is that multiple dependent variables can be tested simultaneously while keeping track of their correlation with each other. This reduces the amount of type I error that can occur and reduces the amount of false differences between the independent variables. Type I error occurs when multiple tests are

performed at a specific p-value because with enough tests you are likely to get a significant result due to chance alone [112]. Furthermore, if the MANOVA analysis showed a significant difference, a LSD post hoc analysis was used to determine specifically how the ALL configurations for each parameter were different from each other.

Table 9 shows the calculated p-values from the MANOVA and LSD post-hoc analysis in the MTS rigidity parameters. The gray shaded boxes represent a significant difference ($p<0.05$) in the MANOVA analysis and the yellow shaded boxes represent a significant difference between the different ALL configurations using the LSD post hoc analysis. The significant differences between the ALL configurations found using the LSD post hoc analyses are also represented in the parameter bar graphs of the MTS rigidity results (Figures 38-41).

The results of the statistical analysis fell in line with the graphical observations made in the fact that significant differences were seen primarily in the parameters driven by FE bending. The MANOVA analysis found a significant difference in the extension EZ stiffness, FE ±6 ROM, and the extension peak moment. After examining the differences in more detail using the LSD post hoc analysis it was discovered that all three ALL configurations were not uniquely different from each other. For the FE ±6 ROM and the extension peak moment the NONE ALL configuration was significantly different from the AVG and STIFF configurations, but the AVG configurations were not significantly different from the STIFF. This indicates that the mere presence of an ALL is important in controlling

these specific parameters. Similarly, for the extension EZ stiffness, the NONE and AVG configurations were found to be significantly different from the STIFF configuration, but were not significantly different from each other. This could mean that an increase from 24 to 60 tows of polyester fiber in the ALL was enough to significantly affect the extension stiffness of the entire lumbar spine segment.

It was of interest to see how analogue spine 1 and 4 (deemed as potential outliers), may have affected the significant differences in the rigidity parameters. Looking at columns 2, 3, and 4 in Table 9, the amount of significant differences between the ALL stiffness configurations seemed to increase with the exclusion of spines 1 and 4. The significant difference, especially between each of the 3 ALL configurations in the extension EZ stiffness and the extension peak moment, became more pronounced with the exclusion of spine 4 from the data set (columns 3 and 4 in Table 9). In addition to this, more significant differences were determined between the other flexion/extension bending parameters. This further supports the hypothesis that the stiffness of the ALL primarily affects the FE rigidity and FE ROM.

4.5.4 Effect of ALL stiffness on kinematics

Another goal of this study was to implement a method, for the first time in the KU Structural Biomaterials Lab, to track the kinematics of a lumbar spine segment. Figures 45-47 show the kinematic results of the L3-L4 spinal segment for each mode of testing. The angular and translation ROMs during FE bending can be seen in (Figure 45). As expected, it was clear that the primary bending direction in this segment was occurring in the flexion/extension direction. On average, about 13° of

total flexion/extension was applied to the spine during testing. The magnitude of the FE rotation was small and only represents around 5% of the overall flexion/extension being applied during the FE bending trial. It is likely that the majority of the FE bending motion was occurring in the adjacent spinal levels that were not captured with the Optotrak. This is discussed more in section 4.5.6. Using the same statistical analysis as with the MTS rigidity data, the different ALL configurations were compared for each kinematic parameter to determine if a significant difference existed (Table 10). In FE bending, a significant difference was determined in all three translational directions as well as the RL bending direction. There was an obvious stepwise decrease in the A/P translational ROM as the ALL stiffness increased. This could be a result of the stiffer ALL better restraining the vertebrae from shifting anteriorly or posteriorly. No significant differences were found in the FE ROM for FE bending. Based on the function of the ALL and the bending rigidity results, it was expected that this was the parameter that would be the most affected by a change in the ALL stiffness.

The RL lateral bending kinematic results are shown in Figure 46. It was expected that the bending angles would be much higher in RL bending because there are not as many structures (i.e. facet joints, longitudinal ligaments) resisting the lateral bending. Kinematics in RL bending are primarily controlled by the intervertebral disc. The ROM in the primary RL bending direction was around 3.5º combined with about 2º of coupled axial rotation. This RL bending ROM in the L3-L4 motion segment represents about 12-13% of the overall bending in the full spine

segment. White and Panjabi et al. [28] stated that this coupled rotation is one of the most common bending patterns in the lumbar spine. It was also determined that the L3 vertebra translated 2 or 3 mm in each direction during the bending trial. As expected, the RL bending kinematics showed no major significant differences when changing the ALL stiffness configuration (Table 10). This reinforces the hypothesis that the ALL stiffness predominately affects the kinematics in FE bending.

The results of the compression kinematics were surprising (Figure 47). During pure compression the L3-L4 motion segment appeared to rotate primarily in flexion and extension. In fact, the angular ROM in this direction was much larger than the ROM when the spine was actually bent in flexion and extension. One hypothesis for this is that the spine may have been buckling under the compressive loads. Since a follower load was not used in this study, the pure axial load was creating a bending moment about the L3-L4 motion segment thus resulting in FE bending. Since the L3-L4 motion segment is at the apex of the lumbar spine's lordotic curve it would naturally experience the largest amount of extension rotation due to buckling since the compression axis was not in line with its axis of rotation. Similar to the FE bending kinematics, there was also a noticeable decrease in A/P translational ROM with increase ALL stiffness.

4.5.5 Sources of Error in the Optotrak Kinematic Data

One source of error in the kinematic analysis may be from the variability in the anatomical probe points. Between the testing of each ALL configuration, the IRED rigid bodies had to be removed from the spinal segment in order to cut off the

ALL or reattach a new ALL. As a result, the anatomic probe points had to be re-probed and may not have been in the exact location each time. This difference may have resulted in error in the final angular rotations and translations that were calculated. In a study by Morton et al. [113], the effect of varying the anatomic probe points in the knee was investigated. They found that measures with a large ROM were particularly susceptible to anatomical location variability. Unlike the knee, the rotations in the lumbar spine are relatively small and variation in anatomic probing may have a large effect on the final ROMs. Another source of error that could be present in the kinematic results include a certain amount of multiplying error. Each time the transformation matrix was multiplied in order to get the desired transformations between the L3 and L4 vertebrae rigid bodies more error was created in the data. Therefore, it is best to calculate the desired transformation matrix with minimal matrix multiplication if possible.

As with any motion tracking equipment, there is a certain amount of error in built into the system. As reported by the manufacturer the RMS accuracy of the system for each individual IRED at a viewing distance of 2.25 meters was ± 0.1 mm for the camera viewing plane and ± 0.15 mm directed towards the camera. It has been assumed that these errors translate down into approximately a ± 0.5 degree accuracy error. The small kinematic values shown for flexion/extension in Figure 45 are very close to the magnitudes of error inherent in the Optotrak equipment and should be considered with great caution.

4.5.6 Comparison of Kinematic Results to Literature

According to the literature, the ROM for a single lumbar motion segment in FE bending appears to be in the range of 7-15º [28, 92, 105, 114, 115]. For RL lateral bending the range found in literature is 10-15º. The ROM magnitudes in the present study seem to be rather small compared to the intersegmental ROMs presented in the literature. One reason for the difference in magnitude is because the L3-L4 motion segment analyzed in the present study was part of a full lumbar segment and acted in situ. Kettler et al. [100] showed that a greater ROM occurred in a FSU as compared to the same segment tested in a polysegmental column. Some of the data presented in the literature is from FSU studies thus possibly causing the ROM values to seem larger than what actually appear in the in-situ motion segment.

Another reason that the L3-L4 motion segment in this study showed such small angles is because it was in the very middle of the T12-S1 segment being tested. Since equal bending occurs on the superior and inferior ends of the spinal column, the L3-L4 motion segment almost floats in the middle (acts as a pivot point) and allows the segments above and below it to do the majority of the rotating. Visual inspection during testing made appeared as though the T12-L1 and L5-S1 segments were rotating the most. Preliminary testing of analogue spine models showed that the intervertebral disc bonds at these levels were the first to fail. This indicated that higher amounts of rotation were occurring compared to the middle motion segments. The IRED rigid bodies that were attached to the L3 and L4 vertebral bodies did,

however, appear to be translating which is evident by the translation ROM in Figures 45 and 46.

The difference in results found in the present study with the kinematic ROMs found in literature can most certainly also be attributed to the differences in test setup and test methods. The MTS test setup in the present study uses displacement control to apply bending to the spine on both ends and measures the resultant bending moments on each end of the spine. A majority of the investigators that measure spinal segment kinematics use a load control or flexibility protocol. One of the major differences in this study's test setup was that the spine was constrained on both the inferior and superior ends and only allowed to move in the one direction that the custom MTS spinal jigs rotate. In addition, only bending moment data in the direction of bending could be collected thus making it difficult to determine if a pure bending moment was truly being transferred through the spinal column. In the load control setups, the spine is constrained only at the base and the superior end is allowed to move freely based on the forces and pure moments applied. The advantage of applying pure moments under load control is that the load is independent of the site of application, and the moment is uniform along the entire length of the spine [116]. It appears that this type of test setup results in larger ROMs under the same bending moments. Because spines tested in the KU Structural Biomaterials Lab are constrained at the top and the bottom, the angles required to produce a certain moment are undoubtedly less.

Chapter 5 – Conclusions and Future Work

5.1 Synthetic Ligament Characterization Tensile Study (Chapter 3)

The current ligament tensile study demonstrated the ability to successfully control the nonlinear mechanical properties of the synthetic soft tissue ligaments of the spine in a repeatable fashion. The parameters of the synthetic spinal ligaments can be altered in order to achieve any non-linear load-deformation response desired. This same approach can be applied to the other spinal ligaments in order to fully control the spine's overall biomechanical response. By successfully controlling the mechanical properties of the analogue spine's soft tissues the biomechanical response of the lumbar spinal column can be controlled. This control also gives greater flexibility to design different types of synthetic spine models, such as scoliotic models or varying ages or laxities of spine representation for future research.

Future work to be done in the development and characterization of the synthetic spinal ligaments is extensive. As seen by the variation in ligament properties in the literature there is a clear lack of consensus on the mechanical properties of the lumbar spinal ligaments. This is due to both the differences in test methods and the inherent interspecimen variability found in biologic tissues. Therefore, it would be beneficial to perform testing of human ALL and PLL ligaments in the KU Structural Biomaterials Lab using methods derived from the ones described in the current study. This would lead to better characterization of the synthetic longitudinal lumbar spinal ligaments. Characterizing the control of the other parameters such as waveform profile and PU matrix stiffness would help to

form a more complete understanding of the synthetic ligament control. More testing is also needed for the other synthetic spinal ligaments, especially the PLL. As the manufacturing techniques from PRL are perfected, it is expected that even more consistent and repeatable results will follow.

5.2 Analogue Spine Study (Chapter 4)

The AVG ALL analogue spine model did a sufficient job in mimicking the rigidity of the human cadaveric spines tested at KU using the same testing protocols. When comparing the analogue spine model to the human cadaveric spines, the NZ stiffness in FE and RL bending appeared to be stiffer than that of the human cadaveric spines. This also resulted in smaller ranges of motion compared to the human spines. The EZ stiffness was very close to that of the human spines indicating that the spinal ligaments were doing their job in limiting extreme bending. In order to decrease the NZ stiffness and thus increase the ROM of the spine, the design of the synthetic intervertebral disc should be reevaluated to allow the spine to move more freely in the initial bending stages. Once the NZ stiffness if further decreased the analogue spine model will be an even better solution in mimicking the biomechanics of the human cadaveric spinal column. While this study effectively demonstrates a global response similar to that of the human spinal column, local parameters such as disc pressure and facet joint loads were not evaluated. In order for the analogue spine model become an even more effective tool for research, these parameters must be reproducible and similar in magnitude to in-vitro cadaveric values.

The variability in the analogue spine models was on average half to a third of the variability found in the human cadaveric dataset. Despite this valuable decrease, it is believed that the variability in the analogue spine model will decrease even more over time. The five analogue spine models used in the present study represent the current state of manufacturing at Pacific Research Labs. A good future study would be to re-evaluate the spine model after at least 10 more spines have been manufactured at PRL. This would allow the materials control and learning curve of the assembly to be dramatically improved. It will be especially important to make sure that the exact same mixture and durometer of PU is used in the soft tissues of the model to ensure the mechanical properties of the soft tissue do not vary.

The current study demonstrates how ALL stiffness has an effect on the bending rigidity of the lumbar spine, particularly in FE bending. The extension NZ, extension EZ, and extension peak moment all increased with increasing ALL stiffness. The ±6 ROM decreased with increasing ALL stiffness. This supports the indicated function of the ALL in preventing hyperextension. This information shows that by altering the soft tissue mechanical properties the biomechanics of the spinal column can be controlled.

In order to better compare the effect of the ALL on the human spinal column it would be of value to perform an ALL transection study on human cadaveric spines using the methods developed in the Structural Biomaterials Lab at KU. Unlike the analogue spine model, it would be difficult to test varying degrees of ALL stiffness, but simple comparison of intact vs. ALL fully cut would provide information about

how the ALL effects the overall spine biomechanics. This would be extremely helpful in the development of the soft tissues of the analogue spine model.

This study successfully demonstrated that kinematic analysis of the lumbar spine is possible with the equipment available in the KU Structural Biomaterials Lab. This study represents a solid first attempt at implementing this valuable type of measurement technology on all future studies. Due to limited funding and materials available, motion tracking was only implemented on one motion segment. In order to better define the overall spine biomechanics, IRED rigid bodies should be placed on every vertebra as well as the moving MTS spine simulator jigs. By tracking every vertebral body, overall multi-segment kinematics as well as individual motion segment kinematics at any level desired can be calculated.

It is difficult to compare the results (rigidity and kinematic) in the present study with results found in the literature because of the fundamental differences between different test methods. The displacement control method using standard MTS spine simulator jigs was chosen because it was easy to describe to other researchers and is very reproducible in other laboratories. Because the test methods used in the KU Structural Biomaterials Lab differ greatly from that shown by other researchers, it will be vitally important to implement the kinematic motion tracking on future human cadaveric spines that are tested. This will allow for a more direct comparison of the synthetic spine model to the human cadaveric spine.

In the future it may be of interest to develop a testing method and test frame that allows for load control or a more advanced application of displacement control

(hybrid approach) that doesn't constrain the spine on both ends. Also, the current test system in the present study did not have the ability to perform axial rotation testing. If this were implemented in a new test system, there would be great benefits to the results that would be able to be obtained. Both methods have their advantages and disadvantages. The displacement control method seems to be best for evaluating changes in spinal segment stiffness while the load control method is better for evaluating changes in spinal kinematics. The load control method does not repeat the kinematics between tests because altering a component of the model will lead to altered kinematics. One good feature of using displacement control is that when something is changed on the model, such as ligament stiffness, the kinematics are similarly repeated. This allows accurate quantification of the mechanical contribution of the ligaments resistance to extension.

According to Wilke in 1998 [77] there are five requirements that a spinal loading simulator should fulfill and may serve as good guidelines in designing a new simulator at KU.

1. The specimen shall be able to move freely in all six degrees of freedom.
2. The simulator shall be capable of simulating the six loading components separately. This includes flexion/extension moments, lateral bending moments right and left, torsion left and right, and axial compression, tension, and shear in the sagittal and frontal planes.
3. All possible loading combinations shall be provided.

4. Loading shall be applied either continuously or in stepwise fashion.
5. The specimen shall be loaded in the positive and negative directions continuously (forward-backward or left-right) in order to obtain load-displacement curves that reflect the full cycle of motion in a given direction.

References:

1. Deyo, R.A. and J.N. Weinstein, *Low back pain.* N Engl J Med, 2001. **344**(5): p. 363-70.
2. Andersson, G.B., *Epidemiological features of chronic low-back pain.* Lancet, 1999. **354**(9178): p. 581-5.
3. Pai, S. and L.J. Sundaram, *Low back pain: an economic assessment in the United States.* Orthop Clin North Am, 2004. **35**(1): p. 1-5.
4. Frymoyer, J.W. and W.L. Cats-Baril, *An overview of the incidences and costs of low back pain.* Orthop Clin North Am, 1991. **22**(2): p. 263-71.
5. Hart, L.G., R.A. Deyo, and D.C. Cherkin, *Physician office visits for low back pain. Frequency, clinical evaluation, and treatment patterns from a U.S. national survey.* Spine, 1995. **20**(1): p. 11-9.
6. Taylor, V.M., et al., *Low back pain hospitalization. Recent United States trends and regional variations.* Spine, 1994. **19**(11): p. 1207-12; discussion 13.
7. Guo, H.R., et al., *Back pain prevalence in US industry and estimates of lost workdays.* Am J Public Health, 1999. **89**(7): p. 1029-35.
8. Maetzel, A. and L. Li, *The economic burden of low back pain: a review of studies published between 1996 and 2001.* Best Pract Res Clin Rheumatol, 2002. **16**(1): p. 23-30.
9. Martin, B.I., et al., *Expenditures and health status among adults with back and neck problems.* JAMA, 2008. **299**(6): p. 656-64.
10. Adams, M.A., *Biomechanics of back pain.* Acupunct Med, 2004. **22**(4): p. 178-88.
11. Martin, B.I., et al., *Reoperation rates following lumbar spine surgery and the influence of spinal fusion procedures.* Spine, 2007. **32**(3): p. 382-7.
12. Denhoy, *Spine Sector Shows Continued Growth*, in *MX Business Strategies for Medical Technology Executives*. 2008, Cannon Communications LLC: http://devicelink.com/mx/issuesupdate/08/08/Spine.html.
13. Deyo, R.A., et al., *United States trends in lumbar fusion surgery for degenerative conditions.* Spine, 2005. **30**(12): p. 1441-5; discussion 1446-7.
14. Viscogliosi Bros., L., *Spine Industry Analysis Series: Spine Non-Fusion. "Beyond Total Disc" the Future of Spine Surgery.* 2004: p. 301.
15. Cunningham, B.W., et al., *Biomechanical evaluation of total disc replacement arthroplasty: an in vitro human cadaveric model.* Spine, 2003. **28**(20): p. S110-7.
16. Chow, D.H., et al., *Effects of short anterior lumbar interbody fusion on biomechanics of neighboring unfused segments.* Spine, 1996. **21**(5): p. 549-55.
17. Dath, R., et al., *Intradiscal pressure changes with dynamic pedicle screw systems.* J Spinal Disord Tech, 2008. **21**(4): p. 241-6.
18. Grauer, J.N., et al., *Biomechanics of two-level Charite artificial disc placement in comparison to fusion plus single-level disc placement combination.* Spine J, 2006. **6**(6): p. 659-66.

19. Nunley, P.D., et al., *Comparison of pressure effects on adjacent disk levels after 2-level lumbar constructs: fusion, hybrid, and total disk replacement.* Surg Neurol, 2008. **70**(3): p. 247-51.
20. Panjabi, M., et al., *Multidirectional testing of one- and two-level ProDisc-L versus simulated fusions.* Spine, 2007. **32**(12): p. 1311-9.
21. Goel, V.K., et al., *Effects of charite artificial disc on the implanted and adjacent spinal segments mechanics using a hybrid testing protocol.* Spine, 2005. **30**(24): p. 2755-64.
22. Shono, Y., et al., *Stability of posterior spinal instrumentation and its effects on adjacent motion segments in the lumbosacral spine.* Spine, 1998. **23**(14): p. 1550-8.
23. Sudo, H., et al., *Biomechanical study on the effect of five different lumbar reconstruction techniques on adjacent-level intradiscal pressure and lamina strain.* J Neurosurg Spine, 2006. **5**(2): p. 150-5.
24. Untch, C., Q. Liu, and R. Hart, *Segmental motion adjacent to an instrumented lumbar fusion: the effect of extension of fusion to the sacrum.* Spine, 2004. **29**(21): p. 2376-81.
25. Yang, J.Y., J.K. Lee, and H.S. Song, *The impact of adjacent segment degeneration on the clinical outcome after lumbar spinal fusion.* Spine, 2008. **33**(5): p. 503-7.
26. Cunningham, B.W., et al., *The effect of spinal destabilization and instrumentation on lumbar intradiscal pressure: an in vitro biomechanical analysis.* Spine, 1997. **22**(22): p. 2655-63.
27. Hongo, M., et al., *Effect of multiple freeze-thaw cycles on intervertebral dynamic motion characteristics in the porcine lumbar spine.* J Biomech, 2008. **41**(4): p. 916-20.
28. White, A. and M. Panjabi, *Clinical Biomechanics of the Spine 2nd Edition*. ed. 2 ed. 1990, Philadelphia: J.B. Lippincott Company.
29. Saladin, K., *Human Anatomy: Custom edition for BIOL 240 University of Kansas*. 2005: Mcgraw Hill.
30. Raj, P.P., *Intervertebral disc: anatomy-physiology-pathophysiology-treatment.* Pain Pract, 2008. **8**(1): p. 18-44.
31. Heuer, F., H. Schmidt, and H.J. Wilke, *The relation between intervertebral disc bulging and annular fiber associated strains for simple and complex loading.* J Biomech, 2008. **41**(5): p. 1086-94.
32. Hukins and M. JR, *Relationship between structure and mechanical function of the tissues of the intervertebral joint.* American Zoologist, 2000. **40**(1): p. 11.
33. Twomey, L.T. and J.R. Taylor, *Age changes in lumbar vertebrae and intervertebral discs.* Clin Orthop Relat Res, 1987(224): p. 97-104.
34. Roberts, S., J. Menage, and J.P. Urban, *Biochemical and structural properties of the cartilage end-plate and its relation to the intervertebral disc.* Spine, 1989. **14**(2): p. 166-74.
35. Inoue, H., *Three-dimensional architecture of lumbar intervertebral discs.* Spine, 1981. **6**(2): p. 139-46.

36. Yu, J., et al., *Elastic fibre organization in the intervertebral discs of the bovine tail.* J Anat, 2002. **201**(6): p. 465-75.
37. Marchand, F. and A.M. Ahmed, *Investigation of the laminate structure of lumbar disc anulus fibrosus.* Spine, 1990. **15**(5): p. 402-10.
38. Hukins, D.W., et al., *Comparison of structure, mechanical properties, and functions of lumbar spinal ligaments.* Spine, 1990. **15**(8): p. 787-95.
39. Panjabi, M.M., V.K. Goel, and K. Takata, *Physiologic strains in the lumbar spinal ligaments. An in vitro biomechanical study 1981 Volvo Award in Biomechanics.* Spine, 1982. **7**(3): p. 192-203.
40. Nachemson, A.L. and J.H. Evans, *Some mechanical properties of the third human lumbar interlaminar ligament (ligamentum flavum).* J Biomech, 1968. **1**(3): p. 211-20.
41. Solomonow, M., et al., *The ligamento-muscular stabilizing system of the spine.* Spine, 1998. **23**(23): p. 2552-62.
42. Stubbs, M., et al., *Ligamento-muscular protective reflex in the lumbar spine of the feline.* J Electromyogr Kinesiol, 1998. **8**(4): p. 197-204.
43. Hindle, R.J., M.J. Pearcy, and A. Cross, *Mechanical function of the human lumbar interspinous and supraspinous ligaments.* J Biomed Eng, 1990. **12**(4): p. 340-4.
44. Chazal, J., et al., *Biomechanical properties of spinal ligaments and a histological study of the supraspinal ligament in traction.* J Biomech, 1985. **18**(3): p. 167-76.
45. Goel, V.K., et al., *The role of lumbar spinal elements in flexion.* Spine, 1985. **10**(6): p. 516-23.
46. Goel, V.K., et al., *Interlaminar shear stresses and laminae separation in a disc. Finite element analysis of the L3-L4 motion segment subjected to axial compressive loads.* Spine, 1995. **20**(6): p. 689-98.
47. Goel, V.K., H. Park, and W. Kong, *Investigation of vibration characteristics of the ligamentous lumbar spine using the finite element approach.* J Biomech Eng, 1994. **116**(4): p. 377-83.
48. Goel, V.K., et al., *Load sharing among spinal elements of a motion segment in extension and lateral bending.* J Biomech Eng, 1987. **109**(4): p. 291-7.
49. Neumann, P., et al., *Mechanical properties of the human lumbar anterior longitudinal ligament.* J Biomech, 1992. **25**(10): p. 1185-94.
50. Pintar, F.A., et al., *Biomechanical properties of human lumbar spine ligaments.* J Biomech, 1992. **25**(11): p. 1351-6.
51. Shirazi-Adl, A., A.M. Ahmed, and S.C. Shrivastava, *Mechanical response of a lumbar motion segment in axial torque alone and combined with compression.* Spine, 1986. **11**(9): p. 914-27.
52. Tkaczuk, H., *Tensile properties of human lumbar longitudinal ligaments.* Acta Orthop Scand, 1968: p. Suppl 115:1+.
53. Nordin, M. and F. VH, *Basic Biomechanics of the Musculoskeletal System*. ed. 2 ed. 1989, Philadelphia, PA: Lea and Febiger.

54. Woo, S.L., et al., *Injury and repair of ligaments and tendons.* Annu Rev Biomed Eng, 2000. **2**: p. 83-118.
55. Sjolander, P., H. Johansson, and M. Djupsjobacka, *Spinal and supraspinal effects of activity in ligament afferents.* J Electromyogr Kinesiol, 2002. **12**(3): p. 167-76.
56. Ebenbichler, G.R., et al., *Sensory-motor control of the lower back: implications for rehabilitation.* Med Sci Sports Exerc, 2001. **33**(11): p. 1889-98.
57. Indahl, A., et al., *Electromyographic response of the porcine multifidus musculature after nerve stimulation.* Spine, 1995. **20**(24): p. 2652-8.
58. Indahl, A., et al., *Interaction between the porcine lumbar intervertebral disc, zygapophysial joints, and paraspinal muscles.* Spine, 1997. **22**(24): p. 2834-40.
59. Panjabi, M.M., *The stabilizing system of the spine. Part II. Neutral zone and instability hypothesis.* J Spinal Disord, 1992. **5**(4): p. 390-6; discussion 397.
60. Solomonow, M., *Sensory-motor control of ligaments and associated neuromuscular disorders.* J Electromyogr Kinesiol, 2006. **16**(6): p. 549-67.
61. Solomonow, M. and M. Krogsgaard, *Sensorimotor control of knee stability. A review.* Scand J Med Sci Sports, 2001. **11**(2): p. 64-80.
62. Kastelic, J. and E. Baer, *Deformation in tendon collagen.* Symp Soc Exp Biol, 1980. **34**: p. 397-435.
63. Ambrosio, L., et al., *Viscoelastic behavior of composite ligament prostheses.* J Biomed Mater Res, 1998. **42**(1): p. 6-12.
64. Guerin, H.A. and D.M. Elliott, *The role of fiber-matrix interactions in a nonlinear fiber-reinforced strain energy model of tendon.* J Biomech Eng, 2005. **127**(2): p. 345-50.
65. Solomonow, M., *Ligaments: a source of work-related musculoskeletal disorders.* J Electromyogr Kinesiol, 2004. **14**(1): p. 49-60.
66. Harris, R.I. and I. Macnab, *Structural changes in the lumbar intervertebral discs; their relationship to low back pain and sciatica.* J Bone Joint Surg Br, 1954. **36-B**(2): p. 304-22.
67. Hirsch, C., B.E. Ingelmark, and M. Miller, *The anatomical basis for low back pain. Studies on the presence of sensory nerve endings in ligamentous, capsular and intervertebral disc structures in the human lumbar spine.* Acta Orthop Scand, 1963. **33**: p. 1-17.
68. Markolf, K.L., *Deformation of the thoracolumbar intervertebral joints in response to external loads: a biomechanical study using autopsy material.* J Bone Joint Surg Am, 1972. **54**(3): p. 511-33.
69. Shirazi-Adl, A., A.M. Ahmed, and S.C. Shrivastava, *A finite element study of a lumbar motion segment subjected to pure sagittal plane moments.* J Biomech, 1986. **19**(4): p. 331-50.
70. Gillespie, K.A. and J.P. Dickey, *Biomechanical role of lumbar spine ligaments in flexion and extension: determination using a parallel linkage robot and a porcine model.* Spine, 2004. **29**(11): p. 1208-16.

71. Neumann, P., et al., *Aging, vertebral density, and disc degeneration alter the tensile stress-strain characteristics of the human anterior longitudinal ligament.* J Orthop Res, 1994. **12**(1): p. 103-12.
72. Nachemson, A.L., A.B. Schultz, and M.H. Berkson, *Mechanical properties of human lumbar spine motion segments. Influence of age, sex, disc level, and degeneration.* Spine, 1979. **4**(1): p. 1-8.
73. Myklebust, J.B., et al., *Tensile strength of spinal ligaments.* Spine, 1988. **13**(5): p. 526-31.
74. Dumas, G.A., L. Beaudoin, and G. Drouin, *In situ mechanical behavior of posterior spinal ligaments in the lumbar region. An in vitro study.* J Biomech, 1987. **20**(3): p. 301-10.
75. Goel, V.K., et al., *Mechanical properties of lumbar spinal motion segments as affected by partial disc removal.* Spine, 1986. **11**(10): p. 1008-12.
76. Kornblatt, M.D., M.P. Casey, and R.R. Jacobs, *Internal fixation in lumbosacral spine fusion. A biomechanical and clinical study.* Clin Orthop Relat Res, 1986(203): p. 141-50.
77. Wilke, H.J., K. Wenger, and L. Claes, *Testing criteria for spinal implants: recommendations for the standardization of in vitro stability testing of spinal implants.* Eur Spine J, 1998. **7**(2): p. 148-54.
78. Goel, V.K., et al., *Biomechanical testing of the spine. Load-controlled versus displacement-controlled analysis.* Spine, 1995. **20**(21): p. 2354-7.
79. Goel, V.K., et al., *Test protocols for evaluation of spinal implants.* J Bone Joint Surg Am, 2006. **88 Suppl 2**: p. 103-9.
80. Goel, V.K., et al., *Kinematics of the whole lumbar spine. Effect of discectomy.* Spine, 1985. **10**(6): p. 543-54.
81. Goel, V.K., et al., *Effects of rigidity of an internal fixation device. A comprehensive biomechanical investigation.* Spine, 1991. **16**(3 Suppl): p. S155-61.
82. Goel, V.K., et al., *Response of the ligamentous lumbar spine to cyclic bending loads.* Spine, 1988. **13**(3): p. 294-300.
83. Panjabi, M., et al., *Hybrid testing of lumbar CHARITE discs versus fusions.* Spine, 2007. **32**(9): p. 959-66; discussion 967.
84. Panjabi, M.M., *Hybrid multidirectional test method to evaluate spinal adjacent-level effects.* Clin Biomech (Bristol, Avon), 2007. **22**(3): p. 257-65.
85. Cheng, B.C., et al., *Immediate biomechanical effects of lumbar posterior dynamic stabilization above a circumferential fusion.* Spine, 2007. **32**(23): p. 2551-7.
86. Patwardhan, A.G., et al., *Compressive preload improves the stability of anterior lumbar interbody fusion cage constructs.* J Bone Joint Surg Am, 2003. **85-A**(9): p. 1749-56.
87. Gardner-Morse, M.G. and I.A. Stokes, *Physiological axial compressive preloads increase motion segment stiffness, linearity and hysteresis in all six degrees of freedom for small displacements about the neutral posture.* J Orthop Res, 2003. **21**(3): p. 547-52.

88. Wilke, H.J., et al., *A universal spine tester for in vitro experiments with muscle force simulation.* Eur Spine J, 1994. **3**(2): p. 91-7.
89. Wilke, H.J., et al., *Biomechanical effect of different lumbar interspinous implants on flexibility and intradiscal pressure.* Eur Spine J, 2008. **17**(8): p. 1049-56.
90. Rousseau, M.A., et al., *The instant axis of rotation influences facet forces at L5/S1 during flexion/extension and lateral bending.* Eur Spine J, 2006. **15**(3): p. 299-307.
91. Glazer, P.A., et al., *Biomechanical analysis of multilevel fixation methods in the lumbar spine.* Spine, 1997. **22**(2): p. 171-82.
92. Heuer, F., et al., *Stepwise reduction of functional spinal structures increase range of motion and change lordosis angle.* J Biomech, 2007. **40**(2): p. 271-80.
93. Zander, T., A. Rohlmann, and G. Bergmann, *Influence of ligament stiffness on the mechanical behavior of a functional spinal unit.* J Biomech, 2004. **37**(7): p. 1107-11.
94. Zander, T., A. Rohlmann, and G. Bergmann, *Analysis of simulated single ligament transection on the mechanical behaviour of a lumbar functional spinal unit.* Biomed Tech (Berl), 2004. **49**(1-2): p. 27-32.
95. Adams, M.A., W.C. Hutton, and J.R. Stott, *The resistance to flexion of the lumbar intervertebral joint.* Spine, 1980. **5**(3): p. 245-53.
96. Lee, K.K. and E.C. Teo, *Material sensitivity study on lumbar motion segment (L2-L3) under sagittal plane loadings using probabilistic method.* J Spinal Disord Tech, 2005. **18**(2): p. 163-70.
97. Brolin, K. and P. Halldin, *Development of a finite element model of the upper cervical spine and a parameter study of ligament characteristics.* Spine, 2004. **29**(4): p. 376-85.
98. Wilke, H.J., et al., *Spinal segment range of motion as a function of in vitro test conditions: effects of exposure period, accumulated cycles, angular-deformation rate, and moisture condition.* Anat Rec, 1998. **251**(1): p. 15-9.
99. Wilke, H.J., S. Krischak, and L. Claes, *Biomechanical comparison of calf and human spines.* J Orthop Res, 1996. **14**(3): p. 500-3.
100. Kettler, A., et al., *Effects of specimen length on the monosegmental motion behavior of the lumbar spine.* Spine, 2000. **25**(5): p. 543-50.
101. Wilke, H.J., A. Kettler, and L.E. Claes, *Are sheep spines a valid biomechanical model for human spines?* Spine, 1997. **22**(20): p. 2365-74.
102. Fagan, M.J., S. Julian, and A.M. Mohsen, *Finite element analysis in spine research.* Proc Inst Mech Eng [H], 2002. **216**(5): p. 281-98.
103. Gilbertson, L.G., et al., *Finite element methods in spine biomechanics research.* Crit Rev Biomed Eng, 1995. **23**(5-6): p. 411-73.
104. Dick, J.C., et al., *Mechanical evaluation of cross-link designs in rigid pedicle screw systems.* Spine, 1997. **22**(4): p. 370-5.
105. Wilke, H.J., et al., *A mechanical model of human spinal motion segments.* Biomed Tech (Berl), 1997. **42**(11): p. 327-31.

106. Friis, E., et al., *Mechanical Analogue Model of the Human Lumbar Spine: Development and Initial Evaluation.*, in *Spinal Implants: Are We Evaluating Them Appropriately?*, M. Melkerson, S. Griffith, and J. Kirkpatrick, Editors. 2002, ASTM International: West Conshohocken, PA.
107. Neumann, P., et al., *Structural properties of the anterior longitudinal ligament. Correlation with lumbar bone mineral content.* Spine, 1993. **18**(5): p. 637-45.
108. Holt, C.A., et al., *Three-dimensional measurement of intervertebral kinematics in vitro using optical motion analysis.* Proc Inst Mech Eng [H], 2005. **219**(6): p. 393-9.
109. Crawford, N.R., G.T. Yamaguchi, and C.A. Dickman, *A new technique for determining 3-D joint angles: the tilt/twist method.* Clin Biomech (Bristol, Avon), 1999. **14**(3): p. 153-65.
110. Grood, E.S. and W.J. Suntay, *A joint coordinate system for the clinical description of three-dimensional motions: application to the knee.* J Biomech Eng, 1983. **105**(2): p. 136-44.
111. Crawford, N.R., *Biomechanics of lumbar arthroplasty.* Neurosurg Clin N Am, 2005. **16**(4): p. 595-602, v.
112. EPA. *Comparison of Statistical Methods*. Statistical Primer 2007 [cited 2008; Available from: http://www.epa.gov/bioiweb1/statprimer/tableall.html.
113. Morton, N.A., et al., *Effect of variability in anatomical landmark location on knee kinematic description.* J Orthop Res, 2007. **25**(9): p. 1221-30.
114. Panjabi, M.M., et al., *Mechanical behavior of the human lumbar and lumbosacral spine as shown by three-dimensional load-displacement curves.* J Bone Joint Surg Am, 1994. **76**(3): p. 413-24.
115. Wilke, H.J., et al., *Load-displacement properties of the thoracolumbar calf spine: experimental results and comparison to known human data.* Eur Spine J, 1997. **6**(2): p. 129-37.
116. Ames, C.P., et al., *Biomechanical comparison of posterior lumbar interbody fusion and transforaminal lumbar interbody fusion performed at 1 and 2 levels.* Spine, 2005. **30**(19): p. E562-6.